MUTATIONAL ANALYSIS AND ENGINEERING OF THE HUMAN VITAMIN D RECEPTOR TO BIND AND ACTIVATE IN RESPONSE TO A NOVEL SMALL MOLECULE LIGAND

A Dissertation
Presented to
The Academic Faculty

by

Hilda S. Castillo

In Partial Fulfillment
of the Requirements for the Degree
Doctorate of Philosophy in the
School of Chemistry & Biochemistry

Georgia Institute of Technology
May 2011

MUTATIONAL ANALYSIS AND ENGINEERING OF THE HUMAN VITAMIN D RECEPTOR TO BIND AND ACTIVATE IN RESPONSE TO A NOVEL SMALL MOLECULE LIGAND

Approved by:

Dr. Donald Doyle, Advisor
School of Chemistry & Biochemistry
Georgia Institute of Technology

Dr. Loren Williams, Co-advisor
School of Chemistry & Biochemistry
Georgia Institute of Technology

Dr. Bahareh Azizi, Advisor
School of Chemistry & Biochemistry
Georgia Institute of Technology

Dr. Nicholas Hud
School of Chemistry & Biochemistry
Georgia Institute of Technology

Dr. Andreas Bommarius, Co-advisor
School of Chemical & Biomolecular Engineering
Georgia Institute of Technology

Dr. Sheldon May
School of Chemistry & Biochemistry
Georgia Institute of Technology

Date Approved: January 20, 2011

Sólo dos legados duraderos podemos dejar a nuestros hijos:
uno, raíces; otro, alas.

~Hodding Carter

Para mis padres, Alex y Felix Castillo.
Soy quien soy gracias a ustedes.

TABLE OF CONTENTS

	Page
LIST OF TABLES	vii
LIST OF FIGURES	ix
ABBREVIATIONS	xii
SUMMARY	xv
CHAPTER 1 NUCLEAR RECEPTORS	1
1.1 The Nuclear Receptor Superfamily	1
1.2 Structure of Nuclear Receptors	2
1.3 Transcriptional Regulation by Nuclear Receptors	7
1.4 Nuclear Receptors: Drug Discovery and Protein Engineering Targets	12
1.5 Literature Cited	15
CHAPTER 2 THE HUMAN VITAMIN D RECEPTOR (hVDR)	19
2.1 The hVDR: Structure and Function	19
2.2 The hVDR: A Drug Discovery Target	27
2.3 The hVDR: A Protein Engineering Target	28
2.4 Chemical Complementation: A Genetic Selection System in Yeast	29
2.5 Characterization of the hVDR in Chemical Complementation	31
2.6 Summary	41
2.7 Materials and Methods	44
2.8 Literature Cited	46
CHAPTER 3 PROTEIN ENGINEERING WITH CHEMICAL COMPLEMENTATION: ENGINEERING THE HUMAN VITAMIN D RECEPTOR TO BIND AND ACTIVATE IN RESPONSE TO A NOVEL SMALL MOLECULE LIGAND	56
3.1 Engineering the hVDR	56
3.2 Rational Mutagenic Approach: hVDR Libraries 1 & 2	59
3.2.1 Rational Mutagenic Approach: Design for hVDR Libraries 1 & 2	59
3.2.2 Rational Mutagenic Approach: Library Construction and Selection of hVDR Libraries 1 & 2 in Chemical Complementation	65
3.2.3 Rational Mutagenic Approach: Troubleshooting hVDR Libraries 1 & 2 Using *Klenow* Polymerase	70
3.2.4 Rational Mutagenic Approach: Troubleshooting hVDR Libraries 1 & 2 Using Commercial *Pfu* Polymerase	72
3.3 Random Mutagenic Approach: hVDR Error-Prone PCR Libraries	78
3.4 Rational Mutagenic Approach: hVDR Subset Libraries: B, C, E & F	84
3.5 hVDR Variant BS4 Binds and Activates in Response to A Novel	

Small Molecule Ligand: Characterization in Mammalian Cell Culture Assays 90
3.6 Summary 95
3.7 Materials and Methods 100
3.8 Literature Cited 105

CHAPTER 4 ENGINEERING THE HVDRC410Y VARIANT AND INVESTIGATING THE MUTATIONAL TOLERANCE OF RESIDUE C410 IN THE HUMAN VITAMIN D RECEPTOR 108

4.1 Engineering hVDRC410Y and Investigating hVDR Residue C410 108
4.2 Engineering hVDRC410Y: Error-Prone PCR Libraries 110
4.3 hVDR Residue C410 and *In-Silico* Docking of wthVDR and hVDRC410Y 112
4.4 Mutational Tolerance of Residue C410 115
4.5 Enhancing the Sensitivity of hVDRC410Y 121
4.6 Summary 125
4.7 Materials and Methods 126
4.8 Literature Cited 130

CHAPTER 5 INVESTIGATING THE ROLE AND MUTATIONAL TOLERANCE OF TYROSINES 143 AND 147 IN THE HUMAN VITAMIN D RECEPTOR'S LIGAND BINDING POCKET 133

5.1 Tyrosines and the Two Anchoring Ends of the hVDR's Ligand Binding Pocket 133
5.2 Reversal of the hVDR Ligand Anchors 135
5.3 Eliminating the Constitutive Activity of A hVDR Variant 140
5.4 Mutational Tolerance of hVDR Residues Y143 and Y147 143
5.5 Summary 153
5.6 Materials and Methods 155
5.7 Literature Cited 159

LIST OF TABLES

		Page
Table 2.1:	Contacts and Interactions Between the hVDR and 1α, 25$(OH)_2D_3$, and within the hVDR that Stabilize Helix 12	24
Table 2.2:	Comparison of the wthVDR EC_{50} Values in Chemical Complementation vs. Literature	42
Table 3.1:	Rational Mutagenic Approach hVDR Library 1: Mutated Residues and Their Predicted Functions	62
Table 3.2:	Rational Mutagenic Approach hVDR Library 2: Mutated Residues and Their Predicted Functions	64
Table 3.3:	Rational Mutagenic Approach hVDR Library 1: Oligonucleotides Containing Randomized Degenerate Codons at the Designated Mutation Sites	67
Table 3.4:	Rational Mutagenic Approach hVDR Library 2: Oligonucleotides Containing Randomized Degenerate Codons at the Designated Mutation Sites	68
Table 3.5:	Rational Mutagenic Approach: hVDR Library 1 (using commercial *Pfu*) Sequencing Results	79
Table 3.6:	Rational Mutagenic Approach: hVDR Library 2 (using commercial *Pfu*) Sequencing Results	80
Table 3.7:	Random Mutagenic Approach: hVDR Error-Prone PCR Libraries Sequencing Results	83
Table 3.8:	Rational Mutagenic Approach hVDR Subset Library B: Oligonucleotides Containing Randomized Degenerate Codons at the Designated Mutation Sites	86
Table 3.9:	Rational Mutagenic Approach hVDR Subset Library C: Oligonucleotides Containing Randomized Degenerate Codons at the Designated Mutation Sites	87
Table 3.10:	Rational Mutagenic Approach hVDR Subset Library E: Oligonucleotides Containing Randomized Degenerate Codons at the Designated Mutation Sites	88
Table 3.11:	Rational Mutagenic Approach hVDR Subset Library F: Oligonucleotides Containing Randomized Degenerate Codons at the Designated Mutation Sites	89
Table 3.12:	Rational Mutagenic Approach: hVDR Subset Library B Sequencing Results	96

Table 3.13: Rational Mutagenic Approach: hVDR Subset Library C Sequencing Results 97

Table 3.14: Rational Mutagenic Approach: hVDR Subset Library E Sequencing Results 98

Table 3.15: Rational Mutagenic Approach: hVDR Subset Library F Sequencing Results 99

Table 4.1: EC_{50} and Fold- Activation Values for hVDR (H305, H397 and C410) Constructs Tested in Mammalian Cell Culture Assays 124

Table 5.1: EC_{50} and Fold- Activation Values for hVDR (Y143 and Y147) Constructs Tested in Mammalian Cell Culture Assays 151

LIST OF FIGURES

	Page
Figure 1.1: Structural Domains of Nuclear Receptors (Human RXRα)	3
Figure 1.2: DNA Binding Domain of Nuclear Receptors (Human RXRα)	4
Figure 1.3: Ligand Binding Domain of Nuclear Receptors (Human RXRα)	6
Figure 1.4: Nuclear Receptor Heterodimer (Human PPAR-γ and Human RXR-α)	8
Figure 1.5: Transcriptional Regulation by Nuclear Receptors	10
Figure 1.6: *Apo* vs. *Holo* Nuclear Receptor Ligand Binding Domains (Human RXR- α)	11
Figure 1.7: Two Current Commonly Prescribed Nuclear Receptor-Targeting Drugs	13
Figure 2.1: hVDR Ligands, Analogs and Mimics	20
Figure 2.2: The hVDR Ligand Binding Domain	22
Figure 2.3: Important Hydrogen Bonds between the hVDR and 1α, 25$(OH)_2D_3$	23
Figure 2.4: The hVDR 'Pi-Cation Activation Switch' and 'Charge Clamp'	26
Figure 2.5: Ligands of Various Nuclear Receptors	30
Figure 2.6: Chemical Complementation	32
Figure 2.7: Cloning the hVDR from cDNA and Co-transformation into the PJ69-4A Yeast Strain	33
Figure 2.8: Liquid Quantitation Assay of Chemical Complementation	35
Figure 2.9: The wthVDR in Chemical Complementation: Adenine selective media with LCA	36
Figure 2.10: The wthVDR in Chemical Complementation: 3-AT Test in histidine selective media	38
Figure 2.11: 1α, 25$(OH)_2D_3$, Lithocholic Acid and their Analogs	39
Figure 2.12: The wthVDR in Chemical Complementation: Histidine selective media with various ligands	40
Figure 2.13: The wthVDR in Chemical Complementation: Adenine selective media with 1α, 25$(OH)_2D_3$	43

Figure 3.1: Engineering the hVDR to Bind and Activate in Response to A Novel Small Molecule: Structures of molecules of Interest 58

Figure 3.2: Rational Mutagenic Approach: Design for hVDR Library 1 61

Figure 3.3: Rational Mutagenic Approach: Design for hVDR Library 2 63

Figure 3.4: Using Hybridization and PCR to Create Full Insert Cassettes, Construction of the Background Plasmid and Transformation into PJ69-4A for hVDR Libraries 1 & 2 69

Figure 3.5: Rational Mutagenic Approach: Streaking for hVDR Library 1 & 2 Variants 71

Figure 3.6: Rational Mutagenic Approach hVDR Libraries 1 & 2: Examples of Cassette Products Obtained Using *Klenow* Polymerase 73

Figure 3.7: Rational Mutagenic Approach hVDR Libraries 1 & 2: Cassette Products Obtained Using Commercial *Pfu* Polymerase 74

Figure 3.8: Rational Mutagenic Approach: Streaking for hVDR Library 1 & 2 Variants (using commercial *Pfu)* *76*

Figure 3.9: Rational Mutagenic Approach: hVDR Library 1 & 2 Variants (obtained using commercial *Pfu*) in Chemical Complementation 77

Figure 3.10: Random Mutagenic Approach: hVDR Error-Prone PCR Variants in Chemical Complementation 82

Figure 3.11: Rational Mutagenic Approach: Design for hVDR Subset Libraries B, C, E & F 85

Figure 3.12: Rational Mutagenic Approach: hVDR Subset Library B Variant BS4 in Chemical Complementation: Histidine selective media with LCA 91

Figure 3.13: Rational Mutagenic Approach: hVDR Subset Library B Variant BS4 in Chemical Complementation: Histidine selective media with chole 92

Figure 3.14: Rational Mutagenic Approach: hVDR Subset Library B Variant BS4 in Mammalian Cell Culture Assay with LCA 93

Figure 3.15: Rational Mutagenic Approach: hVDR Subset Library B Variant BS4 in Mammalian Cell Culture Assay with chole 94

Figure 4.1: Structures of hVDR Ligands and Molecules of Interest 109

Figure 4.2: hVDR Residue C410 113

Figure 4.3: *In-silico* Docking of wthVDR and hVDRC410Y with Various Ligands 116

Figure 4.4: Mutational Tolerance of Residue C410 in the hVDR: hVDRC410 Variants in Chemical Complementation 120

Figure 4.5: Enhancing the Sensitivity of hVDRC410Y: hVDR Variants in Mammalian Cell Culture Assays 123

Figure 5.1: The hVDR and 1α, 25$(OH)_2D_3$ 134

Figure 5.2: *In-silico* Docking of wthVDR 137

Figure 5.3: Reversal of the hVDR Ligand Anchors: hVDR Variants in Chemical Complementation 139

Figure 5.4: Eliminating the Constitutive Activity of A hVDR Variant: hVDR Variants in Chemical Complementation 142

Figure 5.5: hVDR Residues Y143 and Y147 144

Figure 5.6: Mutational Tolerance of hVDR Residue Y143: Single Variants in Chemical Complementation 146

Figure 5.7: Mutational Tolerance of hVDR Residue Y147: Single Variants in Chemical Complementation 147

Figure 5.8: Mutational Tolerance of hVDR Residues Y143 and Y147: Double Variants in Chemical Complementation 148

Figure 5.9: Mutational Tolerance of hVDR Residue Y143: Single Variants in Mammalian Cell Culture Assay 150

Figure 5.10: Mutational Tolerance of hVDR Residue Y147: Single Variants in Mammalian Cell Culture Assay 152

Figure 5.11: Mutational Tolerance of hVDR Residues Y143 and Y147: Double Variants in Mammalian Cell Culture Assay 154

ABBREVIATIONS

1α, 25$(OH)_2D_3$	1α, 25-dihydroxyvitamin D_3
3-AT	3-amino-1, 2, 4-triazole
Ac	Acetyl group
ACTR	Activator for Thyroid and Retinoid receptors
AD	Activation domain
ADE	Adenine
AF-1	Ligand-independent activation function domain
AF-2	Ligand-dependent activation function domain
-ALW	Minus adenine, leucine and tryptophan
AR	Androgen receptor
bp	Base pair
C.A.	Constitutively active
CAR	Constitutive androstane receptor
CC	Chemical complementation
cDNA	Complementary DNA
Chole	Cholecalciferol
CMV	Cytomegalovirus
CoAc	Coactivator
CoR	Corepressor
CoRNR box	CoRepressor Nuclear Receptor Box
DBD	DNA binding domain
DCA	Deoxycholic acid
DNA	Deoxyribonucleic acid
DMSO	Dimethylsulfoxide

dNTPs	Deoxyribonucleotide triphosphate
E.coli	*Escherichia coli*
EC_{50}	Half maximal effective concentration
epPCR	Error-prone PCR
ER	Estrogen receptor
GAD	Gal4 activation domain
GBD	Gal4 DNA binding domain
GR	Glucocorticoid receptor
h	Human
HATs	Histone acetyltransferases
HDACs	Histone deacetylases
HEK 293T	Human embryonic kidney 293T
HIS	Histidine
-HLW	Minus histidine, leucine and tryptophan
LBD	Ligand binding domain
LBP	Ligand bind pocket
LCA	Lithocholic acid
LRH-1	Liver receptor homolog-1
-LW	Minus leucine and tryptophan
LXR	Liver X receptor
µg	Microgram
$MgCl_2$	Magnesium chloride
µM	Micromolar
mM	millimolar
$MnCl_2$	Manganese chloride
NCoR1	Nuclear receptor Corepressor-1

ng	Nanogram
nM	Nanomolar
NR	Nuclear receptor
OD	Optical density
oligos	oligonucleotides
PCR	Polymerase chain reaction
PDB	Protein Data Bank
PPARs	Peroxisome proliferator-activated receptors
PR	Progesterone receptor
PXR	Pregnane X receptor
r	rat
RAR	Retinoic acid receptor
RE	Response element
RNA Pol	Ribonucleic acid polymerase
rpm	Revolutions per minute
RXR	Retinoid X receptor
SC	Synthetic complete media
SHP	Short heterodimer partner receptor
SRC-1	Steroid Receptor Coactivator-1
T_m	Melting temperature
VDR	Vitamin D Receptor
VMD	Visual Molecular Dynamics
wt	Wild type

SUMMARY

Nuclear receptors (NRs) are ligand-activated transcription factors that regulate the expression of genes involved in all physiological activities. Disruption in NR function (e.g. mutations) can lead to a variety of diseases; making these receptors important targets for drug discovery. The ability to bind a broad range of 'drug-like' molecules also make these receptors attractive candidates for protein engineering, such that they can be engineered to bind novel small molecule ligands, for several applications. One application is the creation of potential molecular switches, tools that can be used for controlling gene expression.

Gaining knowledge of specific molecular interactions that occur between a receptor and its ligand is of interest, as they contribute towards the activation or repression of target genes. The focus of this work has been to investigate the structural and functional relationships between the human vitamin D receptor (hVDR) and its ligands. To date, mutational assessments of the hVDR have focused on alanine scanning and residues typically lining the ligand binding pocket (LBP) that are involved in direct interactions with the ligand. A comprehensive analysis of the tolerance of these residues in the binding and activation of the receptor by its ligands has not been performed. Furthermore, residues not in contact with the ligand or that do not line the LBP may also play an important role in determining the activation profiles observed for NRs, and therefore need to be explored further.

In order to engineer and use the hVDR in chemical complementation, a genetic selection system in which the survival of yeast is linked to the activation of a NR by an agonist, the hVDR gene was isolated from cDNA. To gain insight into how chemical and physical changes within the ligand binding domain (LBD) affect receptor-ligand interactions, libraries of hVDR variants exploring the role and tolerance of hVDR residues were created. To develop a comprehensive mutational analysis while also engineering the hVDR to bind a novel small molecule ligand, a rational and a random mutagenic approach were used to create the libraries. A variant,

hVDRC410Y, that displayed enhanced activity with lithocholic acid (LCA), a known hVDR ligand, and novel activation with cholecalciferol (chole), a precursor of the hVDR's natural ligand known not to activate the wild-type hVDR, was discovered.

The presence of a tyrosine at the C410 position resulting in novel activation profiles with both LCA and chole, and the fact that this residue does not line the hVDR's LBP led to interest in determining whether a physical or chemical property of the residue was responsible for the observed activity. When residue C410 was further assessed for its tolerance to varying amino acids, the results indicated that bulkiness at this end of the pocket is important for activation with these ligands. Both LCA and chole have reduced molecular volumes compared to the natural ligand, 1α, 25$(OH)_2D_3$. As a result, increased bulkiness at the C410 position may contribute additional molecular interactions between the receptor and ligands.

Results obtained throughout this work suggest that the end of the hVDR's LBP consisting of two ligand anchoring residues, H305 and H397, and residue C410 tolerates structural variations, as numerous variants with mutations at these positions displayed enhanced activity. The receptor contains two tyrosines, Y143 and Y147, which were targeted for mutagenesis in one of the rationally designed libraries, located at the exact opposite end of the pocket. In an effort to gain further insight into the role of these residues at the other end of the LBP, mutagenesis assessing the tolerance of tyrosines 143 and 147 was performed. Overall, most changes at these positions proved to be detrimental to the function of the receptor supporting the hypothesis that this end of the LBP is less tolerant of structural changes, compared to the opposite end consisting of residues H305, H397 and C410.

Overall, a better understanding of the structural and functional relationships between the human vitamin D receptor (hVDR) and its ligands was achieved. The effects of residue C410 on specificity and activation with the different ligands studied were unforeseen, as this residue does not line the receptor's ligand binding pocket (LBP). However, they serve as an example of the significant impact distant residues can have on receptor activation and also emphasize the

important role physical properties of residues, such as volume, can play for specific ends of the LBP compared to chemical properties.

CHAPTER 1

NUCLEAR RECEPTORS

1.1 The Nuclear Receptor Superfamily

Nuclear receptors (NRs) are a large family of ligand-activated transcription factors. These receptors are found in many organisms, including worms, insects, and humans [1]. As of 2001, the genome of *Caenorhabditis elegans*, a worm, was shown to contain 270 NRs, more than any other organism [2-4]. Upon binding of a small molecule, NRs function as transcription regulators of essential genes involved in all physiological activities, such as development, growth, and homeostasis [1, 5-13]. Due to their essential roles in a complex cascade of biological processes, disruption in NR function can lead to numerous metabolic diseases, such as diabetes, obesity and cancer [5-8, 11, 14]. As a result, NRs are good candidates for drug discovery, with 34 of the top 200 most prescribed drugs targeting a NR in the year 2003 [13].

Historically, the foundation of the NR superfamily was initiated by the cloning and sequencing of the human glucocorticoid receptor (GR) in 1985 and the human estrogen receptor α (ERα) in 1986 [15-17]. The similarity in sequence between these two receptors was indicative of a potential receptor protein family. To date, there are 48 members in the human NR superfamily [5-8, 11-14, 18-20]. Based on their ligands and functions, these receptors are divided into three classes; the endocrine, the adopted orphan and the true orphan NRs [5, 19, 21]. Endocrine receptors bind hormones and vitamins with high affinity [5, 8, 21]. This class includes steroid as well as non-steroidal receptors, such as the progesterone receptor (PR) and the retinoic acid receptor (RAR), respectively. The adopted orphan receptors include receptors that were identified without the discovery of their natural ligand, such as the pregnane X receptor (PXR). These receptors were ‘adopted’, as their natural ligands, ranging from lipids to

xenobiotics, were discovered [5, 8, 21]. The third class of receptors, the true orphan receptors, is composed of receptors for which ligands have yet to be identified, including the short heterodimer partner receptor (SHP) and the liver receptor homolog-1 (LRH-1). However, the biological processes regulated by many of these receptors have been identified [21].

1.2 Structure of Nuclear Receptors

Despite their ability to control a wide variety of processes, NRs share highly conserved sequences and modular protein structures that consist of several domains (Figure 1.1) [1, 5-8, 11, 13, 22]. Most NR structures include an N-terminal region, a DNA binding domain, a hinge region, a ligand binding domain, and a C-terminal region. Each domain plays an essential role in the function of NRs. The N-terminal region contains a ligand-independent activation function domain (AF-1). This highly variable domain serves as the binding site for a variety of proteins including other transcription factors, and is the main target for post-translational modifications [12, 14, 19]. The highly disordered nature of this region has led to limited information about the structure and function of this domain.

The DNA-binding domain (DBD) is the most conserved domain, with members within the NR superfamily sharing high sequence homology. This domain (~70 amino acids) contains two cysteine-rich zinc finger motifs necessary for binding specific DNA sequences called response elements (REs) (Figure 1.2) [12, 14, 19, 21, 23]. Most REs are made up of two hexameric half-sites, usually RGGTCA (where R is a purine), separated by several nucleotides [12, 21, 24, 25]. Binding specificity for REs among different NRs depends on the spacing (usually 3-5 nucleotides) and orientation (direct or indirect repeats) of the two half-sites [24, 25]. Direct repeats are made up of DNA sequences that are identical to each other (e.g. AGGTCAxxxAGGTCA), while indirect

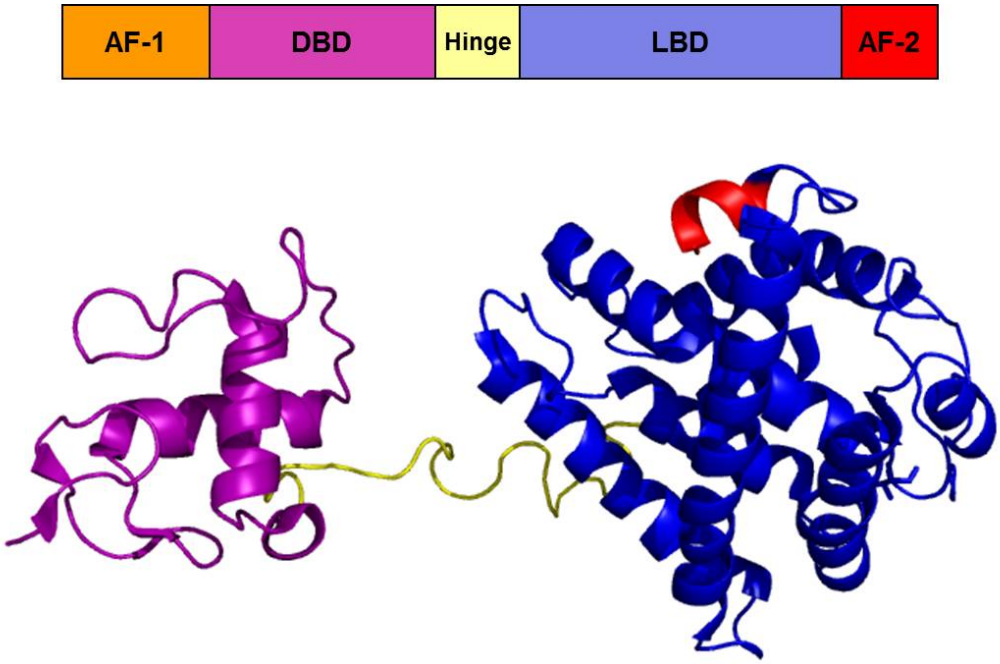

Figure 1.1: Structural Domains of Nuclear Receptors (Human RXRα)
DNA Binding Domain (Magenta), Hinge (Yellow), Ligand Binding Domain (Blue), AF-2 Domain (Red), PDB: 3DZY

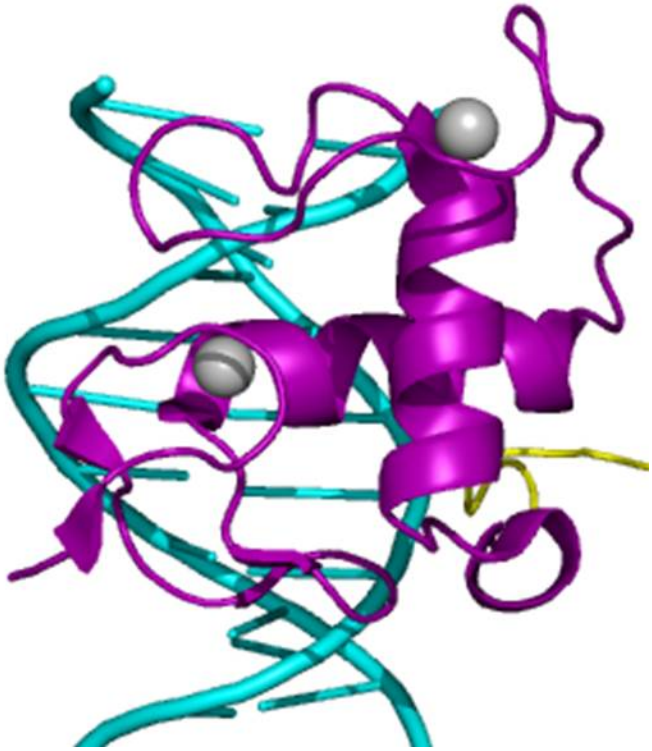

Figure 1.2: DNA Binding Domain of Nuclear Receptors (Human RXRα)
DNA Binding Domain (Magenta), DNA Response Element (Cyan), Zinc (II) Ions (Gray), PDB: 3DZY

repeats are not. Indirect repeats are subdivided into mirror-image and inverted (palindromic) repeats. Mirror-image repeats are made up of DNA sequences that are reverse to each other (e.g. AGGTCAxxxACTGGA), while inverted repeats are made up of DNA sequences that are also reversed but complement each other (e.g. AGGTCAxxxTGACCT).

The DBD is linked to the ligand –binding domain (LBD) via a non-conserved hinge region that provides NRs with flexibility for participation in a diverse array of interactions. This domain also includes a nuclear localization sequence, which facilitates the transport of some NRs from the cytoplasm to the nucleus [1, 5, 10-13, 21].

The LBD's overall structure (~250 amino acids) is well-conserved, but varies enough to allow selective ligand recognition among different NRs [8, 11, 13]. This domain shares a common three-dimensional structure typically composed of 12 α-helices and a three-stranded β sheet, arranged in three layers that form an antiparallel 'α-helical sandwich' (Figure 1.3) [12, 14, 19, 26, 27]. Residues involved in direct interactions/contact with the ligand form the ligand binding pocket (LBP). The specificity of NR ligand-binding depends on the shape and volume of this LBP, the amino acid residues that are in proximity to the ligand and form direct interactions, as well as distant residues that may have indirect structural effects [11]. The LBP's volume can vary significantly among different NRs, for example, the androgen receptor (AR) has a LBP volume of 420 $Å^3$, while the peroxisome proliferator-activated receptors (PPARs) have LBP volumes of ~1300 $Å^3$ [8, 11, 13]. The LBPs of most NRs are generally lined with hydrophobic amino acids and a few polar residues from helices 3, 7 and 10 that mediate ligand positioning and interactions [14, 26, 28]. Helix 12, an essential helix in the LBD, contains the ligand dependent activation function domain (AF-2), which serves as a

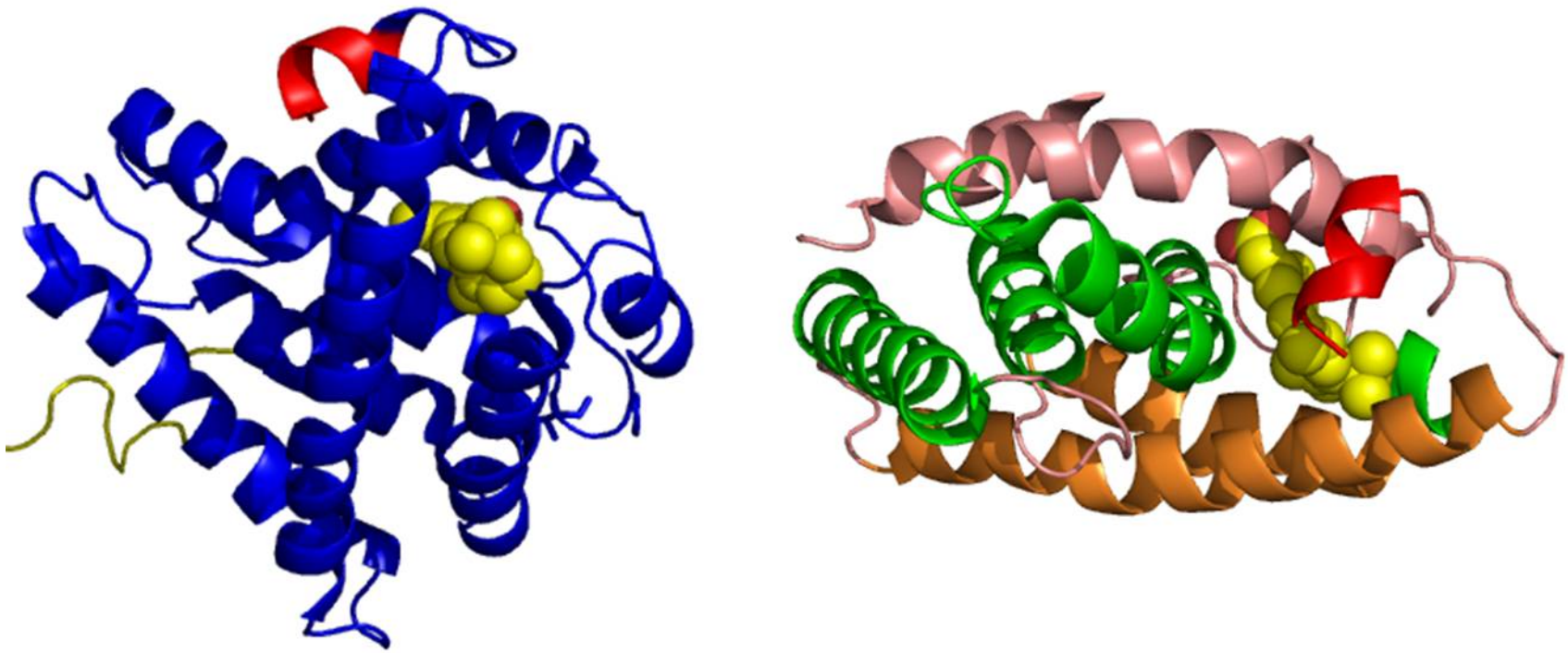

Figure 1.3: Ligand Binding Domain of Nuclear Receptors (Human RXRα) Ligand Binding Domain (Blue), AF-2 Domain (Red), 9-cis Retinoic Acid (Yellow), Layers of the 'α-helical sandwich' (Pink, Green, Orange), PDB: 3DZY

mobile lid over the LBP [12, 14, 19, 28, 29]. This domain is also involved in interactions with transcriptional coregulators, specifically NR corepressors and coactivators, which interact with chromatin-modifying enzymes [12, 14, 20, 30-35].

Crystallization of partial NR structures has furthered the understanding of NR three-dimensional structure and mechanisms of action. However, a significant advancement in the structural analysis of NRs occurred with the crystallization of the full-length liganded NR pair, peroxisome proliferator-activated receptor-γ (PPARγ)-retinoid X receptor-α (RXRα), bound to DNA with coactivator peptides [36, 37]. Unlike previous NR crystallization efforts which focused on isolated DBDs and LBDs, this first full-length crystal structure provided insight into how domain-domain interactions cooperate and ultimately influence NR activity [37].

1.3 Transcriptional Regulation by Nuclear Receptors

Due to their roles in a complex cascade of biological processes, the transcriptional regulation of NRs involves a series of molecular events. Most NRs are regulated by small molecules that are hydrophobic and lipid-soluble in nature [5, 11, 12, 14]. Generally speaking, NR ligands can be divided into two main categories; agonists and antagonists. Agonists are molecules that bind and activate a NR, while antagonists are molecules that bind but do not activate a NR [11, 14]. However, both types of ligands induce changes in the size and shape of NR LBPs, resulting in the recruitment of diverse coregulator complexes (over 300 different proteins identified as of 2007) that interact with chromatin-modifying enzymes necessary for gene transcription [11, 13, 14, 20, 33-35].

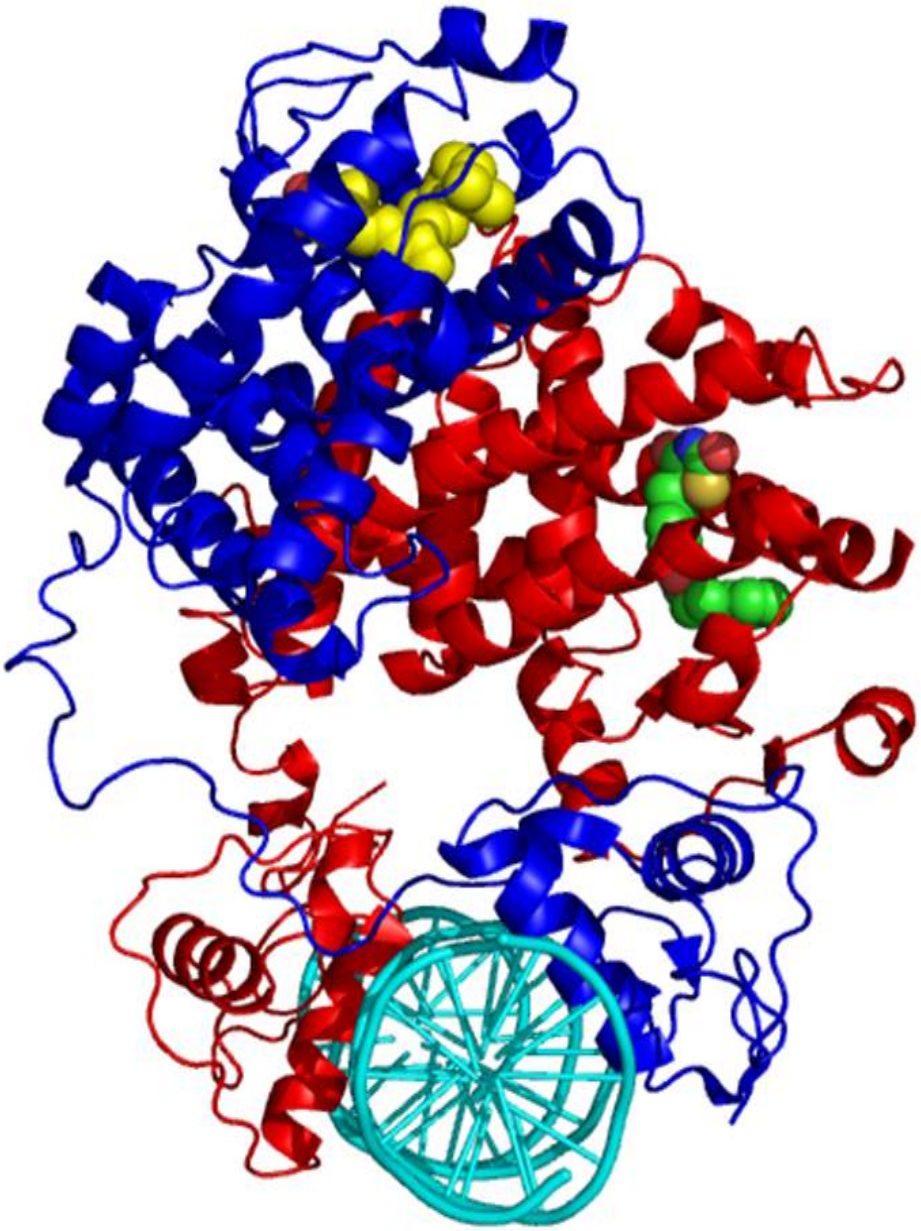

Figure 1.4: Nuclear Receptor Heterodimer (Human PPAR-γ and Human RXR-α)
Full-length PPAR-γ/Rosliglitazone (Red/Green), Full-length RXR-α/9-cis Retinoic Acid (Blue/Yellow), DNA Response Element (Cyan), PDB: 3DZY

Part of the functionality of NRs involves the binding of the NR DBD to specific DNA REs. NRs can bind REs upstream or downstream their target genes as monomers, homodimers, or heterodimers with the heterodimerizing partner, RXR (Figure 1.4) [8, 11, 19, 38, 39]. Based on their activation mode, RXR heterodimer partners are divided into three groups; permissive, conditional, and non-permissive heterodimers [5, 8, 19, 39, 40]. Permissive partners are heterodimers that can be activated by an RXR agonist, the other NR's agonist or both partners' agonists with an overall additive effect (e.g. RXR/LXR (liver X receptor)). Conditional partners do not permit activation by RXR alone and require the partner's agonist for full activation with an RXR agonist (e.g. RXR/RAR). Non-permissive partners do not permit activation by RXR agonists, whether the partner's agonist is present or not (e.g. RXR/VDR (vitamin D receptor)).

In the unliganded *apo*-form, NRs can be located either in the cytoplasm interacting with other proteins (e.g. heat shock proteins and chaperones), or in the nucleus and sometimes bound by corepressor complexes [5, 8, 11, 28]. Corepressor proteins, such as the nuclear receptor corepressor-1 (NCoR1), contain a corepressor nuclear receptor box (CoRNR box) region. An LXXXIXXX(I/L) motif within this box, where L is leucine, I is isoleucine and X is any amino acid, binds a hydrophobic surface commonly formed by helices 3 and 4 of NR LBDs [8, 11, 13, 19, 41]. Corepressors form protein complexes containing histone deacetylases (HDACs). HDACs condense chromatin structure over target promoter regions by deacetylating lysine residues on the histones, leading to tighter interactions between the histones and DNA. This prevents the recruitment of the transcription machinery, resulting in gene repression (Figure 1.5a) [8, 11, 12, 19, 21].

Upon agonist binding, the *holo*-form of NRs undergoes a conformational change, such that helix 12 repositions over the LBP burying the ligand and results in an active conformation of the NR (Figure 1.6) [5, 6, 8, 11, 13, 14, 21, 28, 30]. This leads to the

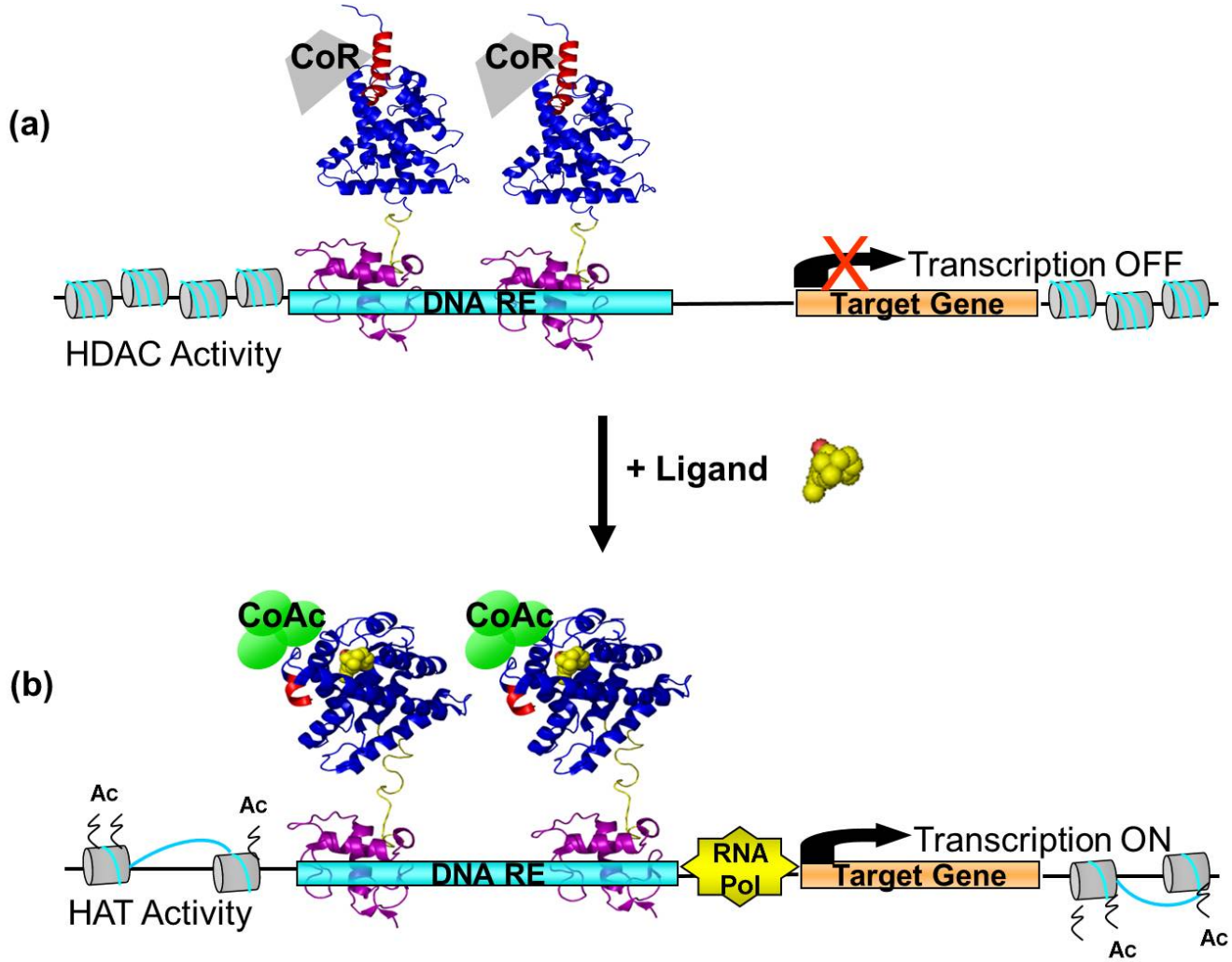

Figure 1.5: Transcriptional Regulation by Nuclear Receptors

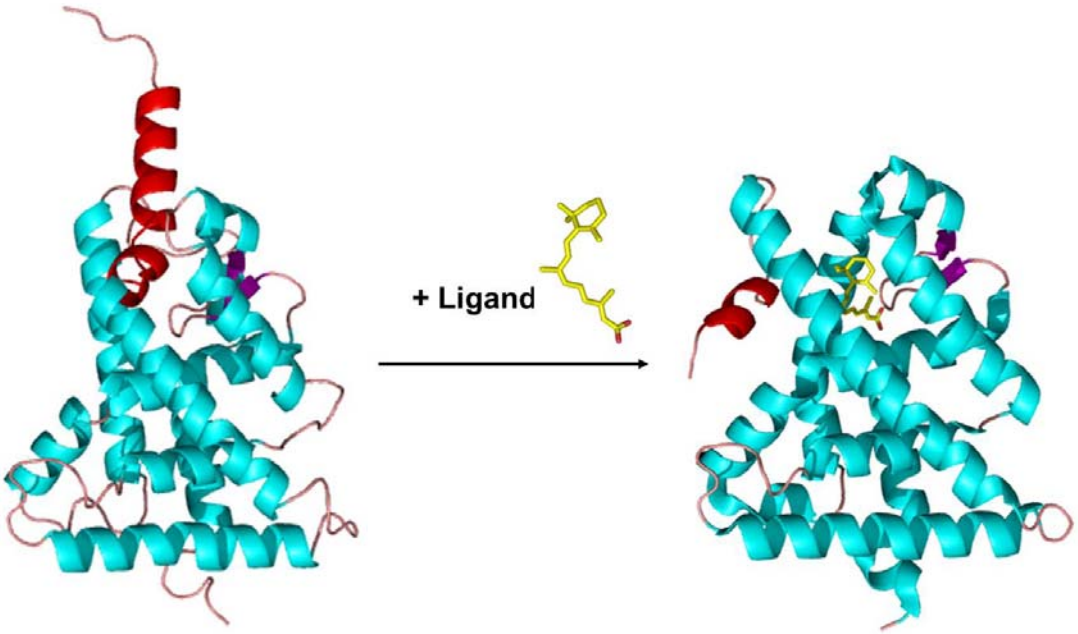

Figure 1.6: *Apo* vs. *Holo* Nuclear Receptor Ligand Binding Domains (Human RXR-α) Ligand Binding Domain (Cyan), AF-2 Domain (Red), 9-cis Retinoic Acid (Yellow), PDBs:1LBD and 1FBY

release of corepressor complexes and the recruitment of coactivator complexes [5, 6, 11, 19, 28, 34, 35]. Coactivator proteins, such as the steroid receptor coactivator-1 (SRC-1), also contain a box region where interactions with NRs occur. An LXXLL motif within this box binds a hydrophobic surface commonly formed by helices 3, 4 and 12 of NR LBDs [8, 11, 13, 14, 19, 42]. Coactivators form protein complexes containing histone acetyltransferases (HATs). These enzymes modify the chromatin structure over target promoter regions by acetylating lysine residues on the histones, weakening the interactions between the histones and DNA. This process facilitates the recruitment of general transcription machinery including RNA polymerase, resulting in gene activation (Figure 1.5b) [11, 12, 21].

1.4 Nuclear Receptors: Drug Discovery and Protein Engineering Targets

As previously mentioned, due to the significant role NRs play in biological processes and their involvement in a variety of serious diseases; NRs are an important target for drug discovery. Owing to the LBD's multiple functionality (e.g. involvement in receptor dimerization, ligand recognition, and coregulator interactions) and ability to bind a broad range of 'drug-like' small molecules, the LBD has been the NR domain predominantly focused on during pharmaceutical development efforts [5, 11, 12, 14, 19, 29]. Two examples of current commonly prescribed NR-targeting drugs include rosiglitazone and tamoxifen (Figure 1.7) [5, 8, 11, 13, 14, 19, 21]. Rosiglitazone targets PPARγ and is used to treat type II diabetes, while tamoxifen targets ER and is used to treat breast cancer. The identification of NR-targeting compounds can be performed using several approaches, including crystallographic methods, library screens, and synthetic chemistry [13, 14, 21, 43].

Crystallographic methods provide a three-dimensional analysis and visualization of the structures of these receptors, identifying important residues involved in receptor-

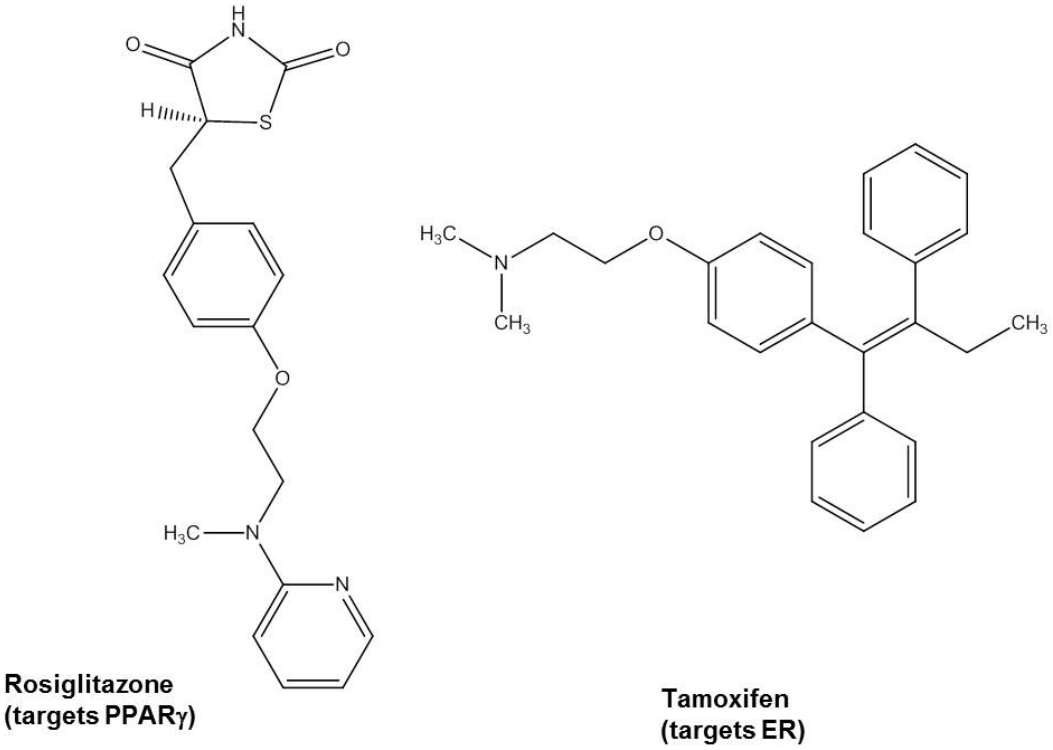

Figure 1.7: Nuclear Receptor-Targeting Drugs

ligand interactions and providing insight on the nature of these proteins in vivo. This information can then be used for designing or identifying small molecules for binding and/or activation. Library screens involve exposing libraries of the target NR to a variety of compounds and assessing their activity, using *in vivo* or *in vitro* assays (e.g. binding assays and transcription assays). Recently, *in-silico* library screens have become a widely used strategy for this approach, involving computational docking of a variety of small molecules into the target NR. The docked receptor-ligand complexes are then evaluated based on chemical interactions. Besides being time efficient, this strategy is also advantageous in that different NR conformations (e.g. *apo* vs. *holo* forms, repositioning of the AF-2 domain), as well as interactions between NRs and other proteins (e.g. coactivator and corepressor proteins) can be explored [21]. Lastly, synthetic chemistry, an approach that can be combined with other methods, involves the design and synthesis of novel small molecules, or derivatives of previously identified compounds using structure-function information. Efforts on identifying new drugs, as well as improving current therapeutic drugs strongly continue to push forward. However, the overall challenge continues to lie in overcoming undesired pharmacological effects due to NR involvement in complex and overlapping pathways [8, 11, 13, 14].

In addition to being important targets for drug discovery, NRs are also attractive candidates for protein engineering. Although most NRs have the same overall structure, the diversity of NRs is partly due to the differences in their ligand binding pockets, thus their ability to bind a large array of small molecules. This makes NRs attractive candidates for protein engineering, such that these receptors can be engineered to bind novel small molecule ligands for several applications. One application is the creation of potential molecular switches, tools that can be used for controlling gene expression [44, 45].

1.5 Literature Cited

1. Mangelsdorf, D.J., C. Thummel, M. Beato, P. Herrlich, G. Schutz, K. Umesono, B. Blumberg, P. Kastner, M. Mark, P. Chambon, and R.M. Evans, *The nuclear receptor superfamily-the 2nd decade.* Cell, 1995. **83**(6): p. 835-839.

2. Enmark, E. and J.A. Gustafsson, *Comparing nuclear receptors in worms, flies and humans.* Trends Pharmacol. Sci., 2001. **22**(12): p. 611-615.

3. Sluder, A.E. and C.V. Maina, *Nuclear receptors in nematodes: themes and variations.* Trends Genet., 2001. **17**(4): p. 206-213.

4. Enmark, E. and J.A. Gustafsson, *Nematode genome sequence dramatically extends the nuclear receptor superfamily.* Trends Pharmacol. Sci., 2000. **21**(3): p. 85-87.

5. Sonoda, J., L.M. Pei, and R.M. Evans, *Nuclear receptors: Decoding metabolic disease.* FEBS Lett., 2008. **582**(1): p. 2-9.

6. Nagy, L. and J.W.R. Schwabe, *Mechanism of the nuclear receptor molecular switch.* Trends Biochem. Sci., 2004. **29**(6): p. 317-324.

7. Laudet, V. and H. Gronemeyer, *The Nuclear Receptor FactsBook.* London: Academic Press, 2002.

8. Gronemeyer, H., J.A. Gustafsson, and V. Laudet, *Principles for modulation of the nuclear receptor superfamily.* Nat. Rev. Drug Discov., 2004. **3**(11): p. 950-964.

9. Chambon, P., *The nuclear receptor superfamily: A personal retrospect on the first two decades.* Mol. Endocrinol., 2005. **19**(6): p. 1418-1428.

10. Evans, R.M., *The nuclear receptor superfamily: A Rosetta Stone for physiology.* Mol. Endocrinol., 2005. **19**(6): p. 1429-1438.

11. Germain, P., B. Staels, C. Dacquet, M. Spedding, and V. Laudet, *Overview of nomenclature of nuclear receptors.* Pharmacol. Rev., 2006. **58**(4): p. 685-704.

12. Noy, N., *Ligand specificity of nuclear hormone receptors: Sifting through promiscuity.* Biochemistry, 2007. **46**(47): p. 13461-13467.

13. Moore, J.T., J.L. Collins, and K.H. Pearce, *The nuclear receptor superfamily and drug discovery.* ChemMedChem, 2006. **1**(5): p. 504-523.

14. Huang, P.X., V. Chandra, and F. Rastinejad, *Structural overview of the nuclear receptor superfamily: Insights into physiology and therapeutics.* Annu. Rev. Physiol., 2010. **72**: p. 247-272.

15. Hollenberg, S.M., C. Weinberger, E.S. Ong, G. Cerelli, A. Oro, R. Lebo, E.B. Thompson, M.G. Rosenfeld, and R.M. Evans, *Primary structure and expression of a functional human glucocorticoid receptor cDNA.* Nature, 1985. **318**(6047): p. 635-641.

16. Green, S., P. Walter, V. Kumar, A. Krust, J.M. Bornert, P. Argos, and P. Chambon, *Human estrogen-receptor cDNA - sequence, expression and homology to v-erb-A.* Nature, 1986. **320**(6058): p. 134-139.

17. Greene, G.L., P. Gilna, M. Waterfield, A. Baker, Y. Hort, and J. Shine, *Sequence and expression of human estrogen-receptor complementary DNA.* Science, 1986. **231**(4742): p. 1150-1154.

18. Robinson-Rechavi, M., A.S. Carpentier, M. Duffraisse, and V. Laudet, *How many nuclear hormone receptors are there in the human genome?* Trends Genet., 2001. **17**(10): p. 554-556.

19. Greschik, I. and D. Moras, *Structure-activity relationship of nuclear receptor-ligand interactions.* Curr. Top. Med. Chem., 2003. **3**(14): p. 1573-1599.

20. Lonard, D.M. and B.W. O'Malley, *Nuclear receptor coregulators: Judges, juries, and executioners of cellular regulation.* Molecular Cell, 2007. **27**(5): p. 691-700.

21. Mukherjee, S. and S. Mani, *Orphan nuclear receptors as targets for drug development.* Pharm. Res., 2010. **27**(8): p. 1439-1468.

22. Wrange, O. and J.A. Gustafsson, *Separation of the hormone-binding and DNA-binding sites of the hepatic glucocorticoid receptor by means of proteolysis.* J. Biol. Chem., 1978. **253**(3): p. 856-865.

23. Ottow, E. and H. Weinmann, *Nuclear Receptors as Drug Targets*. 2008: Weinheim: Wiley-VCH Verlog Gmblt & Co. KGaA.

24. Umesono, K., K.K. Murakami, C.C. Thompson, and R.M. Evans, *Direct repeats as selective response elements for the thyroid-hormone, retinoic acid, and vitamin-D3 receptors.* Cell, 1991. **65**(7): p. 1255-1266.

25. Naar, A.M., J.M. Boutin, S.M. Lipkin, V.C. Yu, J.M. Holloway, C.K. Glass, and M.G. Rosenfeld, *The orientation and spacing of core DNA-binding motifs dictate selective transcriptional responses to 3 nuclear receptors.* Cell, 1991. **65**(7): p. 1267-1279.

26. Wurtz, J.M., W. Bourguet, J.P. Renaud, V. Vivat, P. Chambon, D. Moras, and H. Gronemeyer, *A canonical structure for the ligand-binding domain of nuclear receptors.* Nat. Struct. Biol., 1996. **3**(1): p. 87-94.

27. Bourguet, W., M. Ruff, P. Chambon, H. Gronemeyer, and D. Moras, *Crystal structure of the ligand-binding domain of the human nuclear receptor RXR-alpha.* Nature, 1995. **375**(6530): p. 377-382.

28. Li, Y., M.H. Lambert, and H.E. Xu, *Activation of nuclear receptors: A perspective from structural genomics.* Structure, 2003. **11**(7): p. 741-746.

29. Moras, D. and H. Gronemeyer, *The nuclear receptor ligand-binding domain: structure and function.* Curr. Opin. Cell Biol., 1998. **10**(3): p. 384-391.

30. Bourguet, W., P. Germain, and H. Gronemeyer, *Nuclear receptor ligand-binding domains: three-dimensional structures, molecular interactions and pharmacological implications.* Trends Pharmacol. Sci., 2000. **21**(10): p. 381-388.

31. O'Malley, B.W., J. Qin, and R.B. Lanz, *Cracking the coregulator codes.* Curr. Opin. Cell Biol., 2008. **20**(3): p. 310-315.

32. Wolf, I.M., M.D. Heitzer, M. Grubisha, and D.B. DeFranco, *Coactivators and nuclear receptor transactivation.* J. Cell. Biochem., 2008. **104**(5): p. 1580-1586.

33. McKenna, N.J., R.B. Lanz, and B.W. O'Malley, *Nuclear receptor coregulators: Cellular and molecular biology.* Endocr. Rev., 1999. **20**(3): p. 321-344.

34. McKenna, N.J., J.M. Xu, Z. Nawaz, S.Y. Tsai, M.J. Tsai, and B.W. O'Malley, *Nuclear receptor coactivators: multiple enzymes, multiple complexes, multiple functions.* J. Steroid Biochem. Mol. Biol., 1999. **69**(1-6): p. 3-12.

35. McKenna, N.J. and B.W. O'Malley, *Minireview: Nuclear receptor coactivators - An update.* Endocrinology, 2002. **143**(7): p. 2461-2465.

36. O'Malley, B., *The year in basic science: Nuclear receptors and coregulators.* Mol. Endocrinol., 2008. **22**(12): p. 2751-2758.

37. Chandra, V., P.X. Huang, Y. Hamuro, S. Raghuram, Y.J. Wang, T.P. Burris, and F. Rastinejad, *Structure of the intact PPAR-gamma-RXR-alpha nuclear receptor complex on DNA.* Nature, 2008. **456**(7220): p. 350-356.

38. Brelivet, Y., S. Kammerer, N. Rochel, O. Poch, and D. Moras, *Signature of the oligomeric behaviour of nuclear receptors at the sequence and structural level.* EMBO reports, 2004. **5**(4): p. 423-429.

39. Shulman, A.I., C. Larson, D.J. Mangelsdorf, and R. Ranganathan, *Structural determinants of allosteric ligand activation in RXR heterodimers.* Cell, 2004. **116**(3): p. 417-429.

40. Shulman, A.I. and D.J. Mangelsdorf, *Mechanisms of disease: Retinoid X receptor heterodimers in the metabolic syndrome.* N. Engl. J. Med., 2005. **353**(6): p. 604-615.

41. Hu, X. and M.A. Lazar, *The CoRNR motif controls the recruitment of corepressors by nuclear hormone receptors.* Nature, 1999. **402**(6757): p. 93-96.

42. Heery, D.M., E. Kalkhoven, S. Hoare, and M.G. Parker, *A signature motif in transcriptional co-activators mediates binding to nuclear receptor.* Nature, 1997. **387**(6634): p. 733-736.

43. Gillies, A.R., G. Skretas, and D.W. Wood, *Engineered systems for detection and discovery of nuclear hormone-like compounds.* Biotechnol. Prog., 2008. **24**: p. 8-16.

44. Schwimmer, L.J., P. Rohatgi, B. Azizi, K.L. Seley, and D.F. Doyle, *Creation and discovery of ligand-receptor pairs for transcriptional control with small molecules.* Proc. Natl. Acad. Sci. U. S. A., 2004. **101**(41): p. 14707-14712.

45. Taylor, J.L., P. Rohatgi, H.T. Spencer, D.F. Doyle, and B. Azizi, *Characterization of a molecular switch system that regulates gene expression in mammalian cells through a small molecule.* BMC Biotechnol., 2010. **10**: p. 15.

CHAPTER 2

THE HUMAN VITAMIN D RECEPTOR (hVDR)

2.1 The hVDR: Structure and Function

The human vitamin D receptor (hVDR) is a member of the endocrine receptor class of the nuclear receptor (NR) superfamily [1-4]. This receptor was cloned from human intestine in 1988, with the natural ligand identified as 1α, 25-dihydroxyvitamin D_3 (1α, 25$(OH)_2D_3$) (Figure 2.1) [5, 6]. The hVDR plays a major role in maintaining calcium and phosphate homeostasis, as well as regulating bone metabolism [5, 7-14]. Furthermore, this receptor is involved in anti-proliferative, pro-apoptotic and immunosuppressive activities in human and mouse cells [7, 13, 15-19].

To date, eleven other VDR orthologs, the equivalent receptor in a different organism, have been reported in species such as the mouse, rat, and zebrafish [20]. Additionally, most NRs can exist as isotypes (e.g. α, β, γ) and isoforms (e.g. α1, α2), which are products of post-translational modifications [21]. However, the VDR is the only one of its kind in these organisms where no known isotypes or isoforms exist to date. The hVDR mainly functions in the small intestine, kidney and bone, heterodimerizing with the retinoid X receptor (RXR) as a non-permissive partner (not activated by RXR agonists) and binding 1α, 25$(OH)_2D_3$ [9-11, 22-30]. Liganded hVDR then associates with coactivators of the p160 class including the steroid receptor coactivator-1 (SRC-1), resulting in the transcription of target genes [31-33].

The hVDR is comprised of 427 amino acids, containing a very short N-terminal domain with no ligand independent activation function domain (AF-1) [22, 26, 34, 35]. The receptor's DNA binding domain (DBD) consists of ~65-amino acids and binds response elements (REs) that consist of two directly repeated half-sites of the

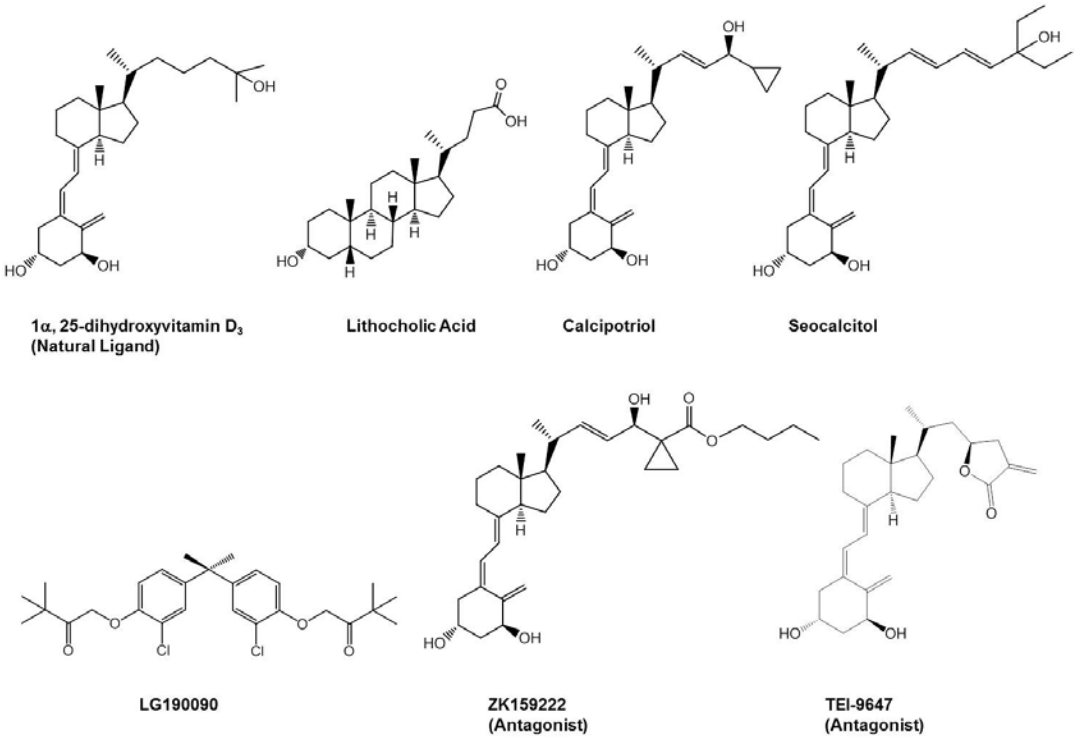

Figure 2.1: hVDR Ligands

consensus sequence RGKTCA (R=Adenine or Guanine, K=Guanine or Thymine) separated by three nucleotides (DR-3), in promoter regions of target genes [4, 11, 22, 26, 36]. Numerous VDR REs have been identified, such as those of osteocalcin and osteopontin, two proteins involved in bone remodeling [22, 37-39]. The hVDR ligand binding domain (LBD) consists of 303 amino acids and forms the canonical 'α-helical sandwich', with 13 α-helices and a three-stranded β-sheet [3, 4, 35, 40, 41].

The first solved VDR crystal structure was that of the hVDR LBD bound to 1α, 25$(OH)_2D_3$ in 2000 [35]. This structure however, lacks a disordered region of 50-amino acids (residues 165-215) between helices 1 and 3 that was removed to facilitate crystallization [5, 35]. As previously mentioned, the receptor's LBD forms the canonical 'α-helical sandwich' but the ligand binding pocket (LBP) is 697 $Å^3$, significantly larger than that of other endocrine receptors (e.g. estrogen receptor (ER) 369 $Å^3$ and progesterone receptor (PR) 422 $Å^3$) and the ligand only occupies 56% of this volume (Figure 2.2a) [5, 35, 42]. The elongated LBP is lined with 36 amino acid residues (34 non-alanine residues), which are mostly hydrophobic [35, 43, 44]. 1α, 25$(OH)_2D_3$'s conformation is such that the A-ring of the structure is positioned towards helices 3 and 5, while the aliphatic chain is positioned towards helices 7 and 10/11 [35].

Interactions between the receptor and 1α, 25 $(OH)_2D_3$ involve both hydrophobic and electrostatic interactions, with residues Y143, S237, R274, S278, H305 and H397 forming important hydrogen bonds (Figure 2.3) [5, 35]. In looking at specific interactions between the ligand and the receptor, when bound to 1α, 25$(OH)_2D_3$, the hVDR's ligand dependent activation function domain (AF-2) is found in the active conformation (Figure 2.2b) [35]. Residues V418 and F422 in helix 12 make Van der Waals contacts with the methyl group of the ligand. The position of this helix overall, is stabilized by hydrophobic contacts and polar interactions (Table 2.1) [35, 42].

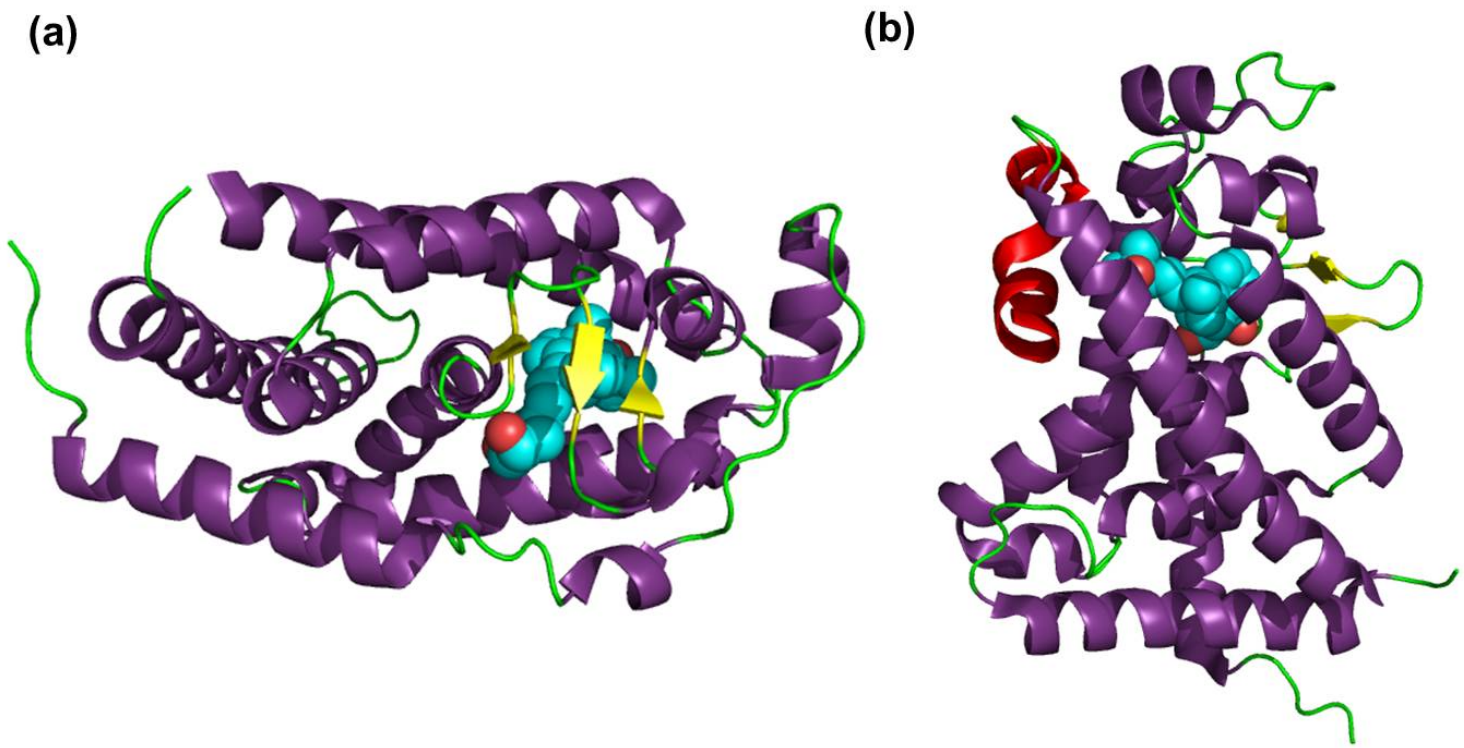

Figure 2.2: The hVDR Ligand Binding Domain Ligand Binding Domain (Purple), 1α, 25$(OH)_2D_3$(Cyan), AF-2 Domain (Red), PDB: 1DB1

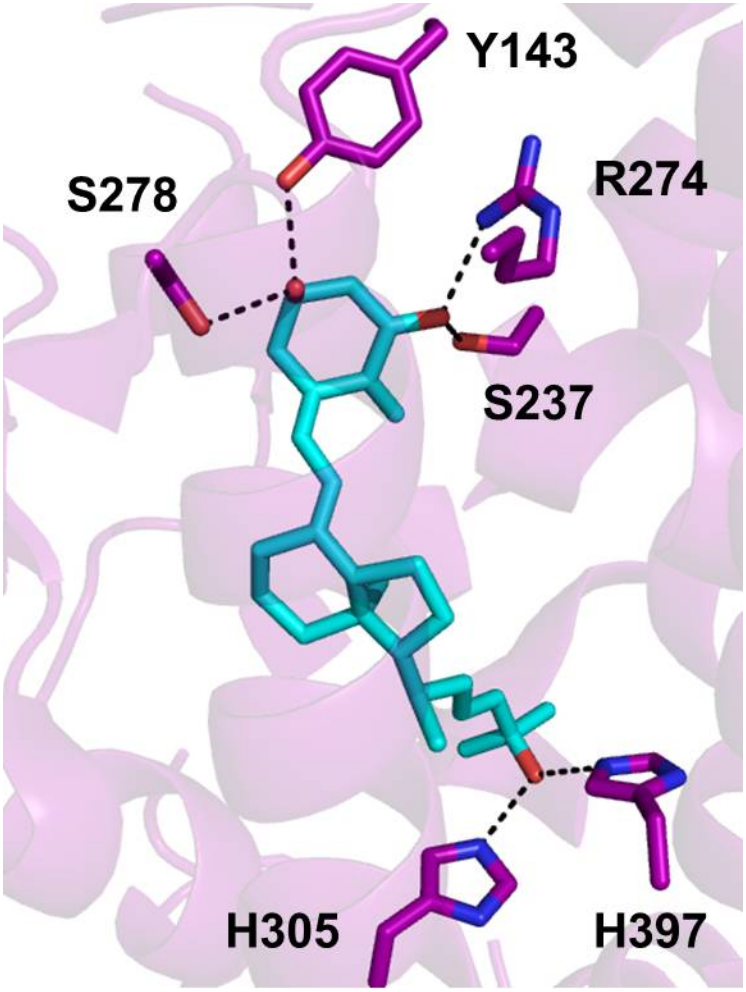

Figure 2.3: Important Hydrogen Bonds between the hVDR and 1α, 25(OH)$_2$D$_3$ hVDR Residues (Purple), 1α, 25(OH)$_2$D$_3$ (Cyan), PDB:1DB1

Table 2.1: Contacts and Interactions Between the hVDR and 1α, 25(OH)$_2$D$_3$, and within the hVDR that Stabilize Helix 12 [35]

Hydrogen Bonds with 1α,25(OH)$_2$D$_3$	Van der Waals Contacts with 1α, 25(OH)$_2$D$_3$	Hydrophobic Contacts	Other Polar Interactions	Other Direct Contacts with 1α, 25(OH)$_2$D$_3$
Y143	V418	T415		V234
S237	F422	L417	**Salt-Bridge**	I268
R274		V418	K264-E420	H397
S278		L419		Y401
H305		V421	**Hydrogen Bond**	
H397		F422	S235-T415	
		D232		
		V234		
		S235		
		I238		
		Q239		
		A267		
		I268		
		H397		
		Y401		

Unlike other ligands which stabilize helix 12 through direct interactions, the hVDR's ligand induced effect on helix 12 with 1α, 25$(OH)_2D_3$ takes place through a 'pi-cation activation switch' conserved among several NRs [45, 46]. This switch involves an electrostatic interaction between H397 in helix 11 and F422 in helix 12. The oxygen group on the aliphatic chain of 1α, 25 $(OH)_2D_3$ directly interacts with H397 but not F422. However, the interaction between these two residues helps stabilize helix 12 in the active conformation [35, 45]. This interaction optimizes the distance between residues K264 in helix 4 and E420 in helix 12, which form a 'charge-clamp' involved in coactivator binding surfaces (Figure 2.4) [4, 47-49].

The hVDR also binds bile acids such as lithocholic acid (LCA), which is produced in the liver, excreted in the bile and partially reabsorbed by the intestines (Figure 2.1). This acid is a carcinogenic compound implicated with the progression of colon cancer [28, 50-52]. Binding to bile acids has been shown to induce activity of enzymes involved in cellular clearance of xenobiotic and endobiotic compounds (e.g. cytochrome P450 genes), which led to the hypothesis of the hVDR's involvement in preventing carcinogenic effects [5, 28, 50, 53-55].

No crystal structure of the hVDR bound to LCA is currently available, however given the structural differences between LCA and 1α, 25$(OH)_2D_3$ different receptor-ligand interactions are involved. For example, LCA lacks the 1α-hydroxyl group on the A-ring and therefore cannot form the hydrogen bond that 1α, 25$(OH)_2D_3$ forms with S237 [28, 35, 50, 52]. Several hypotheses indicate that LCA binding results in a compromised positioning of helix 10 which is involved in dimerization interactions between the hVDR and RXR, and helices 3 and 12 which are involved in coactivator interactions [28]. These differences must account for a certain degree of the lower sensitivity of LCA (EC_{50}= 12.1 μM) for the hVDR, compared to that of 1α, 25$(OH)_2D_3$ (EC_{50}= 2-5 nM)

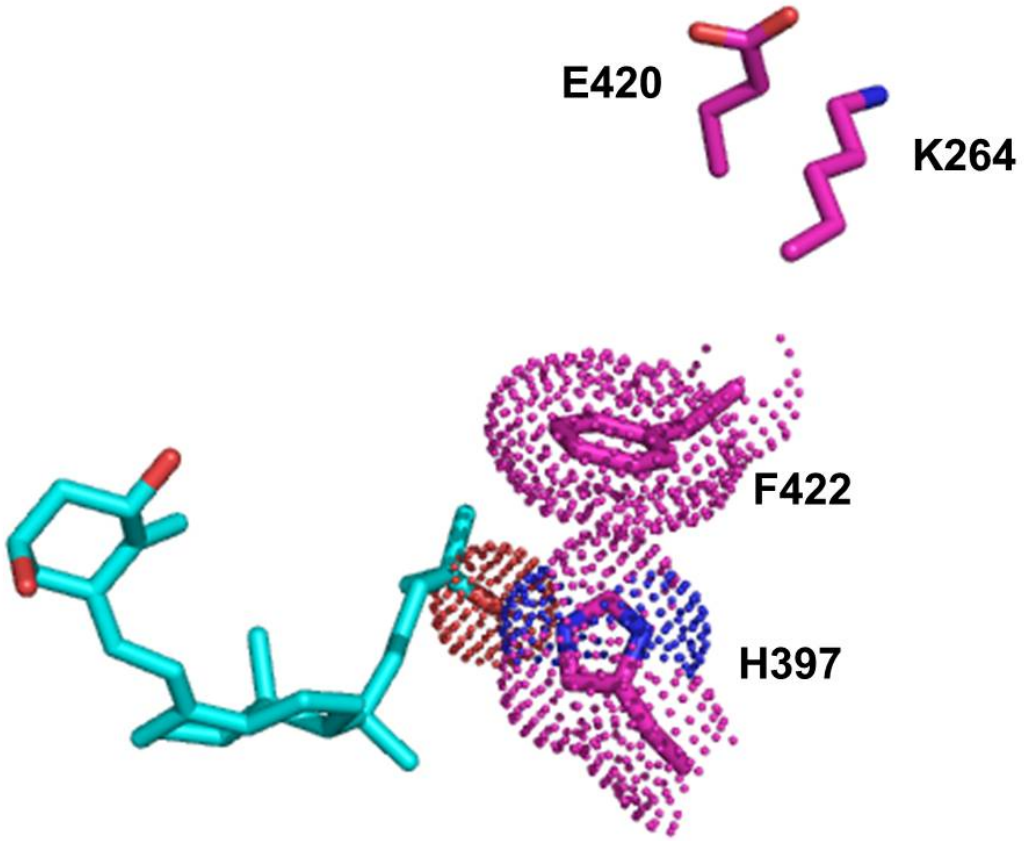

Figure 2.4: The hVDR 'Pi-Cation Activation Switch' and 'Charge Clamp'
hVDR Residues (Purple), 1α, 25-dihydroxyvitamin D_3 (Cyan), PDB:1DB1

[28, 35, 50, 52, 55-60]. Despite differences in receptor-ligand interactions, LCA and 1α, 25$(OH)_2D_3$ may share a similar conformation in the hVDR LBP, as the 3-hydroxyl group on the A-ring of both molecules forms a hydrogen bond with residues Y143 and S278 [28]. Additionally, the functional group on the aliphatic chain of both molecules forms a hydrogen bond with residue H305 [28].

2.2 The hVDR: A Drug Discovery Target

Mutations in the hVDR lead to insufficient ligand activation, thus resulting in an imbalance of physiological levels of 1α, 25$(OH)_2D_3$ and Rickets [5, 35, 61-68]. Rickets is a disease associated with muscle weakness, growth retardation and bone deformity [5, 35, 61-68]. Due to the hVDR's negative-feedback mechanism, certain types of rickets and other related conditions including osteoporosis and psoriasis, can be clinically treated with 1α, 25$(OH)_2D_3$ [5, 13, 59, 69, 70]. However, undesirable calcemic effects that result in hypercalcemia, increased bone resorption, and soft tissue calcification limit the use of pharmacological doses. This has lead to the development of 1α, 25$(OH)_2D_3$ analogs with reduced side effects [5, 7, 13, 35, 52, 71].

To create analogs of 1α, 25$(OH)_2D_3$ without severe side effects, the aliphatic chain of 1α, 25$(OH)_2D_3$ has been the main target of chemical modifications, as the A-D rings have not been successfully changed without loss of ligand activation [35]. Two known examples are calcipotriol and seocalcitol (Figure 2.1). Calcipotriol is used for topical treatment of psoriasis, while seocalcitol underwent clinical studies for cancer treatment [72-77]. Non-secosteroidal mimics such as derivatives of LG190090, have also been developed for potential treatment of cancer, leukemia and psoriasis (Figure 2.1) [60]. More than 3,000 1α, 25$(OH)_2D_3$ analogs have been developed, with few advancing past clinical trials [42, 44, 49, 57, 59, 69, 78-81].

Although agonists have been the focus of hVDR targeted drugs, a few antagonists have also been developed. As previously mentioned, antagonists are small compounds that bind but do not activate a receptor due to improper conformational changes and NR-corepressor interactions, resulting in transcriptional repression of target genes [82]. hVDR antagonists are of interest because of their ability to treat conditions such as Paget's disease, which is associated with excessive breakdown and formation of bone tissue, and as a result bone pain, deformities and fractures [83]. hVDR antagonists have been reported to reduce excessive bone resorption, as well as the formation of cells involved in bone resorption [84, 85]. Two examples of hVDR antagonists are ZK159222 and TEI-9647, and compared to 1α, $25(OH)_2D_3$ (agonist), these compounds have bulky ring structures on their side chains, inhibiting optimal interaction between the positioning of helix 12 and the rest of the receptor (Figure 2.1) [42, 86-88]. ZK159222 is a potent antagonist, binding hVDR with an affinity comparable to that of 1α, $25(OH)_2D_3$, while TEI-9647 is a weaker antagonist [42, 88].

2.3 The hVDR: A Protein Engineering Target

As previously mentioned NRs play essential roles in biological functions and are involved in a variety of diseases. These traits make NRs great targets for drug discovery, specifically discovery of 'drug-like' small molecules that bind the receptor's LBD. The specificity of NR ligand-binding depends on the shape and volume of the LBP within the LBD, the amino acid residues that are in proximity to the ligand and form direct interactions, as well as distant residues that may have indirect structural effects [89]. In addition to being important targets for drug discovery, NRs are also attractive targets for protein engineering. Although most NRs have the same overall structure, they can significantly differ in LBP volumes and can therefore bind a wide array of small

molecules (Figure 2.5) [7, 58]. For example, RXR binds retinoids containing a cyclic end group, a polyene side chain and a polar end group. ER binds estrogens which are steroids consisting of four cyclic rings fused to each other. The pregnane X receptor (PXR), which binds the large macrolide rifampicin, is known as a promiscuous receptor that binds a variety of ligands. This diversity of ligands for NRs, makes NRs attractive candidates for protein engineering, such that these receptors can be engineered to bind novel small molecules for several applications. One application is the creation of molecular switches, tools that can be used for controlling gene expression [90, 91].

The focus of this work has been to investigate the human vitamin D receptor (hVDR), specifically structural and functional relationships between the receptor and its ligands. Throughout this process, the role and mutational tolerance of specific residues within the ligand binding domain of the hVDR were investigated. The hVDR variants engineered by methods of rational and random mutagenesis were tested using chemical complementation [90, 92].

2.4 Chemical Complementation: A Genetic Selection System in Yeast

A genetic selection system like chemical complementation, where the interaction between a protein and a small molecule is evaluated, serves as a powerful tool for protein engineering and drug discovery applications [21, 90-93]. Chemical complementation (CC) is a genetic selection system in which the survival of yeast, *Saccharomyces cerevisiae*, is linked to the binding and activation of a NR by an agonist, as the activation of the NR results in the transcription of an essential gene [90-92]. Yeast is a suitable organism for studying NR-ligand interactions, as they naturally do not have NRs, limiting NR interference in the assay. Additionally, their transcription machinery is similar to mammalian transcriptional machinery, allowing proper expression and functioning of NRs [21, 92].

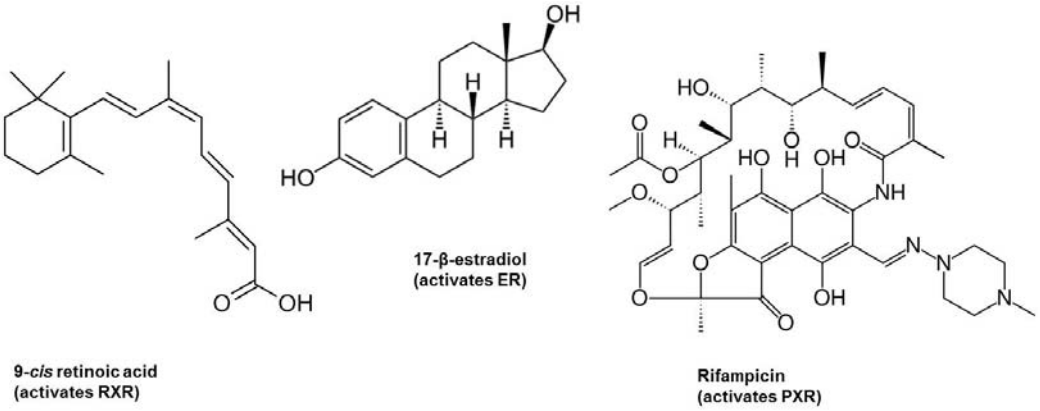

Figure 2.5: Ligands of Various Nuclear Receptors

CC was developed using the PJ69-4A yeast strain, a yeast two-hybrid strain with the expression of genetic selection genes, *HIS*3 and *ADE*2, and a screening gene, *lac*Z, under the control of Gal4 REs [94]. Gal4 is a ligand-independent transcription factor naturally found in yeast [95]. As a modular protein, Gal4 contains a DBD that binds Gal4 REs, and an activation domain (AD) that interacts with transcriptional machinery.

In CC, the Gal4 DBD is fused to a NR LBD, the Gal4 AD is fused to a human coactivator, and a small molecule ligand is introduced (Figure 2.6) [90, 92]. In this system, the Gal4 DBD:NR LBD fusion protein binds Gal4 REs and an agonist binds the NR LBD inducing a conformational change that leads to the recruitment of the corresponding Gal4 AD:coactivator fusion protein and the transcriptional machinery. Hence there is expression of a selective gene; the *HIS3* or *ADE2* gene, essential genes in the corresponding histidine or adenine biosynthetic pathway. Transcription of *HIS3 or ADE2* allows the PJ69-4A yeast strain to produce histidine or adenine and survive on media lacking that nutrient. Therefore, only ligand activated NRs will result in the survival of yeast. Overall, CC provides simple and rapid detection of NR activation, making this selection system useful for semi high-throughput screening [21].

2.5 Characterization of the hVDR in Chemical Complementation

In order to use the hVDR and test the functionality of this receptor in chemical complementation, the hVDR gene was isolated and amplified from skin cDNA using polymerase chain reaction (PCR) and cloned into a yeast expression plasmid. The resulting construct, pGBDhVDR, contained the Gal4 DBD fused to the full length hVDR and a tryptophan marker. This construct along with another yeast expression plasmid, pGAD10BASRC-1, containing the Gal4 AD fused to the SRC-1 coactivator and a leucine marker were co-transformed into the PJ69-4A yeast strain (Figure 2.7). As a positive control, the yeast expression plasmid pGBT9Gal4, containing the *holo* Gal4 gene and a

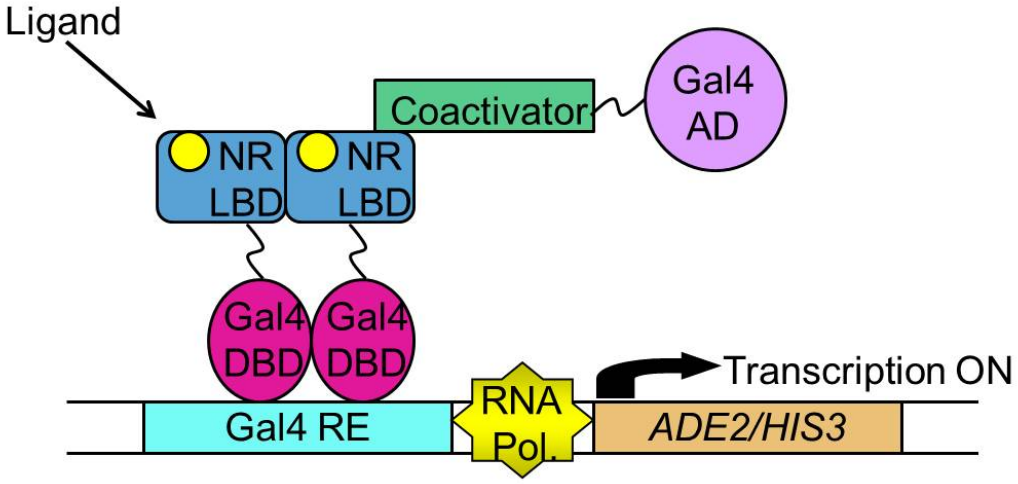

Figure 2.6: Chemical Complementation
A genetic selection system in which the survival of yeast is linked to the binding and activation of a nuclear receptor by an agonist.

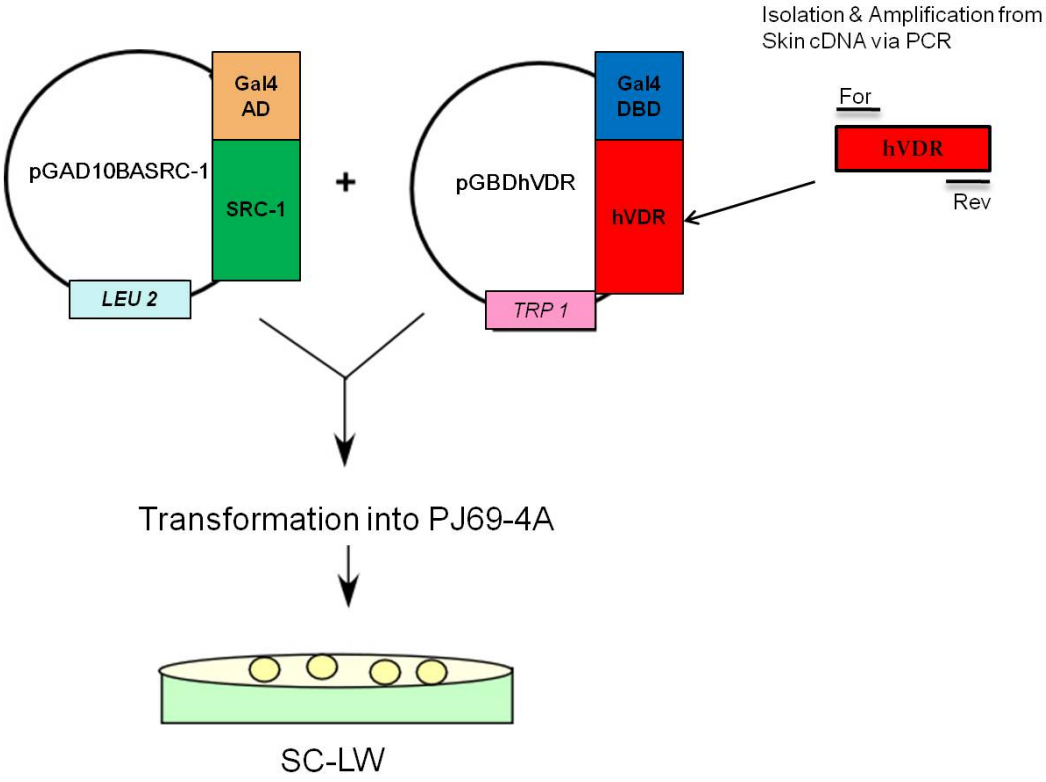

Figure 2.7: Cloning the hVDR from cDNA and Co-transformation into the PJ69-4A Yeast Strain

tryptophan marker was also co-transformed with pGAD10BASRC-1 into the PJ69-4A strain. The resulting transformants were then tested in chemical complementation using a liquid based assay.

Liquid quantitation assays of chemical complementation are performed in 96-well plates, where yeast cells containing the fusion proteins (Gal4 DBD:NR LBD and Gal4 AD:coactivator) of interest are added to wells with and without ligand (Figure 2.8). As previously mentioned, the PJ69-4A yeast strain uses the *HIS3* or *ADE2* gene, essential genes in the corresponding histidine or adenine biosynthetic pathway. As a result, all wells contain selective media lacking an essential nutrient, either synthetic complete media lacking histidine, leucine and tryptophan (SC-HLW) or synthetic complete media lacking adenine, leucine and tryptophan (SC-ALW). Plates are then incubated at 30 ºC with shaking, and optical density readings at a wavelength of 630 nm (OD630) are taken at 0, 24 and 48 hours. Wells with yeast growth are an indication of the small molecule ligand binding and activating the NR, turning on the transcription of the selective gene and consequently yeast survival (ligand activated growth).

The hVDR was first tested in adenine selective media (SC-ALW) with varying concentrations of ligand. Due to the expense of the hVDR's natural ligand, 1α, 25$(OH)_2D_3$, LCA was used to collect this set of data. No ligand activated growth was observed for the hVDR in adenine selective media with LCA, as shown in Figure 2.9 where no curve is observed. Gal4 is a ligand independent transcription factor and is used as a positive control. As expected, Gal4 grew with and without ligand at an optical density of ~0.5 (Figure 2.9).

The *HIS3* gene which encodes imidazoleglycerol-phosphate dehydratase, an essential enzyme in the histidine biosynthetic pathway, is known as a 'leaky gene' with some basal activity [96]. As a result, 3-amino-1, 2, 4-triazole (3-AT), an inhibitor of imidazoleglycerol-phosphate dehydratase, is used to reduce basal growth (Figure 2.8).

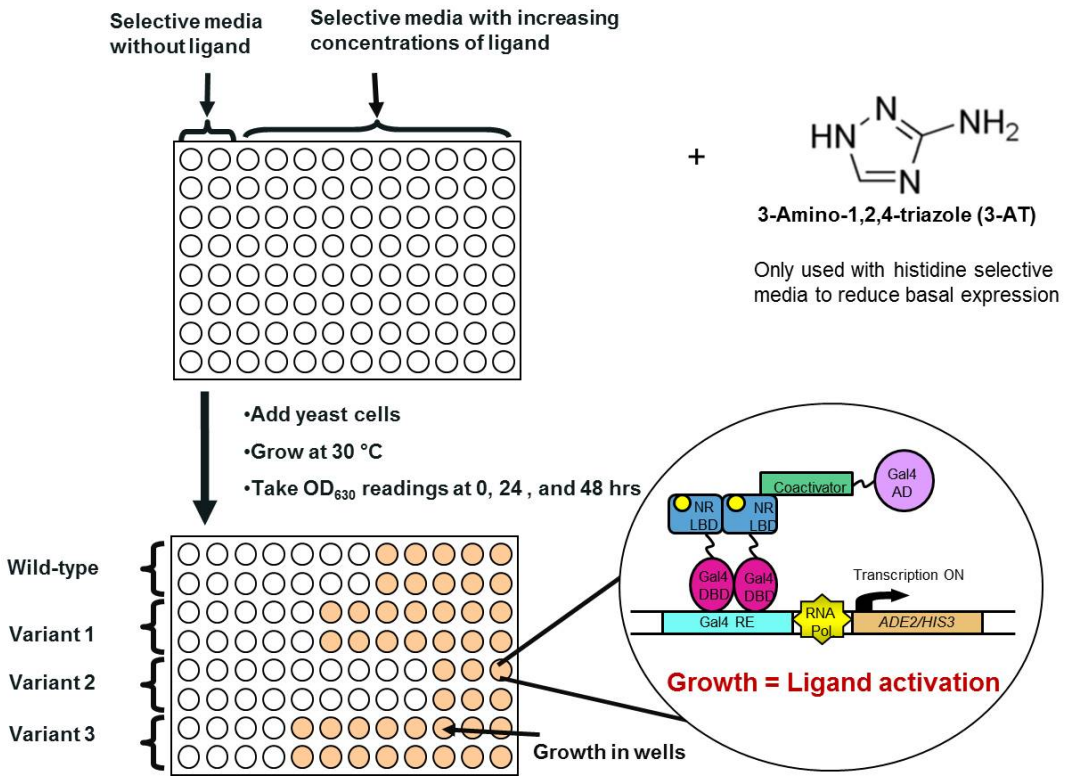

Figure 2.8: Liquid Quantitation Assay of Chemical Complementation

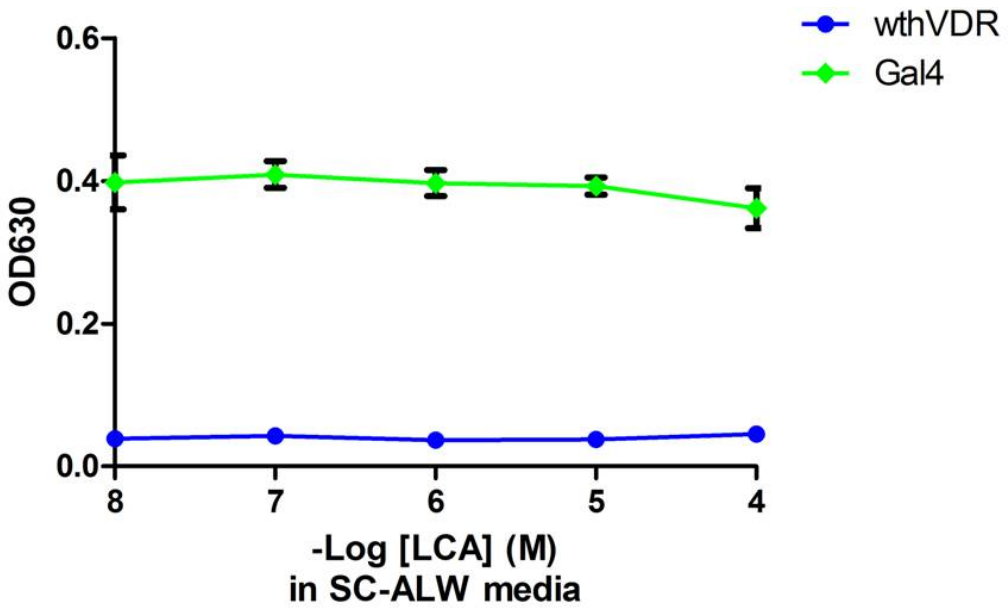

Figure 2.9: The wthVDR in Chemical Complementation
Adenine selective media with LCA

To determine the concentration of 3-AT necessary to reduce the *HIS3* basal expression with the hVDR, the receptor was tested in liquid quantitation assays of chemical complementation in histidine selective media (SC-HLW) with varying concentrations of 3-AT, with and without ligand. Again, due to the expense of 1α, 25$(OH)_2D_3$, LCA (100 μM) was used to collect this set of data. Based on the 3-AT dose response curve without ligand, we determined that an optical density of ~0.145 is the basal growth associated with the hVDR in histidine selective media. This growth was reduced to ~0.093 upon the addition of 0.1 mM 3-AT. Higher concentrations of 3-AT did not reduce the basal growth further (Figure 2.10a). Ligand activated growth above basal was observed for the hVDR in histidine selective media with 0.1 mM 3-AT and 100 μM LCA, with a two-fold activation (Figure 2.10b). As a result, 0.1 mM 3-AT should be used when testing the hVDR in histidine selective media, as this concentration of 3-AT reduced the basal expression associated with the receptor without eliminating ligand activated growth.

The hVDR was then tested in liquid quantitation assays of chemical complementation in histidine selective media with 0.1 mM 3-AT and varying concentrations of 1α, 25$(OH)_2D_3$, lithocholic acid, and various analogs of the two ligands (Figure 2.11). Ligand activated growth was observed with 1α, 25$(OH)_2D_3$, calcipotriol, calcifediol, lithocholic acid and lithocholic acid acetate with four-, five-, five-, three- and four-fold activations, respectively. Besides good fold activations, most ligands resulted in an optical density of ~0.4 at the highest ligand concentration, which is comparable to the growth previously observed with Gal4 (positive control) (Figure 2.12). The EC_{50} values (half maximal effective concentrations), which refer to the ligand concentration that induces a response half-way between the baseline and maximum response, in CC with each ligand were in agreement with previously reported literature EC_{50} values in mammalian cells (Table 2.2) [55, 59, 60]. As expected, no ligand activated growth was

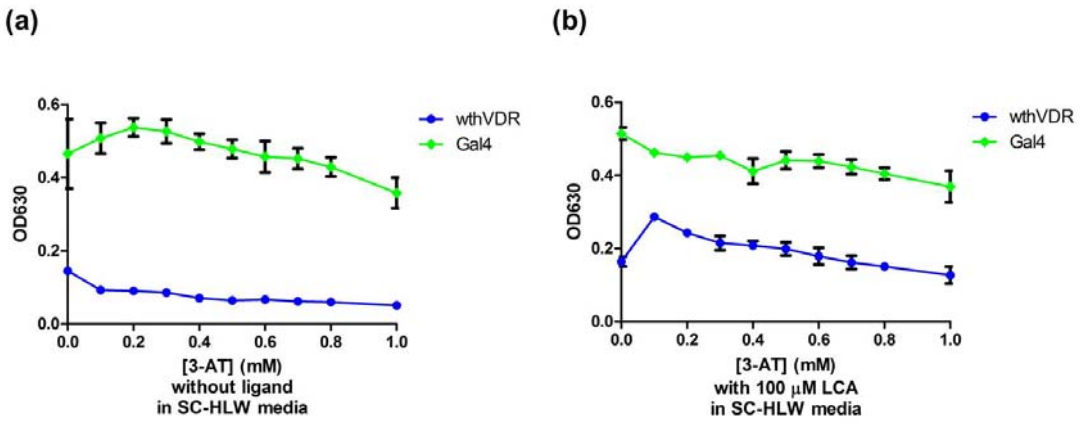

Figure 2.10: The wthVDR in Chemical Complementation
3-AT test in histidine selective media

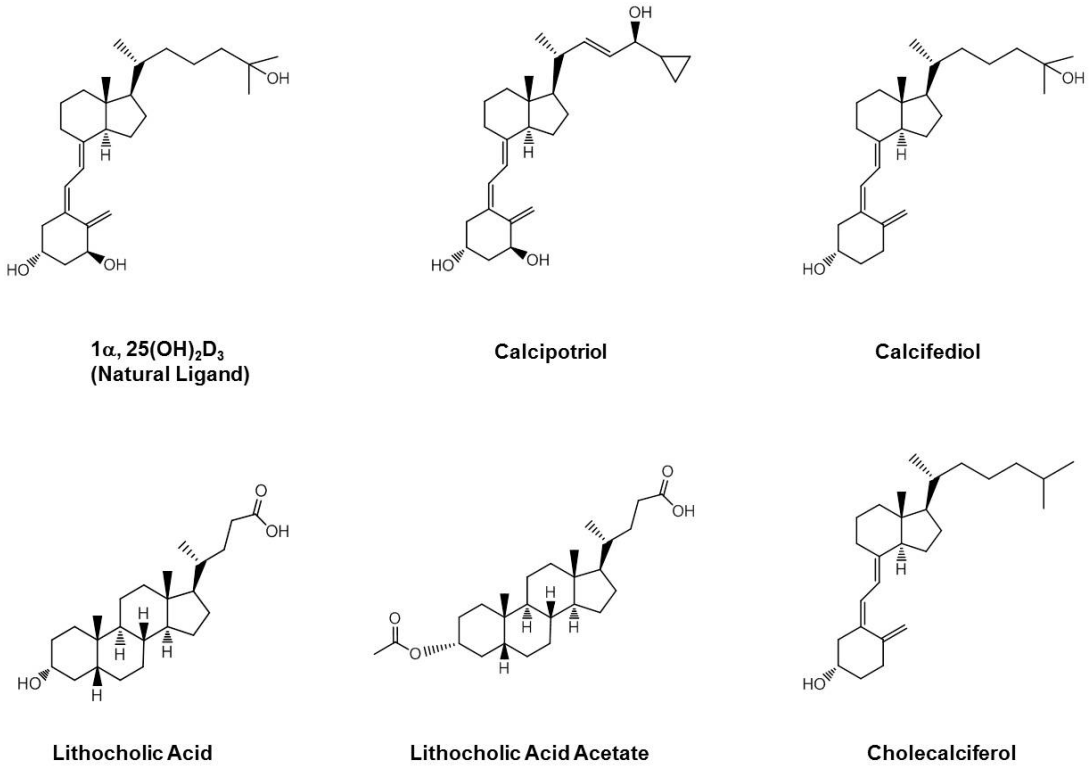

Figure 2.11: 1α, 25(OH)$_2$D$_3$, Lithocholic Acid and their Analogs

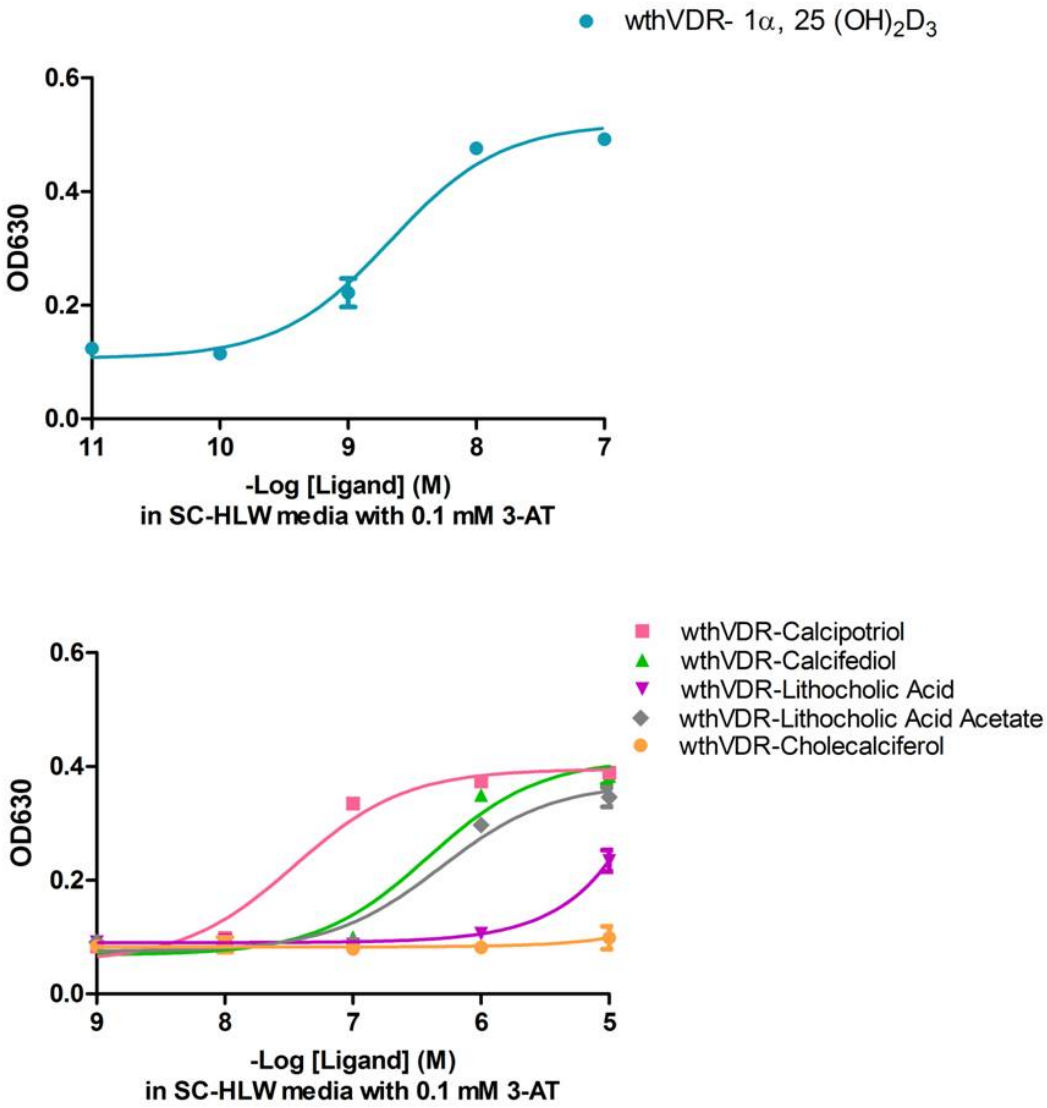

Figure 2.12: The wthVDR in Chemical Complementation
Histidine selective media with various ligands

observed with cholecalciferol, a precursor in the 1α, 25$(OH)_2D_3$ biosynthetic pathway (Figure 2.12). Based on these results, chemical complementation has proven to be a suitable system for studying the human vitamin D receptor.

The hVDR was also tested in liquid quantitation assays of chemical complementation in adenine selective media with varying concentrations of its natural ligand, 1α, 25$(OH)_2D_3$. A 10-fold activated growth and an EC_{50} value of 5.14 nM was observed (Figure 2.13). Based on these results and those previously obtained in adenine selective media with LCA (no ligand activated growth, Figure 2.9), we conclude that the *ADE2* selection system is too stringent for testing hVDR ligands associated with low sensitivity (weak receptor-ligand pairs e.g. hVDR-LCA) but not for ligands associated with high sensitivity (strong receptor-ligand pairs e.g. hVDR-1α, 25$(OH)_2D_3$). Overall, the hVDR can be used in chemical complementation, providing results similar to those obtained in mammalian cell culture.

2.6 Summary

In addition to being important targets for drug discovery, nuclear receptors (NRs) are also attractive candidates for protein engineering. In order to engineer and use the human vitamin D receptor (hVDR) in chemical complementation, a genetic selection system in which the survival of yeast is linked to the activation of a NR by an agonist, the hVDR gene was isolated from cDNA and the receptor's functionality was tested in liquid quantitation assays of chemical complementation. Chemical complementation proved to be a suitable system for studying this receptor, providing results similar to those previously reported for mammalian cell culture assays. As a result, the structural and functional relationships between the hVDR and its ligands can be investigated using chemical complementation as a protein engineering tool.

Table 2.2: Comparison of the wthVDR EC_{50} Values in Chemical Complementation vs. Literature

Ligand	EC_{50} in Chemical Complementation	EC_{50} in Literature [55, 59, 60]
$1\alpha, 25(OH)_2D_3$	2.14 nM	2-5 nM
Calcipotriol	35.1 nM	0.1 nM
Calcifediol	0.39 µM	
Lithocholic Acid	>10 µM	12.1 µM
Lithocholic Acid Acetate	0.49 µM	0.4 µM
Cholecalciferol	———	———

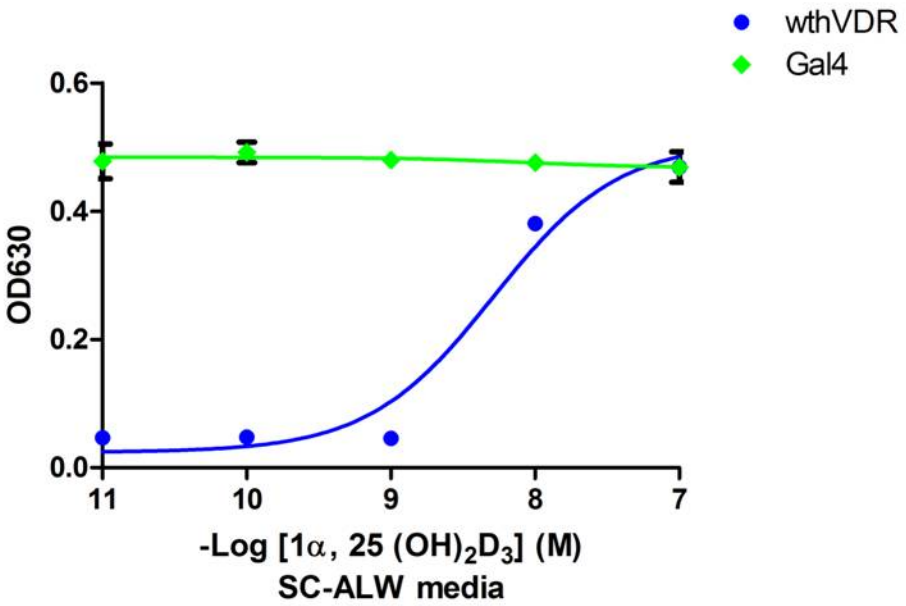

Figure 2.13: The wthVDR in Chemical Complementation
Adenine selective media with 1α, 25$(OH)_2D_3$

2.7 Materials and Methods

Ligands

1α,25-dihydroxyvitamin D_3 and calcifediol were purchased from BIOMOL (Plymouth Meeting, PA). Calcipotriol was purchased from Waterstone Technology (Carmel, IN). Lithocholic acid and lithocholic acid acetate were purchased from MP Biomedicals, LLC (Solon, OH). Cholecalciferol was purchased from Sigma-Aldrich (St. Louis, MO). 10 mM stocks of all ligands, except 1α,25-dihydroxyvitamin D_3, for which a 13.3 μM stock was made, were made with 80 % ethanol: 20 % dimethyl sulfoxide (DMSO) and stored at 4 °C.

hVDR Gene Isolation and Construction of a Yeast Expression Plasmid

The human vitamin D receptor gene was isolated and amplified from human skin cDNA (BioChain, Hayward, CA) via PCR (55 ºC as the annealing temperature) using 125 ng of the following primers: 5'-gcc gga att cat gga ggc aat ggc ggc-3' and 5'-gga cta gtt cag gag atc tca ttg cca aac ac-3' (Operon, Huntsville, AL). The underlined sequences denote *EcoRI* and *SpeI* restriction sites, respectively. The hVDR gene and yeast expression plasmid pGBT9, which contains the Gal4 DBD, were digested with *EcoRI* and *SpeI*, ligated, and transformed into Z-competent™ XL-1 Blue *Escherichia coli* (*E.coli)* cells (Zymo, Orange, CA). The resulting plasmid, pGBDhVDR, contained the Gal4 DBD fused to the full-length hVDR, and a tryptophan marker. All DNA was purified using the QIAprep® Spin Miniprep Kit (Qiagen, Valencia, CA). The pGBDhVDR plasmid was sequenced for confirmation (Operon, Huntsville, AL).

Yeast Transformation Using the PJ69-4A Strain

Using the 1x TRAFCO yeast transformation protocol, ~500 ng of the yeast expression plasmids, pGBDhVDR (containing the Gal4 DBD fused to the full-length

hVDR and a tryptophan marker) and pGAD10BASRC-1 (containing the Gal4 AD fused to SRC-1 and a leucine marker), were co-transformed into the yeast strain PJ69-4A [97]. Transformants were plated onto non-selective synthetic complete agar plates lacking leucine and tryptophan (SC-LW) to select for both fusion plasmids. Plates were incubated at 30 ºC for 3-4 days.

Liquid Quantitation Assays of Chemical Complementation in Yeast

Transformants obtained from the yeast transformation were grown overnight in non-selective SC-LW media, at 30 ºC with shaking at 300 rpm. A 4:1 ratio of selective media (SC-ALW or SC-HLW) with and without ligand at varying concentrations: cells (yeast resuspended in water) were aliquoted into 96-well plates. Plates were then incubated at 30 ºC with shaking at 170 rpm for 48 hours, with optical density readings at a wavelength of 630 nm (OD630) taken at 0, 24 and 48 hours. All data points represent the mean of at least duplicate experiments and the bars indicate standard deviation. The lowest ligand concentration data points for all plots contain no ligand. EC_{50} values were calculated using GraphPad Prism and a non-linear regression extrapolation.

2.8 Literature Cited

1. Evans, R.M., *The steroid and thyroid-hormone receptor superfamily.* Science, 1988. **240**(4854): p. 889-895.

2. Mangelsdorf, D.J. and R.M. Evans, *The RXR heterodimers and orphan receptors.* Cell, 1995. **83**(6): p. 841-850.

3. Mangelsdorf, D.J., C. Thummel, M. Beato, P. Herrlich, G. Schutz, K. Umesono, B. Blumberg, P. Kastner, M. Mark, P. Chambon, and R.M. Evans, *The nuclear receptor superfamily-the 2nd decade.* Cell, 1995. **83**(6): p. 835-839.

4. Carlberg, C., *Molecular basis of the selective activity of vitamin D analogues.* J. Cell. Biochem., 2003. **88**(2): p. 274-281.

5. Moore, D.D., S. Kato, W. Xie, D.J. Mangelsdorf, D.R. Schmidt, R. Xiao, and S.A. Kliewer, *International Union of Pharmacology. LXII. The NR1H and NR1I receptors: Constitutive androstane receptor, pregnene X receptor, farnesoid X receptor alpha, farnesoid X receptor beta, liver X receptor alpha, liver X receptor beta, and vitamin D receptor.* Pharmacol. Rev., 2006. **58**(4): p. 742-759.

6. Baker, A.R., D.P. McDonnell, M. Hughes, T.M. Crisp, D.J. Mangelsdorf, M.R. Haussler, J.W. Pike, J. Shine, and B.W. Omalley, *Cloning and expression of full-length cDNA-encoding human vitamin-D receptor.* Proc. Natl. Acad. Sci. U.S.A., 1988. **85**(10): p. 3294-3298.

7. Greschik, I. and D. Moras, *Structure-activity relationship of nuclear receptor-ligand interactions.* Curr. Top. Med. Chem., 2003. **3**(14): p. 1573-1599.

8. van Leeuwen, J., G. van den Bemd, M. van Driel, C.J. Buurman, and H.A.P. Pols, *24,25-Dihydroxyvitamin D-3 and bone metabolism.* Steroids, 2001. **66**(3-5): p. 375-380.

9. Deluca, H.F., *The vitamin-D story - a collaborative effort of basic science and clinical medicine.* FASEB J., 1988. **2**(3): p. 224-236.

10. Haussler, M.R. and T.A. McCain, *Basic and clinical concepts related to vitamin-D metabolism and action.* N. Engl. J. Med., 1977. **297**(18): p. 974-983.

11. Haussler, M.R., G.K. Whitfield, C.A. Haussler, J.C. Hsieh, P.D. Thompson, S.H. Selznick, C.E. Dominguez, and P.W. Jurutka, *The nuclear vitamin D receptor: Biological and molecular regulatory properties revealed.* J. Bone Miner. Res., 1998. **13**(3): p. 325-349.

12. Jones, G., S.A. Strugnell, and H.F. DeLuca, *Current understanding of the molecular actions of vitamin D.* Physiol. Rev., 1998. **78**(4): p. 1193-1231.

13. Bouillon, R., W.H. Okamura, and A.W. Norman, *Structure-function-relationships in the vitamin-D endocrine system.* Endocr. Rev., 1995. **16**(2): p. 200-257.

14. Hendy, G.N., K.A. Hruska, S. Mathew, and D. Goltzman, *New insights into mineral and skeletal regulation by active forms of vitamin D.* Kidney Int., 2006. **69**(2): p. 218-223.

15. Colston, K.W. and C.M. Hansen, *Mechanisms implicated in the growth regulatory effects of vitamin D in breast cancer.* Endocr. Relat. Cancer, 2002. **9**(1): p. 45-59.

16. Abe, E., C. Miyaura, H. Sakagami, M. Takeda, K. Konno, T. Yamazaki, S. Yoshiki, and T. Suda, *Differentiation of mouse myeloid-leukemia cells induced by 1-alpha,25-dihydroxyvitamin-D3.* Proc. Natl. Acad. Sci. U.S.A., 1981. **78**(8): p. 4990-4994.

17. Colston, K., M.J. Colston, and D. Feldman, *1,25-dihydroxyvitamin-D3 and malignant-melanoma - the presence of receptors and inhibition of cell-growth in culture.* Endocrinology, 1981. **108**(3): p. 1083-1086.

18. Tsoukas, C.D., D.M. Provvedini, and S.C. Manolagas, *1,25-dihydroxyvitamin-D3 - a novel immunoregulatory hormone.* Science, 1984. **224**(4656): p. 1438-1440.

19. Brown, A.J., A. Dusso, and E. Slatopolsky, *Vitamin D.* Am. J. Physiol. Renal, 1999. **277**(2): p. F157-F175.

20. *Nuclear Receptor Signaling Atlas*
10/1/2010; Available from: http://www.nursa.org.

21. Gillies, A.R., G. Skretas, and D.W. Wood, *Engineered systems for detection and discovery of nuclear hormone-like compounds.* Biotechnol. Prog., 2008. **24**: p. 8-16.

22. Jin, C.H. and J.W. Pike, *Human vitamin D receptor-dependent transactivation in Saccharomyces cerevisiae requires retinoid X receptor.* Mol. Endocrinol., 1996. **10**(2): p. 196-205.

23. Schrader, M., K.M. Muller, M. Beckerandre, and C. Carlberg, *Response element selectivity for heterodimerization of vitamin-D receptors with retinoic acid and retinoid-X receptors.* J. Mol. Endocrinol., 1994. **12**(3): p. 327-339.

24. Kliewer, S.A., K. Umesono, D.J. Mangelsdorf, and R.M. Evans, *Retinoid X-receptor interacts with nuclear receptors in retinoic acid, thyroid-hormone and vitamin-D3 signaling.* Nature, 1992. **355**(6359): p. 446-449.

25. Yu, V.C., C. Delsert, B. Andersen, J.M. Holloway, O.V. Devary, A.M. Naar, S.Y. Kim, J.M. Boutin, C.K. Glass, and M.G. Rosenfeld, *RXR-beta- a coregulator that enhances binding of retinoic acid , thyroid-hormone, and vitamin D-receptors to their cognate response elements.* Cell, 1991. **67**(6): p. 1251-1266.

26. Jin, C.H., S.A. Kerner, M.H. Hong, and J.W. Pike, *Transcriptional activation and dimerization functions in the human vitamin D receptor.* Mol. Endocrinol., 1996. **10**(8): p. 945-957.

27. Christakos, S., P. Dhawan, Y. Liu, X.R. Peng, and A. Porta, *New insights into the mechanisms of vitamin D action.* J. Cell. Biochem., 2003. **88**(4): p. 695-705.

28. Jurutka, P.W., P.D. Thompson, G.K. Whitfield, K.R. Eichhorst, N. Hall, C.E. Dominguez, J.C. Hsieh, C.A. Haussler, and M.R. Haussler, *Molecular and functional comparison of 1,25-dihydroxyvitamin D_3 and the novel vitamin D receptor ligand, lithocholic acid, in activating transcription of cytochrome P450 3A4.* J. Cell. Biochem., 2005. **94**(5): p. 917-943.

29. Carlberg, C., *The vitamin D-3 receptor in the context of the nuclear receptor superfamily - The central role of the retinoid X receptor.* Endocrine, 1996. **4**(2): p. 91-105.

30. Shulman, A.I., C. Larson, D.J. Mangelsdorf, and R. Ranganathan, *Structural determinants of allosteric ligand activation in RXR heterodimers.* Cell, 2004. **116**(3): p. 417-429.

31. Onate, S.A., S.Y. Tsai, M.J. Tsai, and B.W. Omalley, *Sequence and characterization of a coactivator for the steroid-hormone receptor superfamily.* Science, 1995. **270**(5240): p. 1354-1357.

32. Gill, R.K., L.M. Atkins, B.W. Hollis, and N.H. Bell, *Mapping the domains of the interaction of the vitamin D receptor and steroid receptor coactivator-1.* Mol. Endocrinol., 1998. **12**(1): p. 57-65.

33. Rachez, C. and L.P. Freedman, *Mechanisms of gene regulation by vitamin D-3 receptor: a network of coactivator interactions.* Gene, 2000. **246**(1-2): p. 9-21.

34. Sone, T., S. Kerner, and J.W. Pike, *Vitamin-D receptor interaction with specific DNA - association as a 1,25-dihydroxyvitamin-D3-modulated heterodimer.* J. Biol. Chem., 1991. **266**(34): p. 23296-23305.

35. Rochel, N., J.M. Wurtz, A. Mitschler, B. Klaholz, and D. Moras, *The crystal structure of the nuclear receptor for vitamin D bound to its natural ligand.* Mol. Cell, 2000. **5**(1): p. 173-179.

36. Umesono, K., K.K. Murakami, C.C. Thompson, and R.M. Evans, *Direct repeats as selective response elements for the thyroid-hormone, retinoic acid, and vitamin-D3 receptors.* Cell, 1991. **65**(7): p. 1255-1266.

37. Kerner, S.A., R.A. Scott, and J.W. Pike, *Sequence elements in the human osteocalcin gene confer basal activation and inducible response to hormonal vitamin-D3.* Proc. Natl. Acad. Sci. U.S.A., 1989. **86**(12): p. 4455-4459.

38. Noda, M., R.L. Vogel, A.M. Craig, J. Prahl, H.F. Deluca, and D.T. Denhardt, *Identification of a DNA-sequence responsible for binding of the 1,25-dihydroxyvitamin-D3 receptor and 1,25-dihydroxyvitamin-D3 enhancement of mouse secreted phosphoprotein-1 (SPP-1 or osteopontin) gene-expression.* Proc. Natl. Acad. Sci. U.S.A., 1990. **87**(24): p. 9995-9999.

39. Ohyama, Y., K. Ozono, M. Uchida, T. Shinki, S. Kato, T. Suda, O. Yamamoto, M. Noshiro, and Y. Kato, *Identification of a vitamin-D-responsive element in the 5-flanking region of the rat 25-hydroxyvitamin D-3 24-hydroxylase gene.* J. Biol. Chem., 1994. **269**(14): p. 10545-10550.

40. Moras, D. and H. Gronemeyer, *The nuclear receptor ligand-binding domain: structure and function.* Curr. Opin. Cell Biol., 1998. **10**(3): p. 384-391.

41. Wurtz, J.M., W. Bourguet, J.P. Renaud, V. Vivat, P. Chambon, D. Moras, and H. Gronemeyer, *A canonical structure for the ligand-binding domain of nuclear receptors.* Nat. Struct. Biol., 1996. **3**(1): p. 87-94.

42. Carlberg, C. and F. Molnar, *Detailed molecular understanding of agonistic and antagonistic vitamin D receptor ligands.* Curr. Top. Med. Chem., 2006. **6**(12): p. 1243-1253.

43. Yamamoto, K., M. Choi, D. Abe, M. Shimizu, and S. Yamada, *Alanine scanning mutational analysis of the ligand binding pocket of the human Vitamin D receptor.* J. Steroid Biochem. Mol. Biol., 2007. **103**(3-5): p. 282-285.

44. Yamada, S. and K. Yamamoto, *Ligand recognition by vitamin D receptor: Total alanine scanning mutational analysis of the residues lining the ligand binding pocket of vitamin D receptor.* Curr. Top. Med. Chem., 2006. **6**(12): p. 1255-1265.

45. Huang, P.X., V. Chandra, and F. Rastinejad, *Structural overview of the nuclear receptor superfamily: Insights into physiology and therapeutics.* Annu. Rev. Physiol., 2010. **72**: p. 247-272.

46. Williams, S., R.K. Bledsoe, J.L. Collins, S. Boggs, M.H. Lambert, A.B. Miller, J. Moore, D.D. McKee, L. Moore, J. Nichols, D. Parks, M. Watson, B. Wisely, and T.M. Willson, *X-ray crystal structure of the liver X receptor beta ligand binding domain - Regulation by a histidine-tryptophan switch.* J. Biol. Chem., 2003. **278**(29): p. 27138-27143.

47. Jimenez-Lara, A.M. and A. Aranda, *Lysine 246 of the vitamin D receptor is crucial for ligand-dependent interaction with coactivators and transcriptional activity.* J. Biol. Chem., 1999. **274**(19): p. 13503-13510.

48. Vanhooke, J.L., M.M. Benning, C.B. Bauer, J.W. Pike, and H.F. DeLuca, *Molecular structure of the rat vitamin D receptor ligand binding domain complexed with 2-carbon-substituted vitamin D-3 hormone analogues and a LXXLL-containing coactivator peptide.* Biochemistry, 2004. **43**(14): p. 4101-4110.

49. Molnar, F., M. Perakyla, and C. Carlberg, *Vitamin D receptor agonists specifically modulate the volume of the ligand-binding pocket.* J. Biol. Chem., 2006. **281**(15): p. 10516-10526.

50. Makishima, M., T.T. Lu, W. Xie, G.K. Whitfield, H. Domoto, R.M. Evans, M.R. Haussler, and D.J. Mangelsdorf, *Vitamin D receptor as an intestinal bile acid sensor.* Science, 2002. **296**(5571): p. 1313-1316.

51. Kawaura, A., N. Tanida, K. Sawada, M. Oda, and T. Shimoyama, *Supplemental administration of 1-alpha-hydroxyvitamin-D3 inhibits promotion by intrarectal instillation of lithocholic acid in N-methyl-N-nitrosourea-induced colonic tumorigenesis in rats.* Carcinogenesis, 1989. **10**(4): p. 647-649.

52. Adachi, R., A.I. Shulman, K. Yamamoto, I. Shimomura, S. Yamada, D.J. Mangelsdorf, and M. Makishima, *Structural determinants for vitamin D receptor response to endocrine and xenobiotic signals.* Mol. Endocrinol., 2004. **18**(1): p. 43-52.

53. Guyton, K.Z., T.W. Kensler, and G.H. Posner, *Cancer chemoprevention using natural vitamin D and synthetic analogs.* Annu. Rev. Pharmacol. Toxicol., 2001. **41**: p. 421-442.

54. Honkakoski, P. and M. Negishi, *Regulation of cytochrome P450 (CYP) genes by nuclear receptors.* Biochem. J., 2000. **347**: p. 321-337.

55. Adachi, R., Y. Honma, H. Masuno, K. Kawana, L. Shimomura, S. Yamada, and M. Makishima, *Selective activation of vitamin D receptor by lithocholic acid acetate, a bile acid derivative.* J. Lipid Res., 2005. **46**(1): p. 46-57.

56. Yamada, S., M. Shimizu, and K. Yamamoto, *Structure-function relationships of vitamin D including ligand recognition by the vitamin D receptor.* Med. Res. Rev., 2003. **23**(1): p. 89-115.

57. Choi, M., K. Yamamoto, T. Itoh, M. Makishima, D.J. Mangelsdorf, D. Moras, H.F. DeLuca, and S. Yamada, *Interaction between vitamin D receptor and vitamin D ligands: Two-dimensional alanine scanning mutational analysis.* Chem. Biol., 2003. **10**(3): p. 261-270.

58. Noy, N., *Ligand specificity of nuclear hormone receptors: Sifting through promiscuity.* Biochemistry, 2007. **46**(47): p. 13461-13467.

59. Bury, Y., D. Ruf, C.M. Hansen, A.M. Kissmeyer, L. Binderup, and C. Carlberg, *Molecular evaluation of vitamin D-3 receptor agonists designed for topical treatment of skin diseases.* J. Invest. Dermatol., 2001. **116**(5): p. 785-792.

60. Boehm, M.F., P. Fitzgerald, A.H. Zou, M.G. Elgort, E.D. Bischoff, L. Mere, D.E. Mais, R.P. Bissonnette, R.A. Heyman, A.M. Nadzan, M. Reichman, and E.A. Allegretto, *Novel nonsecosteroidal vitamin D mimics exert VDR-modulating activities with less calcium mobilization than 1,25-dihydroxyvitamin D-3.* Chem. Biol., 1999. **6**(5): p. 265-275.

61. Kato, S., T. Yoshizazawa, S. Kitanaka, A. Murayama, and K. Takeyama, *Molecular genetics of vitamin D-dependent hereditary rickets.* Horm. Res., 2002. **57**(3-4): p. 73-78.

62. Haussler, M.R., C.A. Haussler, P.W. Jurutka, P.D. Thompson, J.C. Hsieh, L.S. Remus, S.H. Selznick, and G.K. Whitfield, *The vitamin D hormone and its nuclear receptor: molecular actions and disease states.* J. Endocrinol., 1997. **154**: p. S57-S73.

63. Hughes, M.R., P.J. Malloy, D.G. Kieback, R.A. Kesterson, J.W. Pike, D. Feldman, and B.W. Omalley, *Point mutations in the human vitamin-D receptor gene associated with hypocalcemic rickets.* Science, 1988. **242**(4886): p. 1702-1705.

64. Malloy, P.J., T.R. Eccleshall, C. Gross, L. VanMaldergem, R. Bouillon, and D. Feldman, *Hereditary vitamin D resistant rickets caused by a novel mutation in the vitamin D receptor that results in decreased affinity for hormone and cellular hyporesponsiveness.* J. Clin. Invest., 1997. **99**(2): p. 297-304.

65. Malloy, P.J., Z. Hochberg, D. Tiosano, J.W. Pike, M.R. Hughes, and D. Feldman, *The molecular basis of hereditary 1,25-dihydroxyvitamin-D_3 resistant rickets in seven related families.* J. Clin. Invest., 1990. **86**(6): p. 2071-2079.

66. Malloy, P.J., J.W. Pike, and D. Feldman, *The vitamin D receptor and the syndrome of hereditary 1,25-dihydroxyvitamin D-resistant rickets.* Endocr. Rev., 1999. **20**(2): p. 156-188.

67. Kristjansson, K., A.R. Rut, M. Hewison, J.L.H. Oriordan, and M.R. Hughes, *2 Mutations in the hormone-binding domain of the vitamin-D receptor cause tissue resistance to 1,25-dihydroxyvitamin-D3.* J. Clin. Invest., 1993. **92**(1): p. 12-16.

68. Whitfield, G.K., S.H. Selznick, C.A. Haussler, J.C. Hsieh, M.A. Galligan, P.W. Jurutka, P.D. Thompson, S.M. Lee, J.E. Zerwekh, and M.R. Haussler, *Vitamin D receptors from patients with resistance to 1,25-dihydroxyvitamin D-3: Point mutations confer reduced transactivation in response to ligand and impaired interaction with the retinoid X receptor heterodimeric partner.* Mol. Endocrinol., 1996. **10**(12): p. 1617-1631.

69. Pols, H.A.P., J.C. Birkenhager, and J. Vanleeuwen, *Vitamin-D analogs - from molecule to clinical-application.* Clinical Endocrinology, 1994. **40**(3): p. 285-292.

70. Smith, E.L., S.H. Pincus, L. Donovan, and M.F. Holick, *A novel-approach for the evaluation and treatment of psoriasi- oral or topical use of 1,25-dihydroxyvitamin-D3 can be a safe and effective therapy for psoriasis.* J. Am. Acad. Dermatol., 1988. **19**(3): p. 516-528.

71. Hourai, S., T. Fujishima, A. Kittaka, Y. Suhara, H. Takayama, N. Rochel, and D. Moras, *Probing a water channel near the A-ring of receptor-bound 1 alpha,25-dihydroxyvitamin D3 with selected 2 alpha-substituted analogues.* J. Med. Chem., 2006. **49**(17): p. 5199-5205.

72. Tocchini-Valentini, G., N. Rochel, J.M. Wurtz, and D. Moras, *Crystal structures of the vitamin D nuclear receptor liganded with the vitamin D side chain analogues calcipotriol and seocalcitol, receptor agonists of clinical importance. Insights into a structural basis for the switching of calcipotriol to a receptor antagonist by further side chain modification.* J. Med. Chem., 2004. **47**(8): p. 1956-1961.

73. Calverley, M.J., *Synthesis of MC-903, a biologically-active vitamin-D metabolite analog.* Tetrahedron, 1987. **43**(20): p. 4609-4619.

74. Kragballe, K. and L. Iversen, *Calcipotriol - a new topical antipsoriatic.* Dermatol. Clin. , 1993. **11**(1): p. 137-141.

75. Colston, K.W., A.G. Mackay, S.Y. James, L. Binderup, S. Chander, and R.C. Coombes, *EB1089 - A new vitamin-D analog that inhibits the growth of breast-cancer cells invivo and invitro.* Biochem. Pharmacol., 1992. **44**(12): p. 2273-2280.

76. Hansen, C.M., K.J. Hamberg, E. Binderup, and L. Binderup, *Seocalcitol (EB 1089): A vitamin D analogue of anti-cancer potential. Background, design, synthesis, pre-clinical and clinical evaluation.* Curr. Pharm. Des., 2000. **6**(7): p. 803-828.

77. Evans, T.R.J., K.W. Colston, F.J. Lofts, D. Cunningham, D.A. Anthoney, H. Gogas, J.S. de Bono, K.J. Hamberg, T. Skov, and J.L. Mansi, *A phase II trial of the vitamin D analogue Seocalcitol (EB 1089) in patients with inoperable pancreatic cancer.* Br. J. Cancer, 2002. **86**(5): p. 680-685.

78. Stein, M.S. and J.D. Wark, *An update on the therapeutic potential of vitamin D analogues.* Expert Opin. Invest. Drugs, 2003. **12**(5): p. 825-840.

79. Bouillon, R., L. Verlinden, G. Eelen, P. De Clercq, M. Vandewalle, C. Mathieu, and A. Verstuyf, *Mechanisms for the selective action of Vitamin D analogs.* J. Steroid Biochem. Mol. Biol., 2005. **97**(1-2): p. 21-30.

80. Rochel, N., S. Hourai, X. Perez-Garcia, A. Rumbo, A. Mourino, and D. Moras, *Crystal structure of the vitamin D nuclear receptor ligand binding domain in complex with a locked side chain analog of calcitriol.* Arch. Biochem. Biophys., 2007. **460**(2): p. 172-176.

81. Tocchini-Valentini, G., N. Rochel, J.M. Wurtz, A. Mitschler, and D. Moras, *Crystal structures of the vitamin D receptor complexed to superagonist 20-epi ligands.* Proc. Natl. Acad. Sci. U.S.A., 2001. **98**(10): p. 5491-5496.

82. Smith, C.L. and B.W. O'Malley, *Coregulator function: A key to understanding tissue specificity of selective receptor modulators.* Endocr. Rev., 2004. **25**(1): p. 45-71.

83. Roodman, G.D. and J.J. Windle, *Paget disease of bone.* J. Clin. Invest., 2005. **115**(2): p. 200-208.

84. Ishizuka, S., N. Kurihara, S.V. Reddy, J. Cornish, T. Cundy, and G.D. Roodman, *(23S)-25-dehydro-1 alpha-hydroxyvitamin D-3-26,23-lactone, a vitamin D receptor antagonist that inhibits osteoclast formation and bone resorption in bone marrow cultures from patients with Paget's disease.* Endocrinology, 2005. **146**(4): p. 2023-2030.

85. Ishizuka, S., N. Kurihara, Y. Hiruma, D. Miura, J.I. Namekawa, A. Tamura, Y. Kato-Nakamura, Y. Nakano, K. Takenouchi, Y. Hashimoto, K. Nagasawa, and G.D. Roodman, *1 alpha,25-dihydroxyvitamin D-3-26,23-lactam analogues function as vitamin D receptor antagonists in human and rodent cells.* J. Steroid Biochem. Mol. Biol., 2008. **110**(3-5): p. 269-277.

86. Herdick, M., A. Steinmeyer, and C. Carlberg, *Antagonistic action of a 25-carboxylic ester analogue of 1 alpha,25-dihydroxyvitamin D-3 is mediated by a lack of ligand-induced vitamin D receptor interaction with coactivators.* J. Biol. Chem., 2000. **275**(22): p. 16506-16512.

87. Miura, D., K. Manabe, K. Ozono, M. Saito, Q.Z. Gao, A.W. Norman, and S. Ishizuka, *Antagonistic action of novel 1 alpha,25-dihydroxyvitamin D-3-26,23-lactone analogs on differentiation of human leukemia cells (HL-60) induced by 1 alpha,25-dihydroxyvitamin D-3.* J. Biol. Chem., 1999. **274**(23): p. 16392-16399.

88. Toell, A., M.M. Gonzalez, D. Ruf, A. Steinmeyer, S. Ishizuka, and C. Carlberg, *Different molecular mechanisms of vitamin D-3 receptor antagonists.* Mol. Pharmacol., 2001. **59**(6): p. 1478-1485.

89. Germain, P., B. Staels, C. Dacquet, M. Spedding, and V. Laudet, *Overview of nomenclature of nuclear receptors.* Pharmacol. Rev., 2006. **58**(4): p. 685-704.

90. Schwimmer, L.J., P. Rohatgi, B. Azizi, K.L. Seley, and D.F. Doyle, *Creation and discovery of ligand-receptor pairs for transcriptional control with small molecules.* Proc. Natl. Acad. Sci. U.S.A., 2004. **101**(41): p. 14707-14712.

91. Taylor, J.L., P. Rohatgi, H.T. Spencer, D.F. Doyle, and B. Azizi, *Characterization of a molecular switch system that regulates gene expression in mammalian cells through a small molecule.* BMC Biotechnol., 2010. **10**: p. 15.

92. Azizi, B., E.I. Chang, and D.F. Doyle, *Chemical complementation: small-molecule-based genetic selection in yeast.* Biochem. Biophys. Res. Commun., 2003. **306**(3): p. 774-780.

93. Drees, B.L., *Progress and variations in two-hybrid and three-hybrid technologies.* Curr. Opin. Chem. Biol., 1999. **3**(1): p. 64-70.

94. James, P., J. Halladay, and E.A. Craig, *Genomic libraries and a host strain designed for highly efficient two-hybrid selection in yeast.* Genetics, 1996. **144**(4): p. 1425-1436.

95. Lohr, D., P. Venkov, and J. Zlatanova, *Transcriptional regulation in the yeast GAL gene family: A complex genetic network.* FASEB J., 1995. **9**(9): p. 777-787.

96. Struhl, K. and R.W. Davis, *Production of a functional eukaryotic enzyme in escherichia-coli - Cloning and expression of yeast structural gene for imidazoleglycerolphosphate dehydratase (HIS3).* Proc. Natl. Acad. Sci. U.S.A., 1977. **74**(12): p. 5255-5259.

97. Gietz, R.D. and R.A. Woods, *Transformation of yeast by lithium acetate/single-stranded carrier DNA/polyethylene glycol method*, in *Guide to Yeast Genetics and Molecular and Cell Biology, Pt B*. 2002, Academic Press Inc: San Diego. p. 87-96.

CHAPTER 3

PROTEIN ENGINEERING WITH CHEMICAL COMPLEMENTATION: ENGINEERING THE HUMAN VITAMIN D RECEPTOR TO BIND AND ACTIVATE IN RESPONSE TO A NOVEL SMALL MOLECULE LIGAND

3.1 Engineering the hVDR

The human vitamin D receptor's (hVDR) significant role in biological processes and involvement in diseases makes this receptor an important target for drug discovery, and an attractive candidate for protein engineering. Based on this fact and the severe effects of mutations on the hVDR's function (discussed in Chapter 2), investigating the structure- function relationships between the hVDR and its ligands is of interest. The information gained can be applied towards further understanding of the functionality of the receptor, its ability to bind various ligands, and for further development of new small molecules as potential therapeutic drugs.

Previous structural and mutational analyses of the hVDR have focused on alanine scanning mutagenesis and site-directed mutagenesis of the residues lining the receptor's ligand binding pocket (LBP). These studies have provided a fundamental understanding of the key interactions between the hVDR and various ligands; however work on the mutational tolerance of LBP residues or the indirect effects of residues outside the LBP have been limited.

To investigate the structural and functional parameters of the hVDR further, as well as gain insight into the role and tolerance of specific residues, a mutational assessment of residues in the hVDR ligand binding domain (LBD) was performed. To develop a comprehensive mutational analysis, libraries of hVDR variants were engineered using two approaches. In the first approach, structural analyses allowed the

rational design of two libraries using randomized codons at chosen positions. The second approach involved random mutagenesis, using error-prone PCR (epPCR) to create libraries of variants. All of the variants obtained were tested with small molecule ligands of interest using chemical complementation. As discussed in Chapter 2, chemical complementation proved to be a suitable system for studying the hVDR, providing results similar to those obtained in mammalian cell culture assays.

While evaluating and developing a deeper understanding of the hVDR, part of the goal was to engineer this receptor to bind and activate in response to a novel small molecule and not its natural ligand, 1α, 25$(OH)_2D_3$. The diversity of ligand binding among different nuclear receptors (NRs) suggests the possibility of engineering these receptors to bind novel small molecules for several applications [1, 2]. Specific interest laid in determining whether selective pressure would allow for the directed evolution of a variant that would be activated by cholecalciferol (chole) or a β-lactam antibiotic (Figure 3.1a). Chole, a precursor in the 1α, 25$(OH)_2D_3$ biosynthetic pathway lacks two of the three hydroxyl groups present in 1α, 25$(OH)_2D_3$ and does not activate the hVDR, confirming the importance of precise molecular interactions required for ligand activation.

β-lactam antibiotics, on the other hand, are a large component of the pharmaceutical industry worldwide. However, some of the major challenges faced in the synthesis and manufacturing of these drugs are high costs and excessive waste production, as well as patient drug resistance [3]. As a result, alternatives to current synthetic approaches are needed. One such approach would be to develop microbial ‘factories’ that produce β-lactam antibiotics, resulting in reduced costs and labor, yet higher yields. Engineering NRs to bind these antibiotics in chemical complementation provides a selection method for detection of the small molecules being produced in yeast (Figure 3.1b). The selective pressure placed on the yeast ensures that the

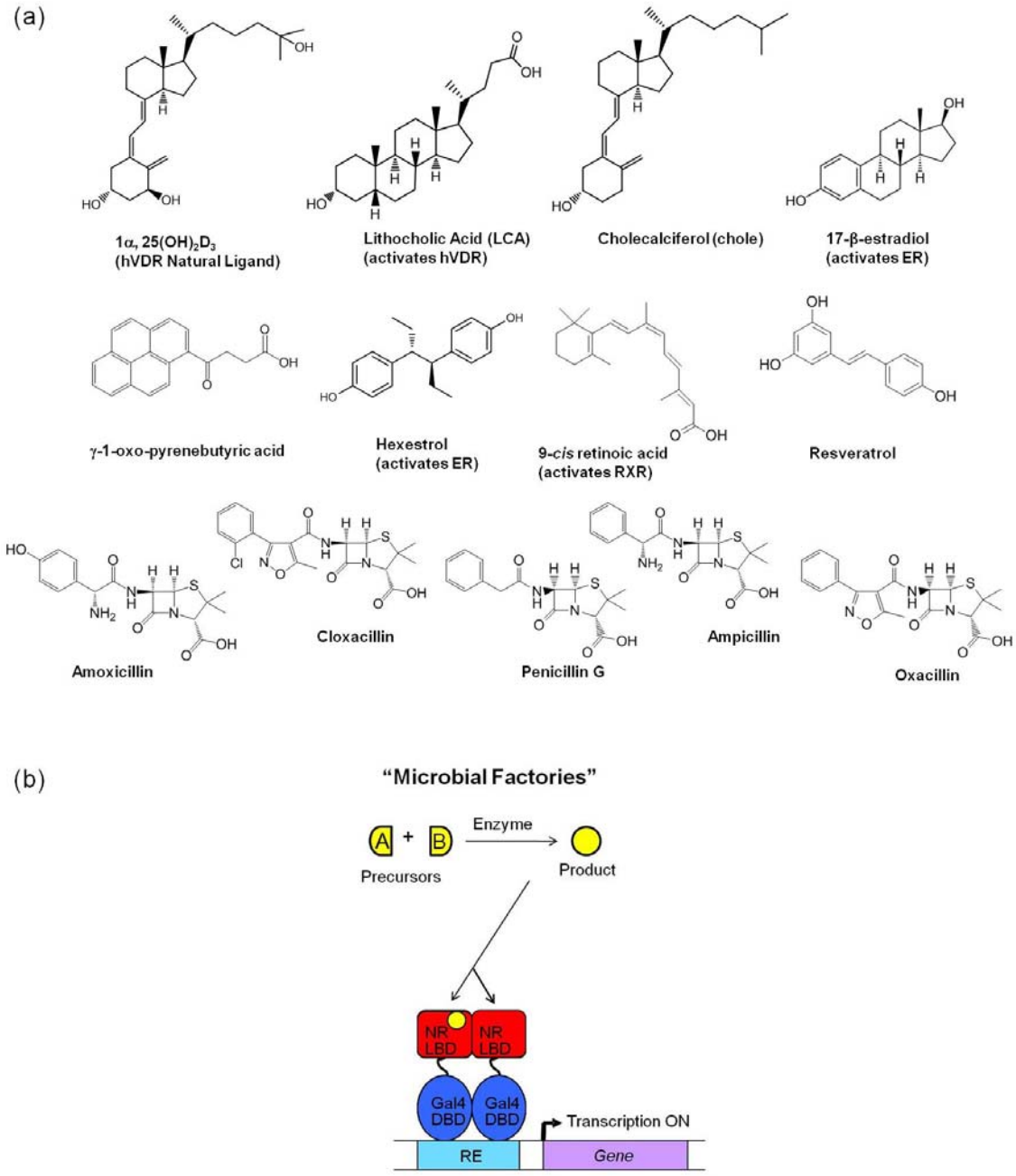

Figure 3.1: Engineering the hVDR to Bind and Activate in Response to a Novel Small Molecule Ligand (a) Structures of molecules of interest (b) Engineering nuclear receptors for the development of microbial systems that produce antibiotics

biosynthetic genes required are maintained by the organism, allowing the production of the β-lactam antibiotics in this microbial system. If selective pressure is not present, yeast would eventually lose the need to produce these antibiotics over several generations.

The goal of this project was to use rational and random mutagenic approaches, along with chemical complementation to engineer the hVDR to activate in response to a β-lactam antibiotic for future use in antibiotic production, and chole to explore how a molecule extremely similar to the natural ligand can contribute to a completely different activation profile with the wild-type receptor. The latter is a result likely due to differing receptor-ligand structure-function relationships between the receptor and these two molecules (Figure 3.1).

3.2 Rational Mutagenic Approach: hVDR Libraries 1 & 2

3.2.1 Rational Mutagenic Approach: Design for hVDR Libraries 1 & 2

Rational design of proteins is a process in which knowledge of the structure and function of a protein is used to create desired changes or mutations. A rational mutagenic approach consisting of multiple strategies was utilized to engineer hVDR libraries. First, the hVDR's crystal structure with 1α, 25$(OH)_2D_3$ (PDB:1DB1) was analyzed for residues within five angstroms of the ligand [4]. Using the molecular graphics software program, Visual Molecular Dynamics (VMD), as a visualization and analysis tool of the three-dimensional crystal structure, key molecular interactions in the hVDR's LBP were determined [5]. Previous literature on mutational analyses assessing the structure-function relationship between the receptor and the ligand was also used as a determinant for the specific residues that were to be mutated, minimizing library size in our rational design to the coverage capabilities of yeast [6-11]. Yeast transformations generate a maximum of ~10^6 transformants/μg plasmid DNA [12]. Ideally, in order to

obtain complete library coverage, library size in yeast should be limited to ~10^5-10^6 variants or smaller. Overall, 14 residues were chosen and mutations at each position were designed based on amino acid properties (e.g. polarity, shape and volume). Mutations were also chosen based on sequencing alignments of the hVDR with other NRs, including the pregnane X receptor (PXR), retinoid X receptor (RXRα) and estrogen receptor (ERα), focusing on evolutionarily conserved and non-conserved residues [13].

Two rationally designed hVDR libraries (1 & 2) were created in quest of exploring how chemical and physical changes within the LBP affect receptor-ligand interactions, thus receptor function. For hVDR library 1, several residues that interact directly with 1α, 25$(OH)_2D_3$ and/or predicted to have an effect on stabilizing the active conformation of the receptor were chosen for mutagenesis [8-10]. For example, residues S237 (helix 3), R274 (helix 4/5) and H397 (helix 11) form important hydrogen bonds with the ligand, while residues I238 (helix 3) and F422 (helix 12) are located in helices that interact with coactivator proteins, thus stabilizing the active conformation of the receptor [4, 14]. Seven residues were targeted for mutagenesis in library 1: S237, I238, I271, R274, H397, Y401 and F422 (Figure 3.2 and Table 3.1).

For hVDR library 2, a different subset of residues predicted to have an effect on stabilizing the active conformation of the receptor and/or ligand- mediated conformational changes of the receptor were chosen for mutagenesis [8-10]. For example, residues Y147 (loop 1-3) and L233 (helix 3) not only interact with the ligand, but also form interactions with other residues that contribute to structural changes of the receptor upon ligand binding, leading to the active conformation. Seven residues were targeted for mutagenesis in library 2: Y143, Y147, F150, L227, L233, Y295 and V418

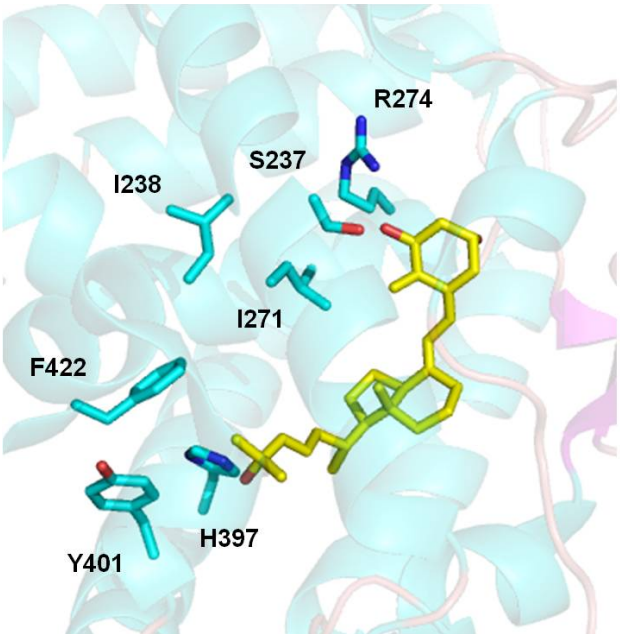

Mutated Residues and Designed Changes

S237: S_2TCFI

I238: $LIV_2FMA_2S_2T_2$

I271: LIV_2FM

R274: $LIV_2FMA_2S_3T_2CRWG_2$

H397: HYNKQStop

Y401: Saturated

F422: FSYCLPHRITNSVADG

Theoretical Library Size:
Amino Acid Level: 5×10^6
Nucleotide Level: 24×10^6

Figure 3.2: Rational Mutagenic Approach: Design for hVDR Library 1
Mutated hVDR Residues (Cyan), 1α, $25(OH)_2D_3$ (Yellow), PDB:1DB1
Subscripts indicate amino acids that appear with more than one codon at the randomized amino acid position and are represented multiple times in the design.

Table 3.1: Rational Mutagenic Approach hVDR Library 1: Mutated Residues and Their Predicted Functions [8-10]

Residue	Designed Changes	Location	Distance from ligand (Å)	Predicted Functions
S237	S_2TCFI	Helix 3	<3	Forms hydrogen bond with natural ligand
I238	$LIV_2FMA_2S_2T_2$	Helix 3	>5	Connection of H3 and H4/5 and folding of the active conformation (hydrophobic interaction with H4/5)
I271	LIV_2FM	Helix 4/5	3-4	Binding of H3 and H4/5 and folding of the active conformation (hydrophobic interaction with ligand and H3)
R274	$LIV_2FMA_2S_3T_2CRWG_2$	Helix 4/5	<3	Forms hydrogen bond with natural ligand, Ligand mediated packing of H3 and H4/5 and folding of the active conformation
H397	HYNKQstop	Helix 11	<3	Forms hydrogen bond with natural ligand, Positioning of H11 and folding of the active conformation
Y401	saturated	Helix 11	4-5	Binding of H11 and H12 and folding of AF-2 surface (Hydrophobic interaction with H12)
F422	FSYCLPHRITNSVADG	Helix 12	4-5	Packing of H12 against H3, H4/5 and H11 and folding of AF-2 surface

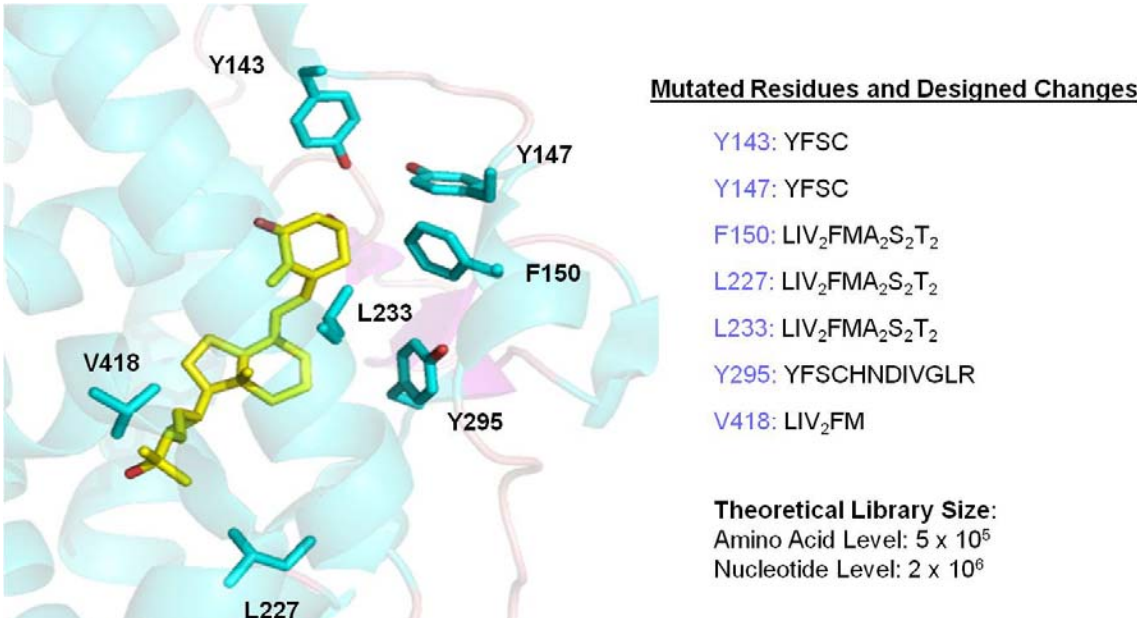

Figure 3.3: Rational Mutagenic Approach: Design for hVDR Library 2
Mutated hVDR Residues (Cyan), 1α, 25$(OH)_2D_3$ (Yellow), PDB:1DB1
Subscripts indicate amino acids that appear with more than one codon at the randomized amino acid position and are represented multiple times in the design.

Table 3.2: Rational Mutagenic Approach hVDR Library 2: Mutated Residues and Their Predicted Functions [8-10]

Residue	Designed Changes	Location	Distance from ligand (Å)	Predicted Functions
Y143	YFSC	Helix 1	<3	Forms hydrogen bond with natural ligand, Ligand mediated folding
Y147	YFSC	Loop 1-3	3-4	Ligand mediated folding
F150	$LIV_2FMA_2S_2T_2$	Loop 1-3	4-5	Ligand mediated folding
L227	$LIV_2FMA_2S_2T_2$	Helix 3	3-4	Folding of AF-2 surface
L233	$LIV_2FMA_2S_2T_2$	Helix 3	3-4	Ligand holding
Y295	YFSCHNDIVGLR	β-turn	3-4	Ligand mediated folding
V418	LIV_2FM	Helix 12	3-4	Ligand mediated folding of AF-2 surface

(Figure 3.3 and Table 3.2). Overall, these residues were predicted to be important for the function of the hVDR and hypothesized to exhibit low tolerance for mutation.

As previously mentioned, mutations at each position targeted for mutagenesis were designed based on amino acid properties and sequencing alignments of the hVDR with other NRs. Overall, hydrophobic residues were mutated to residues with similar chemical properties, maintaining the hydrophobicity of the LBP. For example, residues I271 and V418 were mutated to leucine, isoleucine, valine, phenylalanine and methionine. Residue Y401 is a conserved leucine in PXR, RXRα and ERα; thus this residue was saturated with all amino acids to explore whether amino acids besides tyrosine or leucine would be tolerated in the hVDR. Residue Y295 on the other hand is conserved among PXR and the hVDR, but is a valine in RXRα and a leucine in ERα. As a result, this position was mutated to amino acids of similar properties such as serine, phenylalanine and isoleucine, as well as residues of significantly different properties such aspartic acid and arginine. The theoretical library size at the amino acid level for library 1 was 5 x 10^6 variants, and 5 x 10^5 variants for library 2 (Figures 3.2 and 3.3).

3.2.2 Rational Mutagenic Approach: Library Construction and Selection of hVDR Libraries 1 & 2 in Chemical Complementation

The variants of each hVDR library were constructed using oligonucleotides with randomized degenerate codons at the chosen mutation sites (Tables 3.3 and 3.4). These synthetic oligonucleotides (oligos) were designed to contain overlapping complementary ends with the former and latter oligonucleotide in sequence, forming a full insert cassette via a combination of hybridization and PCR [15]. The 5’ and 3’ ends of the full insert cassette also contained complementary sequences (~100 bp) to the background plasmid (pGBDhVDRBackground), a vector used for decreasing the

expression of the wild-type hVDR (wthVDR) in the libraries. This yeast expression plasmid contains the Gal4 DNA binding domain (DBD) fused to a portion of the hVDR followed by a random sequence of DNA that introduces multiple STOP codons. This results in a non-functional protein when translated and therefore decreases the presence of the wthVDR in the libraries. Once transformed into the PJ69-4A yeast strain, through homologous recombination, the insert cassettes and digested background plasmid recombine generating yeast expression plasmids that contain the Gal4 DBD fused to the hVDR variants, and a tryptophan marker (Figure 3.4).

For each hVDR library, the full insert cassette, the digested background plasmid (pGBDhVDRBackground), and the yeast expression plasmid pGAD10BAACTR (containing a leucine marker and the Gal4 activation domain (GAD) fused to the activator for thyroid and retinoid receptors (ACTR)), were transformed into the PJ69-4A yeast strain. Transformants were plated onto non-selective synthetic complete agar plates lacking leucine and tryptophan (SC-LW) to select for both plasmids and to determine whether homologous recombination occurred. As discussed in Chapter 2, the PJ69-4A yeast strain contains the *HIS3* and *ADE2* genes, essential genes in the corresponding histidine or adenine biosynthetic pathway, under the control of Gal4 response elements. As a result, transformants were also plated onto adenine or histidine selective agar plates (SC-ALW or SC-HLW+0.1mM 3AT) containing β-lactam antibiotics and several additional small molecule ligands. The first ligand set contained amoxicillin, cloxacillin, and penicillin G, as well as, 17-β-estradiol (ligand for ER) and γ-1-oxo-pyrenebutyric acid (Figure 3.1a). The second ligand set contained ampicillin and oxacillin, as well as, hexestrol (ligand for ER), 9-*cis* retinoic acid (ligand for RXR), and resveratrol (a natural product) (Figure 3.1a). LCA and chole were put on individual plates.

Table 3.3: Rational Mutagenic Approach hVDR Library 1: Oligonucleotides Containing Randomized Degenerate Codons at the Designated Mutation Sites

Oligonucleotide	Oligonucleotide Sequences 5'→3' (overlap regions underlined (T_Ms≈ 52-57 ºC) and mutation sites highlighted)
1	ATGATCCTGAAGCGGAAGGAGGAGGAGGCCTTGAAGGACAGTCTGCGGCCCAAGCTGTCTGAGGA
2	ATGGTGGGCGTCCAGCAGTATGGCAATGATGCGCTGCTGCTCCTCAGACAGCTTGGGCC
3	TGCTGGACGCCCACCATAAGACCTACGACCCCACCTACTCCGACTTCTGCCAGTTCCGGCCTCCAGTTCGT
4	AGCTGGGACAGCTCTAGGGTCACAGAAGGGTCATCTGAATCTTCTTCACTCAGATCCAGATTGGAGAAGCTGGAC GAGTCCATCATGTCTGAAGAGGTGATACAGTGATCTGAGCAGGAGGAGGAGGAGTCCCCAGAGAAGCTGGGAGT GTGTCTGGAGTTGGGCCTGGAAGGATGGCTCCCTCCACCATCATTCACACGAACTGGAGGCCGGAA
5	TGACCCTAGAGCTGTCCCAGCTCTCCATGCTGCCCCACCTGGCTGACCTGGTCAGTTACWBCDYSCAAAAGGTCA TTGGCTTTGCTAAGATGATAC S237 I238
6	AATGGCACTTGACTTCAGCAGTACGATCTGGTCCTCAGAGGTGAGGTCTCTGAATCCTGGTATCATCTTAGCAAAG CCAATGA
7	CTGCTGAAGTCAAGTGCCATTGAGGTCDTSATGTTGDBSTCCAATGAGTCCTTCACCATGGACGACATGTCCTGGA CCTG I271 R274
8	CCAGGCTGTGTCCGGCTTTGGTCACGTCACTGACGCGGTACTTGTAGTCTTGGTTGCCACAGGTCCAGGACATGT CGTCC
9	AGCCGGACACAGCCTGGAGCTGATTGAGCCCCTCATCAAGTTCCAGGTGGGACTGAAGAAGCTGAACTTGCATGA GGAGGAGCATGTCCTGCTCATGGCCATCTGCATCGTCTCCCCAGATCGTCCTGGGGTGCAGGACGCCGCGCTGA TTGAGGCCATCCAGGACCGCCTGTCCAACACACTGCAGACGTACATCCGCTGCCGCCACCCGCCCCCGGGCAGC CACCTGCTCTATGCCAAGATGATCCAGAAGCTAGCCGACCTGCGCAGCCTCA
10	ATGCTGCACTCAGGCTGGAAGGAGAGGCAGCGMNNCTGCTTGGAMTDCTCCTCATTGAGGCTGCGCAGGTCG Y401 H397
11	TTCCAGCCTGAGTGCAGCATGAAGCTAACGCCCCTTGTGCTCGAAGTGNNTGGCAATGAGATCTCCTGAACTAGT CCATCCTTTG F422
12	CGTCCAGGCAGGGTGGCCAGAACGGGTGGGCACAAAGGATGGACTAGTTCAGGAGATCT
13	GCCACCCTGCCTGGACGCCAGCTGTTCTTCTCAGCCTGAGCCCTGTCCCTG
14	TGACAGGCTGTGCCCCAAAGTCCAAACAGGCCAGGCAGAGAAGGGCAGGGACAGGGCTCAGGCT

Table 3.4: Rational Mutagenic Approach hVDR Library 2: Oligonucleotides Containing Randomized Degenerate Codons at the Designed Mutation Sites

Oligonucleotide	Oligonucleotide Sequences 5'→3' (overlap regions underlined (T_Ms≈ 52-57 ºC) and mutation sites highlighted)
1	ATGATCCTGAAGCGGAAGGAGGAGGAGGCCTTGAAGGACAGTCTGCGGCCCAAGCTGTCTGAGGA
2	ATGGTGGGCGTCCAGCAGTATGGCAATGATGCGCTGCTGCTCCTCAGACAGCTTGGGCC
3	TGCTGGACGCCCACCATAAGACCTNCGACCCCACCTNCTCCGACDYSTGCCAGTTCCGGCCTCCAGTTCGT Y143 Y147 F150
4	AGCTGGGACAGCTCTAGGGTCACAGAAGGGTCATCTGAATCTTCTTCACTCAGATCCAGATTGGAGAAGCTGGAC GAGTCCATCATGTCTGAAGAGGTGATACAGTGATCTGAGCAGGAGGAGGAGGAGTCCCCAGAGAAGCTGGGAGT GTGTCTGGAGTTGGGCCTGGAAGGATGGCTCCCTCCACCATCATTCACACGAACTGGAGGCCGGAA
5	TGACCCTAGAGCTGTCCCAGCTCTCCATGDYSCCCCACCTGGCTGACDYSGTCAGTTACAGCATCCAAAAGGTCA TTGGCTTTGCTAAGATGATAC L227 L233
6	AATGGCACTTGACTTCAGCAGTACGATCTGGTCCTCAGAGGTGAGGTCTCTGAATCCTGGTATCATCTTAGCAAAG CCAATGA
7	CTGCTGAAGTCAAGTGCCATTGAGGTCATCATGTTGCGCTCCAATGAGTCCTTCACCATGGACGACATGTCCTGG ACCTG
8	CCAGGCTGTGTCCGGCTTTGGTCACGTCACTGACGCGGHNCTTGTAGTCTTGGTTGCCACAGGTCCAGGACATGT CGTCC Y295
9	AGCCGGACACAGCCTGGAGCTGATTGAGCCCCTCATCAAGTTCCAGGTGGGACTGAAGAAGCTGAACTTGCATGA GGAGGAGCATGTCCTGCTCATGGCCATCTGCATCGTCTCCCCAGATCGTCCTGGGGTGCAGGACGCCGCGCTGA TTGAGGCCATCCAGGACCGCCTGTCCAACACACTGCAGACGTACATCCGCTGCCGCCACCCGCCCCCGGGCAGC CACCTGCTCTATGCCAAGATGATCCAGAAGCTAGCCGACCTGCGCAGCCTCA
10	ATGCTGCACTCAGGCTGGAAGGAGAGGCAGCGGTACTGCTTGGAGTGCTCCTCATTGAGGCTGCGCAGGTCG
11	TTCCAGCCTGAGTGCAGCATGAAGCTAACGCCCCTTDTSCTCGAAGTGTTTGGCAATGAGATCTCCTGAACTAGTC CATCCTTTG V418
12	CGTCCAGGCAGGGTGGCCAGAACGGGTGGGCACAAAGGATGGACTAGTTCAGGAGATCT
13	GCCACCCTGCCTGGACGCCAGCTGTTCTTCTCAGCCTGAGCCCTGTCCCTG
14	TGACAGGCTGTGCCCCAAAGTCCAAACAGGCCAGGCAGAGAAGGGCAGGGACAGGGCTCAGGCT

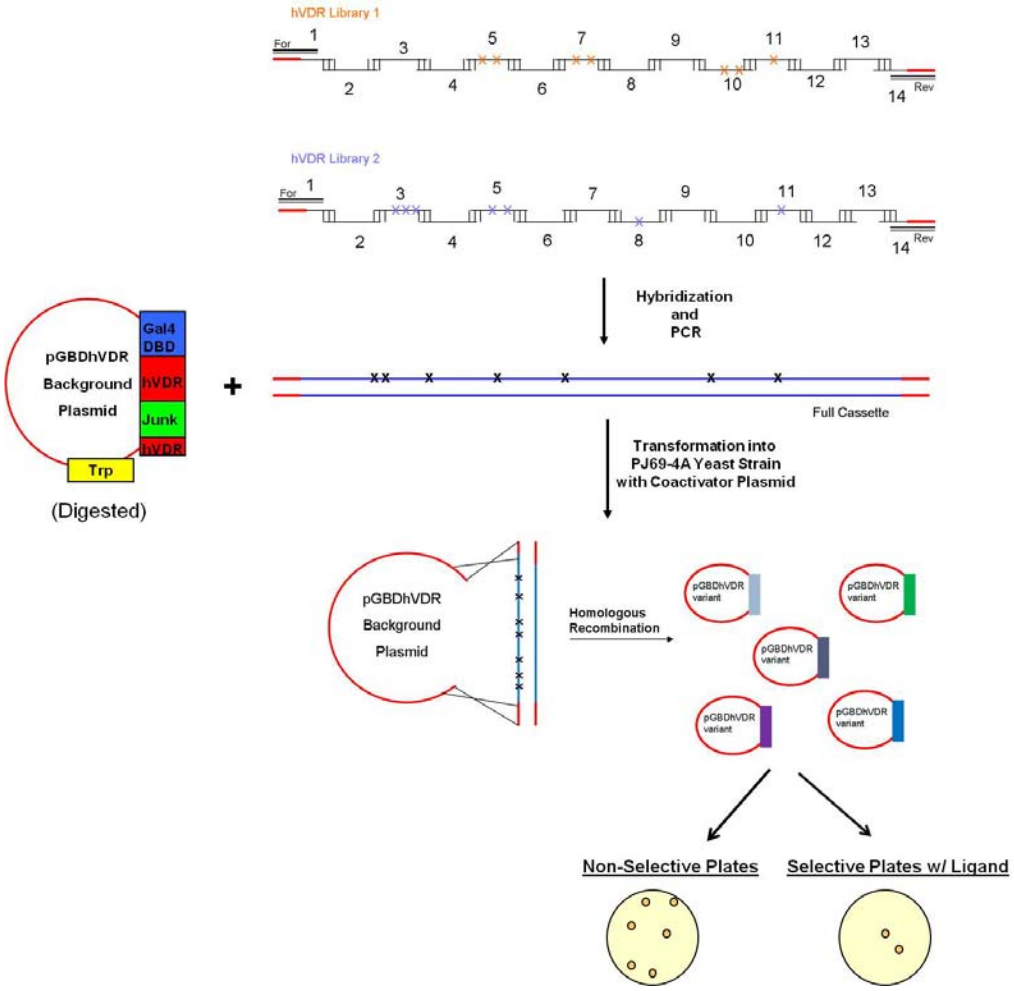

Figure 3.4: Using Hybridization and PCR to Create Full Insert Cassettes, Construction of the Background Plasmid and Transformation into PJ69-4A for hVDR Libraries 1 & 2

Rational Mutagenic Approach: Results for hVDR Libraries 1 & 2

The non-selective (SC-LW) plates were used to determine the experimental library size at the amino acid level and transformation efficiency of each hVDR library. The transformation produced a library size of 3.7 x 10^3 variants with a 6.15 x 10^4 cfu/µg plasmid DNA transformation efficiency for library 1, and 5.3 x 10^3 variants and 1.08 x 10^5 cfu/µg plasmid DNA for library 2, respectively. Potentially ligand activated variants selected from the various ligand plates (~2-3 % of each experimental library) were re-tested on solid media plates for constitutive activity. Constitutive activity is growth observed in selective media without the presence of an exogenous small molecule ligand. For each hVDR library, selective colonies were streaked onto non-selective plates (SC-LW), as well as adenine and histidine selective plates (SC-ALW and SC-HLW+0.1 mM 3-AT) with and without ligand. A subset of variants was also tested in liquid quantitation assays of chemical complementation (data not shown). Streaking indicated that most of the variants were constitutively active, displaying growth on selective plates lacking ligand, as shown in Figure 3.5.

Twelve variants from each hVDR library were submitted for sequencing, and over 95 % of the sequenced variants contained frame-shift mutations due to random insertions and deletions of bases. After careful evaluation of all the sequences, the majority of the sequenced variants displayed insertions and deletions in the overlap regions between oligos, indicating a failure in the hybridization and PCR protocol. Several strategies were pursued in an attempt to solve this problem.

3.2.3 Rational Mutagenic Approach: Troubleshooting hVDR Libraries 1 & 2 Using Klenow Polymerase

The first strategy to reduce the number of frame-shifts observed in the rationally designed libraries was using *Klenow* polymerase to create the full insert cassette of each

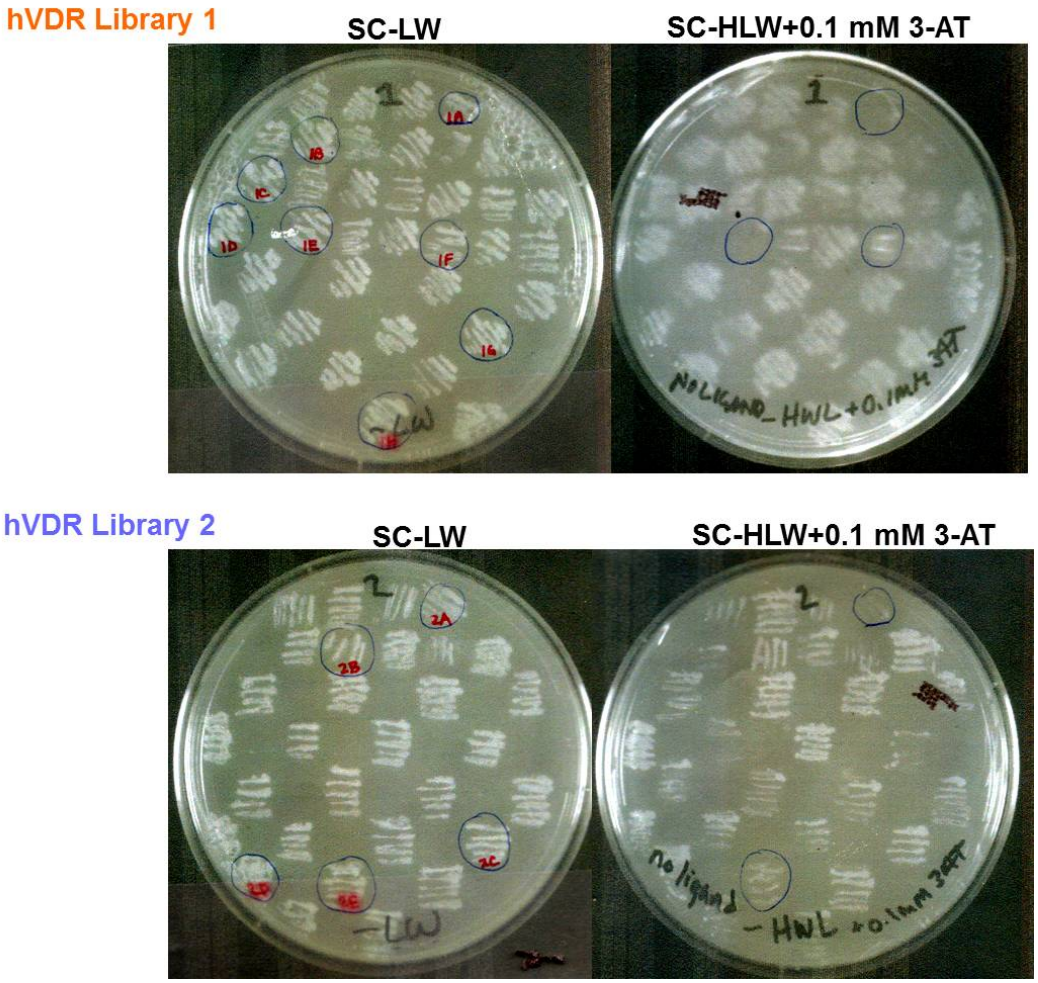

Figure 3.5: Rational Mutagenic Approach: Streaking for hVDR Library 1 & 2 Variants Most of the variants were constitutively active, displaying growth on selective plates lacking ligand. Please disregard circles.

library. Like *Pfu*, *Klenow* is a high fidelity polymerase facilitating DNA synthesis with a reduced error frequency, compared to other polymerases [16, 17]. A combination of *Klenow* and *Pfu* was used, where the hybridization step was followed by an extension step, with *Klenow* completing the overhang pieces of DNA from the 5' to 3' direction [17]. *Klenow* instead of *Pfu* in essence should reduce the number of insertions and deletions. The number of cassettes was exponentially amplified via PCR, with *Pfu* and the corresponding forward and reverse primers. Several conditions with *Klenow* were used to construct the full insert cassette of hVDR libraries 1 & 2: (1) varying the concentration of each oligo and primers (2) varying the number of oligos combined at a time (3) varying PCR conditions for the amplification step (e.g. annealing temperature and number of cycles) and (4) using longer amplification primers. Small cassettes were successfully created using *Klenow* polymerase, however the full insert cassette (1096 bp) of each hVDR library was not obtained. Most of the conditions resulted in smaller cassettes or smears when analyzed on agarose gels, as shown in Figure 3.6.

3.2.4 Rational Mutagenic Approach: Troubleshooting hVDR Libraries 1 & 2 Using Commercial Pfu Polymerase

Another strategy taken to reduce the number of frame-shifts observed in the rationally designed libraries was the use of a commercial *Pfu* polymerase (Stratagene, Santa Clara, CA), instead of the *Pfu* polymerase expressed and purified in-house. Several conditions (as described above for *Klenow* polymerase) using a combination of *Klenow* and the commercial *Pfu* were used to create the full insert cassette of each library, but yielded no success. However, cassettes 1 (oligos 1-8, 607 bp) (Figure 3.7a, lanes 2 and 4) and cassettes 2 (oligos 9-14, 506 bp) (Figure 3.7a, lanes 3 and 5) were successfully made and combined using the commercial *Pfu* alone to form the full insert cassette (oligos 1-14, 1096 bp) of hVDR libraries 1 & 2 (Figure 3.7b, lanes 2-5).

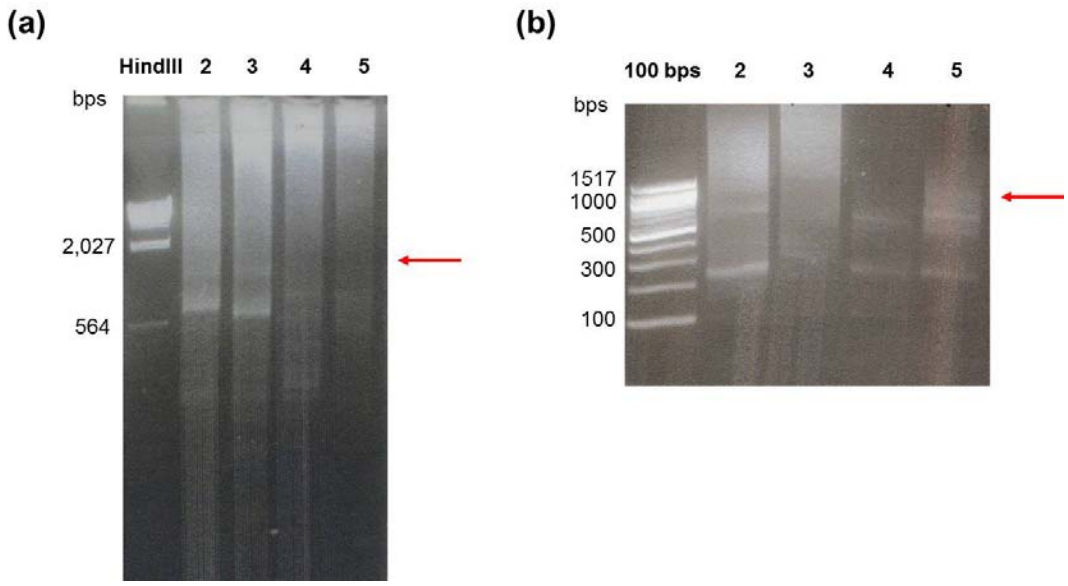

Figure 3.6: Rational Mutagenic Approach hVDR Libraries 1 & 2: Examples of Cassette Products Obtained Using *Klenow* Polymerase
(a) **Lane 1:** λ DNA-HindIII marker, **Lane 2:** cassette 1 (oligos 1-8) + oligos 9, 10, 11, 12, 13 and 14 for hVDR library 1, **Lane 3:** same as lane 2, except for hVDR library 2, **Lane 4:** cassette 1(oligos 1+2) + cassette 2 (oligos 3+4) + cassette 3 (oligos 5+6) + cassette 4 (oligos 7+8) + oligos 9, 10, 11, 12, 13 and 14 for hVDR Library 1, **Lane 5:** same as lane 4, except for hVDR Library 2
(b) **Lane 1:** 100 bp marker, **Lane 2:** cassette 1(oligos 1-8) + cassette 2 (oligos 9+10) + cassette 3 (oligos 11+12) + oligos 13 and 14, **Lane 3:** same as lane 2, except for hVDR library 2, **Lane 4:** cassette 1 (oligos 1+2) + cassette 2 (oligos 3+4) + cassette 3 (oligos 5+6) + cassette 4 (oligos 7+8) + cassette 5 (9+10) + cassette 6 (oligos 11+12) + oligos 13 and 14, **Lane 5:** same as lane 4, except for hVDR library 2.
The full insert cassette (1096 bp) of each library was not obtained, but was expected in lanes 2-5 where the red arrows are shown.

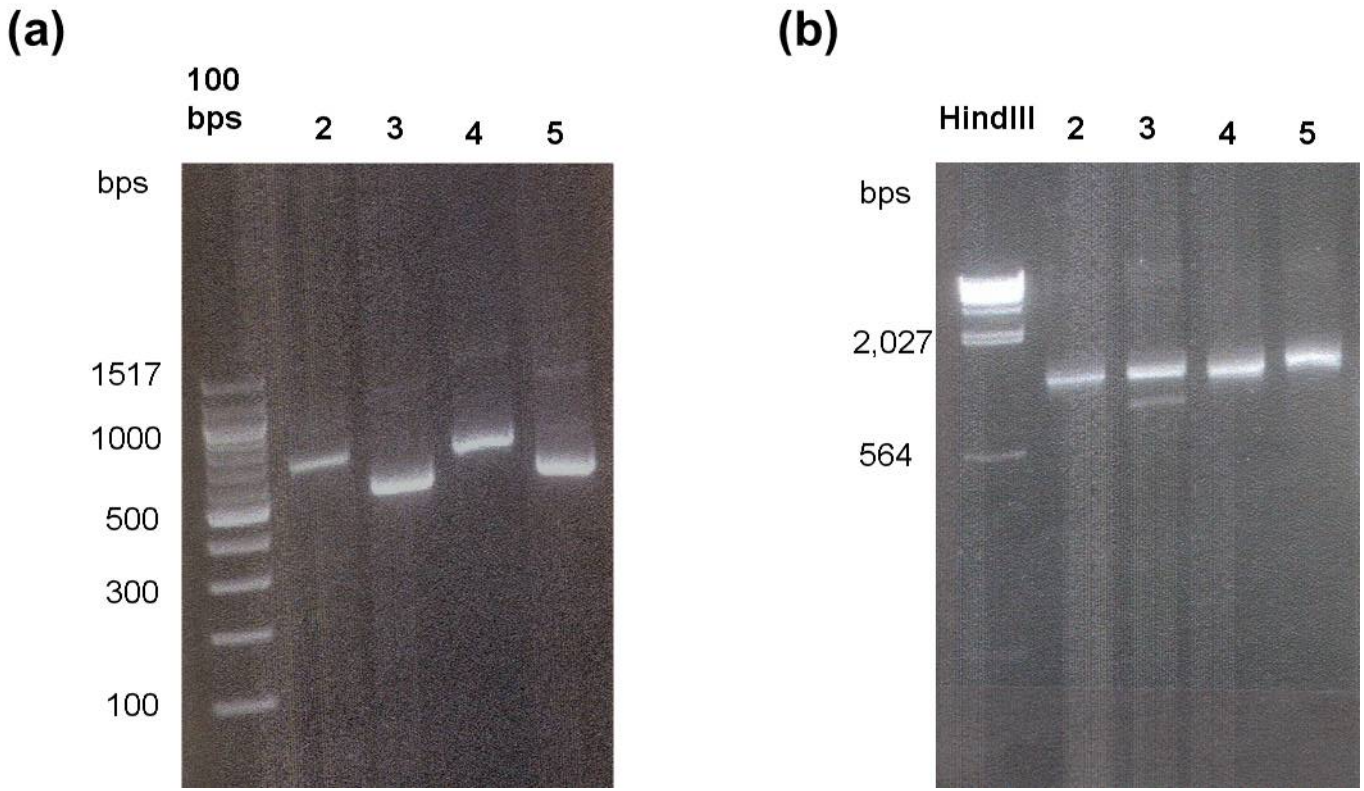

Figure 3.7: Rational Mutagenic Approach hVDR Libraries 1 & 2: Cassette Products Obtained Using Commercial *Pfu* Polymerase
(a) **Lane 1:** 100 bp marker, **Lane 2:** cassette 1 (oligos 1-8) for hVDR library 1, **Lane 3:** cassette 2 (oligos 9-14) for hVDR library 1, **Lane 4:** same as lane 2, except for hVDR library 2, **Lane 5:** same as lane 3, except for hVDR library 2. Cassettes 1 are 607 bp and cassettes 2 are 506 bp.
(b) **Lane 1:** λ DNA-HindIII marker, **Lanes 2 and 3:** cassettes 1 + 2 (full insert cassette) for hVDR library 1, **Lanes 4 and 5:** same as lanes 2 and 3, except for hVDR library 2. The full insert cassettes are 1096 bp.

For each hVDR library, the full insert cassette (3.5 µg), the digested background plasmid (pGBDhVDRBackground) (1 µg), and the coactivator plasmid (pGAD10BAACTR) (1 µg) were transformed into the PJ69-4A yeast strain. Transformants were plated onto non-selective agar plates (SC-LW), as well as adenine and histidine selective agar plates (SC-ALW and SC-HLW+0.1 mM 3-AT) with ligand sets containing β-lactam antibiotics and several additional small molecule ligands, as previously mentioned (Section 3.2.2).

Rational Mutagenic Approach: Results for hVDR Libraries 1 & 2 (using commercial Pfu)

The non-selective plates (SC-LW) were used to determine the experimental library size (at the amino acid level, ~10^2-10^3 variants for each library) and transformation efficiency (~1.4 x 10^4 cfu/µg plasmid DNA for each library) of each hVDR library. Potentially ligand activated variants selected from the histidine selective ligand set 2 and LCA plates (~5 % of each experimental library) were re-tested on solid media plates for constitutive activity, as previously discussed.

While most variants (~75-80 % of the tested variants) were non-functional (Figure 3.8, circled in yellow) or constitutively active (Figure 3.8, circled in red), some showed ligand activated growth with LCA on histidine selective plates (Figure 3.8, circled in blue). A subset of these variants (22 variants) was also tested in liquid quantitation assays of chemical complementation. However, as shown in Figure 3.9 very little to no ligand activated growth was observed for these variants with LCA in histidine selective media. As previously observed, ligand activated growth for the wild-type hVDR was obtained with 10 µM LCA (blue growth profile) (Figure 3.9). Gal4 is a ligand independent transcription factor and was used as a positive control.

Twelve variants from each hVDR library were submitted for sequencing (Tables

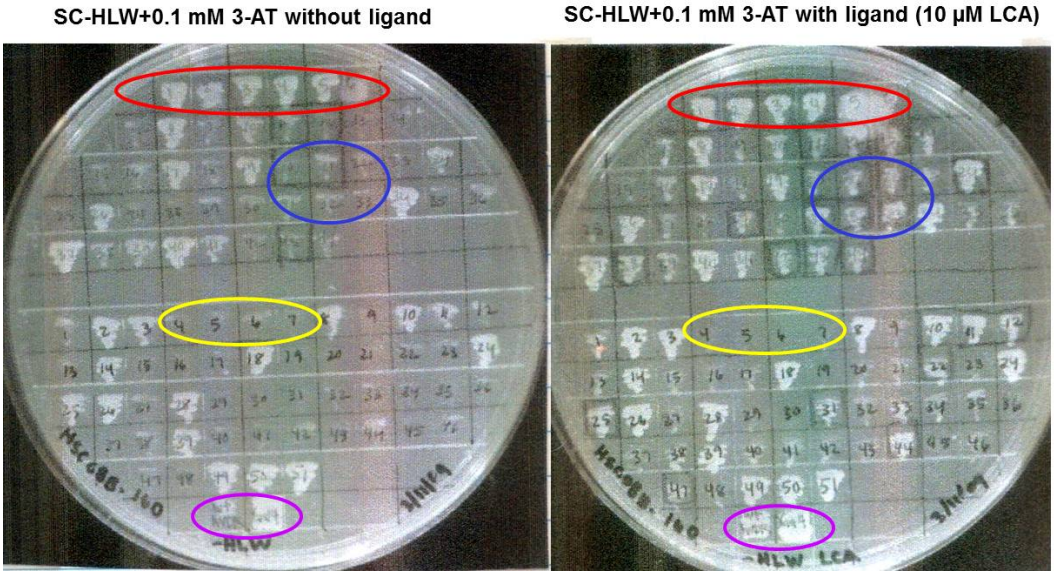

Figure 3.8: Rational Mutagenic Approach: Streaking for hVDR Library 1 & 2 Variants (using commercial *Pfu)* Examples of non-functional variants are circled in yellow, of constitutively active variants are circled in red and of ligand activated variants are circled in blue. The controls, wild-type hVDR (left) and Gal4 (right) are circled in purple.

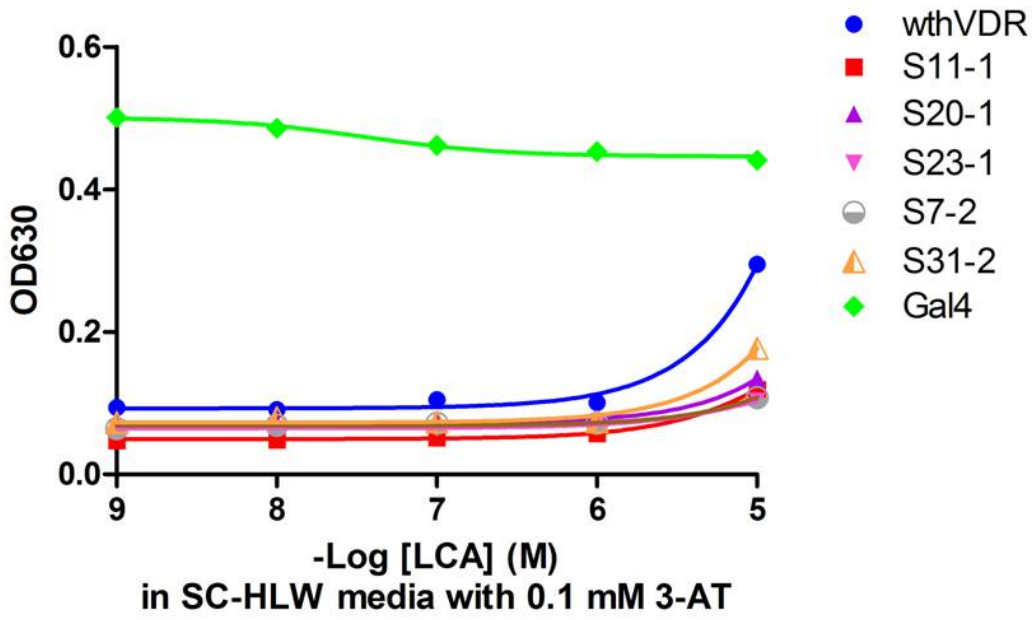

Figure 3.9: Rational Mutagenic Approach: hVDR Library 1 & 2 Variants (obtained using commercial *Pfu*) in Chemical Complementation
Histidine selective media with LCA

3.5 and 3.6). Overall, both libraries showed mutational diversity at the mutated positions. For example, positions S237, I271 and H397 from hVDR library 1 and positions Y143 and L277 from hVDR library 2 (Tables 3.5 and 3.6) had most of the amino acids designed at those positions appear in the obtained variants. Despite the mutational diversity, again a high percentage (~55-65 %) of the sequenced variants showed frame-shifts caused by random insertions and deletions of bases.

3.3 Random Mutagenic Approach: hVDR Error-Prone PCR Libraries

In order to overcome the five angstroms bias introduced in the rational mutagenic approach and to determine if selective pressure would allow for the directed evolution of variants with mutations outside of those explored in the designed libraries, error-prone PCR (epPCR) was used for the random mutagenic approach. Error-prone PCR involving the use of *Taq* polymerase was the method of choice for random mutagenesis, as this approach has successfully been used to engineer new receptor-ligand pairs [18]. *Taq* lacks proof-reading capabilities, hence the high number of random errors [17, 19]. In this epPCR approach, $MnCl_2$ was used as a method to control the fidelity of the polymerase [20]. Manganese is very similar in properties to magnesium, the cofactor for *Taq* polymerase. As a result, both metals compete for binding with the polymerase. Manganese binding decreases the fidelity of the polymerase, increasing the number of mutations. Various concentrations of $MnCl_2$ (2-500 μM) were used to amplify the hVDR LBD (full insert cassette) via PCR.

For each hVDR library, the full insert cassette, the digested background plasmid (pGBDhVDRBackground), and the coactivator plasmid (pGAD10BAACTR) were transformed into the PJ69-4A yeast strain. Transformants were plated onto non-selective agar plates (SC-LW), as well as adenine and histidine selective agar plates (SC-ALW and SC-HLW+0.1 mM 3-AT) with ligand sets containing β-lactam antibiotics and several

Table 3.5: Rational Mutagenic Approach: hVDR Library 1 (using commercial *Pfu*) Sequencing Results

Possible Changes:	S_2TCFI	$LIV_2FMA_2S_2T_2$	LIV_2FM	$LIV_2FMA_2S_3T_2CRWG_2$	HYNKQstop	saturated	FSYCLPHRITNSVADG
Residue:	**S237**	**I238**	**I271**	**R274**	**H397**	**Y401**	**F422**
Nonselective Variants							
*NS1	S	S	L	V	Q	T	L
NS2	S	A	L	G	H	Y	A
*NS4	I	A	V	V	H	T	G
*NS6	C	T	wt	G	K	P	wt
*NS7	C	A	V	L	N	R	R
*NS9	C	A	V	V	Y	K	L
Selective Variants							
*S3	T	A	F	L	N	I	C
S11	T	M	V	L	K	I	V
*S12	S	A	V	G	K	Q	L
*S15	S	F	M	V	N	P	wt
S20	F	S	V	R	K	H	S
S23	S	L	F	V	Y	I	A

*= Variant contains insertions/deletions
Blue= Silent Mutation

Table 3.6: Rational Mutagenic Approach: hVDR Library 2 (using commercial *Pfu*) Sequencing Results

Possible Changes:	YFSC	YFSC	$LIV_2FMA_2S_2T_2$	$LIV_2FMA_2S_2T_2$	$LIV_2FMA_2S_2T_2$	YFSCHNDIVGLR	LIV_2FM
Residue:	**Y143**	**Y147**	**F150**	**L227**	**L233**	**Y295**	**V418**
Nonselective Variants							
NS2	C	C	wt	A	wt	N	wt
*NS3	S	C	V	V	S	N	F
*NS4	S	F	V	T	V	wt	wt
NS6	C	C	A	wt	S	R	wt
*NS10	S	S	V	wt	wt	L	wt
Selective Variants							
*S1	S	C	wt	wt	wt	H	L
S7	S	C	A	wt	wt	I	wt
S10	S	C	L	V	T	L	F
*S13	C	S	S	wt	V	N	L
*S22	F	C	L	wt	wt	N	L
S31	S	S	L	L	V	H	wt

*= Variant contains insertions/deletions
Blue= Silent Mutation

additional small molecule ligands, as previously mentioned (Section 3.2.2).

Random Mutagenic Approach: Results for hVDR Error-Prone PCR Libraries

The experimental library size at the amino acid level (~10^2 variants for each library) and transformation efficiency (~10^3-10^4 cfu/µg plasmid DNA for each library) of each hVDR library were determined using the non-selective plates. Potentially ligand activated variants (~5-20 % of each experimental library) from the 2, 20 and 150 µM $MnCl_2$ libraries were re-tested on solid media plates for constitutive activity. For each hVDR library, selective colonies were streaked onto non-selective plates (SC-LW), as well as adenine and histidine selective plates (SC-ALW and SC-HLW+0.1 mM 3-AT) with and without ligand (data not shown). A subset of variants was also tested in liquid quantitation assays of chemical complementation. However, compared to the wild-type hVDR no variant had increased sensitivity for LCA (~EC_{50}>10 µM) in histidine selective media. Again, ligand activated growth for the wild-type hVDR was obtained with 10 µM LCA (blue growth profile) and as expected, Gal4, the positive control grew with and without ligand at an optical density of ~0.5 in histidine selective media (green growth profile), as shown in Figure 3.10.

Twenty variants were submitted for sequencing. As expected, an overall increase in mutations was observed with increasing concentration of $MnCl_2$ (Table 3.7). In addition, the number of frame-shifts was reduced drastically (compared to previous sequencing results), where only ~10 % of the sequenced variants had frame-shifts due to random insertions and deletions of bases.

A comparison of the variants obtained from the two mutagenic approaches tried thus far suggested that the rational libraries contained a large number of mutations at once (seven target residues), over-challenging the receptor's tolerance and resulting in mostly non-functional variants. As shown in Table 3.7 and Figure 3.10, most of the

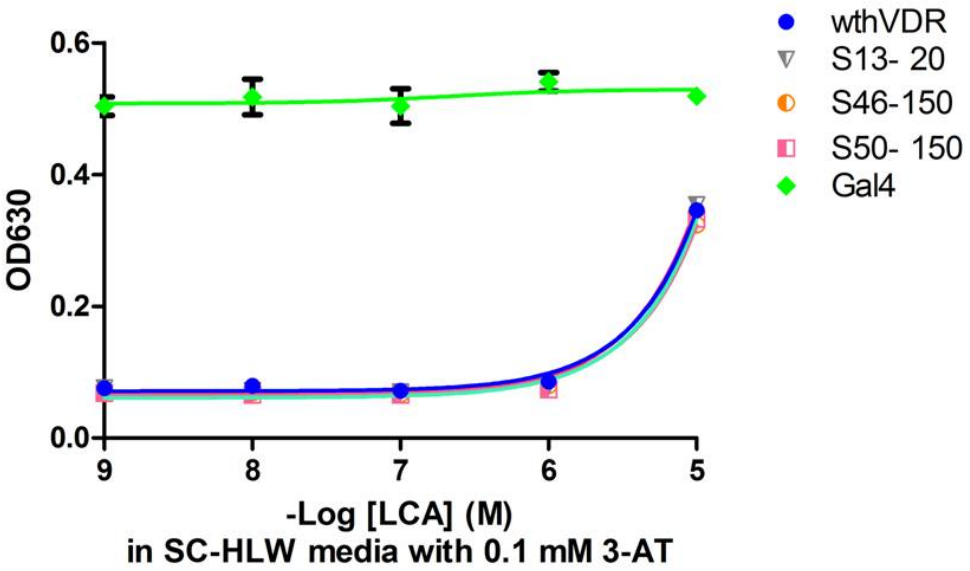

Figure 3.10: Random Mutagenic Approach: hVDR Error-Prone PCR Variants in Chemical Complementation
Histidine selective media with LCA

Table 3.7: Random Mutagenic Approach: hVDR Error-Prone PCR Libraries Sequencing Results

Variant	Mutations
S5-2	wthVDR
NS4-2	S193P
S13-20	D17N
	H189L
NS4-20	M247L
	D357G
	L414P
S46-150	S185P
	S266C
	Q317L
NS8-150	H35Y
	I134T
	L136P
	F178L
S50-150	V270A
NS3-200	L224P
	Q277V
	G304R
	P341S
	R358S

variants obtained from the epPCR libraries contained two or three mutations and ligand activated growth profiles similar to that of the wild-type hVDR were observed for these variants. As a result, we predict that smaller libraries with fewer residues chosen for mutagenesis would be a better approach for discovering functional variants with novel properties.

3.4 Rational Mutagenic Approach: hVDR Subset Libraries B, C, E & F

In an attempt to explore hVDR libraries 1 & 2 further, four smaller subset libraries (hVDR libraries B, C, E & F) were constructed. In this case, one to two residues from each library were targeted for mutagenesis at a time (Figure 3.11). The variants of each hVDR library were constructed using oligonucleotides containing randomized degenerate codons at the chosen mutation sites, as previously described (Tables 3.8, 3.9, 3.10 and 3.11). For each library, the full insert cassette, the digested background plasmid (pGBDhVDRBackground), and the coactivator plasmid (pGAD10BAACTR) were transformed into the PJ69-4A yeast strain. Transformants were plated onto non-selective agar plates (SC-LW), as well as adenine and histidine selective agar plates (SC-ALW and SC-HLW+0.1 mM 3-AT) with ligand sets containing β-lactam antibiotics and several additional small molecule ligands, as previously mentioned (Section 3.2.2).

Rational Mutagenic Approach: Results for hVDR Subset Libraries B, C, E & F

The non-selective SC-LW plates were used to determine the experimental library size at the amino acid level and transformation efficiency of hVDR libraries B, C, E & F. The library size for the various libraries was ~1.6 x 10^3 variants, with a transformation efficiency of ~2.9 x 10^4 cfu/μg plasmid DNA for each library. Due to the small size of these subset libraries (<200 at amino acid and nucleotide level), complete library coverage was obtained. Potentially ligand activated variants selected from the various

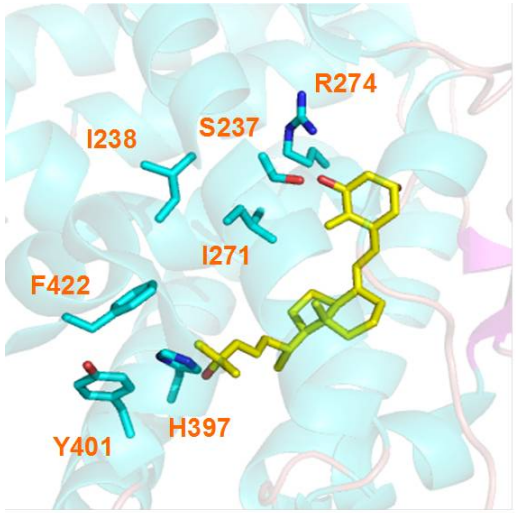

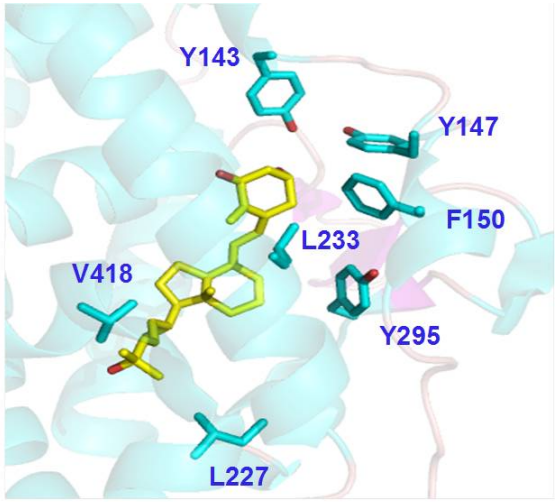

hVDR Subset Library	Mutated Residues and Designed Changes
B	L227: $LIV_2FMA_2S_2T_2$ L233: $LIV_2FMA_2S_2T_2$
C	S237: S_2TCFI I238: $LIV_2FMA_2S_2T_2$
E	Y295: YFSCHNDIVGLR
F	H397: HYNKQStop Y401: Saturated

Figure 3.11: Rational Mutagenic Approach: Design for hVDR Subset Libraries B, C, E & F
hVDR Residues (Cyan), 1α, 25$(OH)_2D_3$ (Yellow), PDB:1DB1, Residues originally from library 1 are labeled orange. Residues originally from library 2 are labeled blue.

Table 3.8: Rational Mutagenic Approach hVDR Subset Library B: Oligonucleotides Containing Randomized Degenerate Codons at the Designed Mutation Sites

Oligonucleotide	Oligonucleotide Sequences 5'→3' (overlap regions underlined (T_Ms≈ 55-59 ºC) and mutation sites highlighted)
1	GATCCTGAAGCGGAAGGAGGAGGAGGCCTTGAAGGACAGTCTGCGGCCCAAGCTGTCTGAGGAGCAGCAGCGC ATCATTGCCATACTGCTGGACGCCCACCATAAGACCTACGACCCCACCTACTCCGACTTCTGCCAGTTCCGGCCT CCAGTTCGTGTGAATGATGGTGGAGGGAGCCATCCTTCCAGGCCCAACTCCAGACACACTCCCAGCTTCTCTGGG GACTCCTCCTCCTCCTGCTCAGATCACTGTATCACCTCTTCAGACATGATGGACTCGTCCAGCTTCTCCAATCTGG ATCTGAGTGAAGAAGATTCAGATGACCCTTCTGTGACCCTAGAGCTGTCCCAGCTCTCCAT
2	AGCAAAGCCAATGACCTTTTGGATGCTGTAACTGACSRHGTCAGCCAGGTGGGGSRHCATGGAGAGCTGGGACA GCTCTAG L233 L227
3	CCAAAAGGTCATTGGCTTTGCTAAGATGATACCAGGATTCAGAGACCTCACCTCTGAGGACCAGATCGTACTGCT GAAGTCAAGTGCCATTGAGGTCATCATGTTGCGCTCCAATGAGTCCTTCACCATGGACGACATGTCCTGGACCTG TGGCAACCAAGACTACAAGTACCGCGTCAGTGACGTGACCAAAGCC
4	TCCCACCTGGAACTTGATGAGGGGCTCAATCAGCTCCAGGCTGTGTCCGGCTTTGGTCACGTCACTGACG
5	CCTCATCAAGTTCCAGGTGGGACTGAAGAAGCTGAACTTGCATGAGGAGGAGCATGTCCTGCTCATGGCCATCTG CATCGTCTCCCCAGATCGTCCTGGGGTGCAGGACGCCGCGCTGATTGAGGCCATCCAGGACCGGGTGTCCAACA CACTGCAGACGTACATCCGCTGCCGCCACCCGCCCCCGGGCAGCCACCTGCTCTATGCCAAGATGATCCAGAAG CTAGCCGACCTGCGCAGCCTCAATG
6	CAGGCTGGAAGGAGAGGCAGCGGTACTGCTTGGAGTGCTCCTCATTGAGGCTGCGCAGGTC
7	CTGCCTCTCCTTCCAGCCTGAGTGCAGCATGAAGCTAACGCCCCTTGTGCTCGAAGTGTTTGGCAATGAGAT
8	GTCCAGGCAGGGTGGCCAGAACGGGTGGGCACAAAGGATGGACTAGTTCAGGAGATCTCATTGCCAAACACTTC GAG

Table 3.9: Rational Mutagenic Approach hVDR Subset Library C: Oligonucleotides Containing Randomized Degenerate Codons at the Designed Mutation Sites

Oligonucleotide	Oligonucleotide Sequences 5'→3' (overlap regions underlined (T_Ms≈ 55-57 ºC) and mutation sites highlighted)
1	GATCCTGAAGCGGAAGGAGGAGGAGGCCTTGAAGGACAGTCTGCGGCCCAAGCTGTCTGAGGAGCAGCAGCGC ATCATTGCCATACTGCTGGACG
2	CTGGCAGAAGTCGGAGTAGGTGGGGTCGTAGGTCTTATGGTGGGCGTCCAGCAGTATGGCAATGA
3	CACCTACTCCGACTTCTGCCAGTTCCGGCCTCCAGTTCGTGTGAATGATGGTGGAGGGAGCCATCCTTCCAGGCC CAACTCCAGACACACTCCCAGCTTCTCTGGGGACTCCTCCTCCTCCTGCTCAGATCACTGTATCACCTCTTCAGAC ATGATGGACTCGTCCAGCTTCTCCAATCTGGATCTGAGTGAAGAAGATTCAGATGACCCTTCTGTGACCCTAGAGC TGTCCCAGCTCTCCATGCTGCCCCACCTGGCTGACCTGGTCAG
4	AGGTGAGGTCTCTGAATCCTGGTATCATCTTAGCAAAGCCAATGACCTTTTGSRHGVWGTAACTGACCAGGTCAG CCAGGTG I238 S237
5	ATACCAGGATTCAGAGACCTCACCTCTGAGGACCAGATCGTACTGCTGAAGTCAAGTGCCATTGAGGTCATCATG TTG
6	TTGTAGTCTTGGTTGCCACAGGTCCAGGACATGTCGTCCATGGTGAAGGACTCATTGGAGCGCAACATGATGACC TCAATGGCAC
7	ACCTGTGGCAACCAAGACTACAAGTACCGCGTCAGTGACGTGACCAAAGCCGGACACAGCCTGGAGCTGATTGA GCC
8	CATTGAGGCTGCGCAGGTCGGCTAGCTTCTGGATCATCTTGGCATAGAGCAGGTGGCTGCCCGGGGGCGGGTG GCGGCAGCGGATGTACGTCTGCAGTGTGTTGGACAGGCGGTCCTGGATGGCCTCAATCAGCGCGGCGTCCTGCA CCCCAGGACGATCTGGGGAGACGATGCAGATGGCCATGAGCAGGACATGCTCCTCCTCATGCAAGTTCAGCTTC TTCAGTCCCACCTGGAACTTGATGAGGGGCTCAATCAGCTCCAGGCT
9	GACCTGCGCAGCCTCAATGAGGAGCACTCCAAGCAGTACCGCTGCCTCTCCTTCCAGCCTG
10	GTCCAGGCAGGGTGGCCAGAACGGGTGGGCACAAAGGATGGACTAGTTCAGGAGATCTCATTGCCAAACACTTC GAGCACAAGGGGCGTTAGCTTCATGCTGCACTCAGGCTGGAAGGAGAGGCA

Table 3.10: Rational Mutagenic Approach hVDR Subset Library E: Oligonucleotides Containing Randomized Degenerate Codons at the Designed Mutation Sites

Oligonucleotide	Oligonucleotide Sequences 5'→3' (overlap regions underlined (T_Ms≈ 55-57 °C) and mutation sites highlighted)
1	GATCCTGAAGCGGAAGGAGGAGGAGGCCTTGAAGGACAGTCTGCGGCCCAAGCTGTCTGAGGAGCAGCAGCGC ATCATTGCCATACTGCTGGACG
2	CTGGCAGAAGTCGGAGTAGGTGGGGTCGTAGGTCTTATGGTGGGCGTCCAGCAGTATGGCAATGA
3	CACCTACTCCGACTTCTGCCAGTTCCGGCCTCCAGTTCGTGTGAATGATGGTGGAGGGAGCCATCCTTCCAGGCC CAACTCCAGACACACTCCCAGCTTCTCTGGGGACTCCTCCTCCTCCTGCTCAGATCACTGTATCACCTCTTCAGAC ATGATGGACTCGTCCAGCTTCTCCAATCTGGATCTGAGTGAAGAAGATTCAGATGACCCTTCTGTGACCCTAGAGC TGTCCCAGCTCTCCATGCTGCCCCACCTGGCTGACCTGGTCAG
4	AGGTGAGGTCTCTGAATCCTGGTATCATCTTAGCAAAGCCAATGACCTTTTGGATGCTGTAACTGACCAGGTCAGC CAGGTG
5	ATACCAGGATTCAGAGACCTCACCTCTGAGGACCAGATCGTACTGCTGAAGTCAAGTGCCATTGAGGTCATCATG TTG
6	TTGTAGTCTTGGTTGCCACAGGTCCAGGACATGTCGTCCATGGTGAAGGACTCATTGGAGCGCAACATGATGACC TCAATGGCAC
7	ACCTGTGGCAACCAAGACTACAAGNDCCGCGTCAGTGACGTGACCAAAGCCGGACACAGCCTGGAGCTGATTGA GCC Y295
8	CATTGAGGCTGCGCAGGTCGGCTAGCTTCTGGATCATCTTGGCATAGAGCAGGTGGCTGCCCGGGGGCGGGTG GCGGCAGCGGATGTACGTCTGCAGTGTGTTGGACAGGCGGTCCTGGATGGCCTCAATCAGCGCGGCGTCCTGCA CCCCAGGACGATCTGGGGAGACGATGCAGATGGCCATGAGCAGGACATGCTCCTCCTCATGCAAGTTCAGCTTC TTCAGTCCCACCTGGAACTTGATGAGGGGCTCAATCAGCTCCAGGCT
9	GACCTGCGCAGCCTCAATGAGGAGCACTCCAAGCAGTACCGCTGCCTCTCCTTCCAGCCTG
10	GTCCAGGCAGGGTGGCCAGAACGGGTGGGCACAAAGGATGGACTAGTTCAGGAGATCTCATTGCCAAACACTTC GAGCACAAGGGGCGTTAGCTTCATGCTGCACTCAGGCTGGAAGGAGAGGCA

Table 3.11: Rational Mutagenic Approach hVDR Subset Library F: Oligonucleotides Containing Randomized Degenerate Codons at the Designed Mutation Sites

Oligonucleotide	Oligonucleotide Sequences 5'→3' (overlap regions underlined (T_Ms≈ 55-59 °C) and mutation sites highlighted)
1	GATCCTGAAGCGGAAGGAGGAGGAGGCCTTGAAGGACAGTCTGCGGCCCAAGCTGTCTGAGGAGCAGCAGCG CATCATTGCCATACTGCTGGACGCCCACCATAAGACCTACGACCCCACCTACTCCGACTTCTGCCAGTTCCGGC CTCCAGTTCGTGTGAATGATGGTGGAGGGAGCCATCCTTCCAGGCCCAACTCCAGACACACTCCCAGCTTCTCT GGGGACTCCTCCTCCTCCTGCTCAGATCACTGTATCACCTCTTCAGACATGATGGACTCGTCCAGCTTCTCCAA TCTGGATCTGAGTGAAGAAGATTCAGATGACCCTTCTGTGACCCTAGAGCTGTCCCAGCTCTCCAT
2	AGCAAAGCCAATGACCTTTTGGATGCTGTAACTGACCAGGTCAGCCAGGTGGGGCAGCATGGAGAGCTGGGAC AGCTCTAG
3	CCAAAAGGTCATTGGCTTTGCTAAGATGATACCAGGATTCAGAGACCTCACCTCTGAGGACCAGATCGTACTGC TGAAGTCAAGTGCCATTGAGGTCATCATGTTGCGCTCCAATGAGTCCTTCACCATGGACGACATGTCCTGGACC TGTGGCAACCAAGACTACAAGTACCGCGTCAGTGACGTGACCAAAGCC
4	TCCCACCTGGAACTTGATGAGGGGCTCAATCAGCTCCAGGCTGTGTCCGGCTTTGGTCACGTCACTGACG
5	CCTCATCAAGTTCCAGGTGGGACTGAAGAAGCTGAACTTGCATGAGGAGGAGCATGTCCTGCTCATGGCCATCT GCATCGTCTCCCCAGATCGTCCTGGGGTGCAGGACGCCGCGCTGATTGAGGCCATCCAGGACCGGGTGTCCA ACACACTGCAGACGTACATCCGCTGCCGCCACCCGCCCCCGGGCAGCCACCTGCTCTATGCCAAGATGATCCA GAAGCTAGCCGACCTGCGCAGCCTCAATG
6	CAGGCTGGAAGGAGAGGCAGCGMNNCTGCTTGGAMTDCTCCTCATTGAGGCTGCGCAGGTC **Y401** **H397**
7	CTGCCTCTCCTTCCAGCCTGAGTGCAGCATGAAGCTAACGCCCCTTGTGCTCGAAGTGTTTGGCAATGAGAT
8	GTCCAGGCAGGGTGGCCAGAACGGGTGGGCACAAAGGATGGACTAGTTCAGGAGATCTCATTGCCAAACACTT CGAG

ligand plates (~0.3-1.8% of each experimental library) were re-tested on solid media plates for constitutive activity, as previously discussed (data not shown). A subset of variants was also tested in liquid quantitation assays of chemical complementation.

One variant from hVDR library B, BS4, showed ligand activated growth with LCA in histidine selective media at 100 nM, drastically showing approximately a 100-fold increase in sensitivity compared to the wild-type receptor (EC_{50}= 29 nM and 6-fold activation vs. ~EC_{50}> 10 μM and 4-fold activation) (Figure 3.12, red growth profile vs. blue growth profile). Furthermore, this variant showed ligand activated growth with a novel small molecule, cholecalciferol, at 10 μM with a 4-fold activation in histidine selective media, as shown in Figure 3.13 (red growth profile). Cholecalciferol is a precursor in the 1α, 25$(OH)_2D_3$ biosynthetic pathway and does not activate the wild-type hVDR, as shown in Figure 3.13 by the blue line.

3.5 hVDR Variant BS4 Binds and Activates in Response to A Novel Small Molecule Ligand: Characterization in Mammalian Cell Culture Assays

To determine whether the results obtained in yeast with variant BS4 were consistent with mammalian cell culture assays, the variant and the wild-type hVDR were cloned into a mammalian expression plasmid, pCMX (with a cytomegalovirus promoter), and transfected into human embryonic kidney 293T (HEK 293T) cells along with the p17*4TATALuc (containing a luciferase gene under the control of four Gal4 response elements) reporter plasmid (as described by Taylor *et al*.) [2]. Cell culture assays were performed with LCA and chole, where luciferase activity would be an indication of a small molecule binding and activating the variant. The wild-type hVDR (which has previously been shown to display activation at 100 μM) and variant BS4 displayed EC_{50} values of >32 μM and 3 μM, and <10- and 34-fold activations respectively, with LCA as shown in Figure 3.14. BS4 displayed an EC_{50} value of 4 μM and a 25-fold activation with

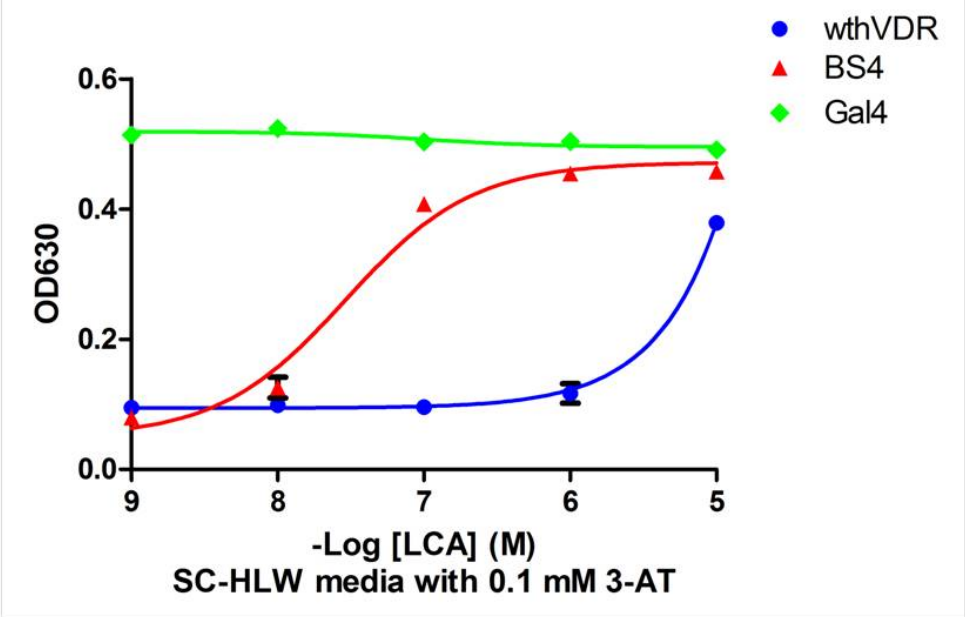

	EC_{50}	Fold- Activation
wthVDR	> 10 μM	4
BS4	29 nM	6

Figure 3.12: Rational Mutagenic Approach: hVDR Subset Library B Variant BS4 in Chemical Complementation
Histidine selective media with LCA

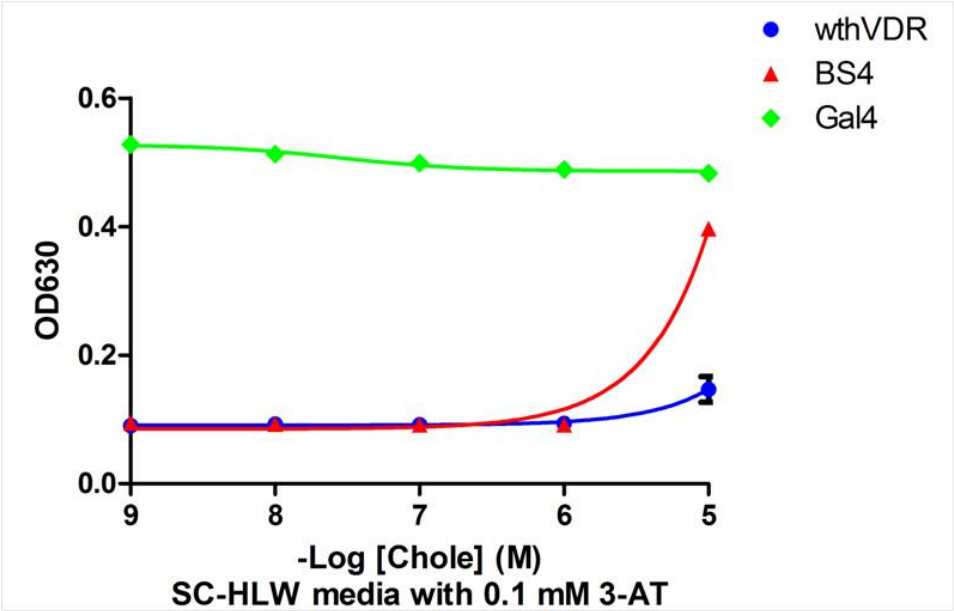

	EC_{50}	Fold- Activation
BS4	>10 µM	4

Figure 3.13: Rational Mutagenic Approach: hVDR Subset Library B Variant BS4 in Chemical Complementation
Histidine selective media with chole

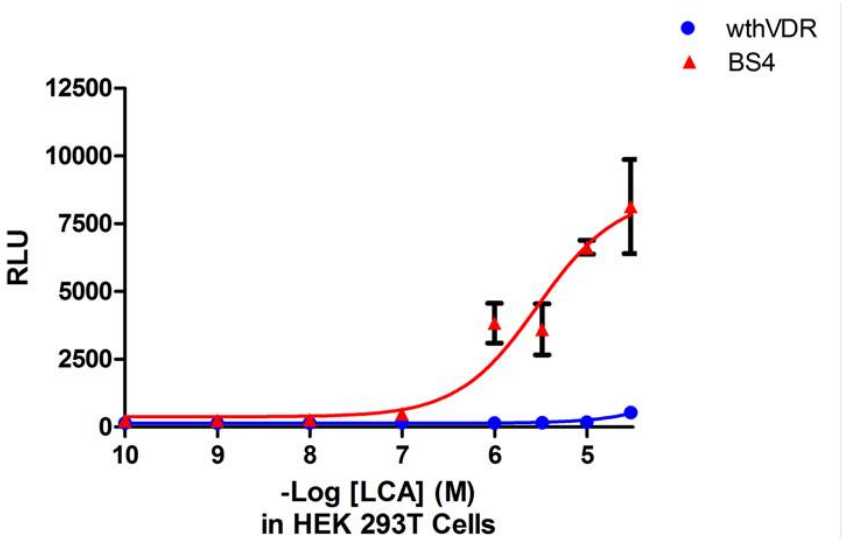

	EC_{50}	Fold- Activation
wthVDR	> 32 μM	<10
BS4	3 μM	34±7

Figure 3.14: Rational Mutagenic Approach: hVDR Subset Library B Variant BS4 in Mammalian Cell Culture Assay with LCA

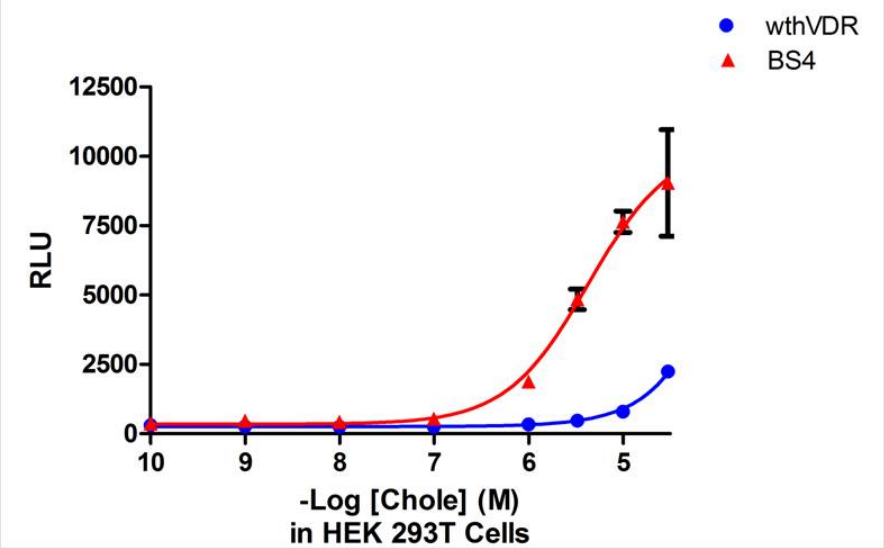

	EC_{50}	Fold- Activation
wthVDR	> 32 μM	<10
BS4	4 μM	25±5

Figure 3.15: Rational Mutagenic Approach: hVDR Subset Library B Variant BS4 in Mammalian Cell Culture Assay with chole

chole, as shown in Figure 3.15. The mammalian cell culture data confirms that we engineered a hVDR variant that is activated by lithocholic acid with enhanced sensitivity in comparison to the wild-type hVDR, and that this variant is also activated by the novel small molecule, cholecalciferol, which does not activate the wild-type hVDR.

Several variants from each hVDR subset library were submitted for sequencing (Tables 3.12, 3.13, 3.14 and 3.15). Overall, the subset libraries showed poor mutational diversity suggesting that the targeted positions do not tolerate much change. The BS4 variant from hVDR library B contained an undesigned mutation, C410Y. Interestingly, residue C410 was not one of the positions chosen for mutation in the designed libraries, yet through the power of genetic selection with chemical complementation, this variant was obtained in the designed libraries numerous times. This variant will be explored further in the next chapter.

3.6 Summary

To gain further insight into the role of residues important for the stability and function of the human vitamin D receptor (hVDR), as well as the types of chemical and physical changes that these and other residues in the receptor's ligand binding domain (LBD) can tolerate, a mutational analysis of the hVDR's LBD was performed. Previous structural and mutational work on the hVDR was used to rationally design two hVDR libraries using randomized codons at chosen positions, while error-prone PCR allowed us to create libraries of variants using random mutagenesis. All of the variants obtained were tested with small molecule ligands of interest, including cholecalciferol and β-lactam antibiotics, using chemical complementation. A variant, hVDRC410Y, that is activated by lithocholic acid with a 100-fold enhanced sensitivity in comparison to the wild-type hVDR, and is also activated by the novel small molecule ligand, cholecalciferol, which does not activate the wild-type hVDR, was discovered.

Table 3.12: Rational Mutagenic Approach: hVDR Subset Library B Sequencing Results
*= variant contains frame-shift

hVDR Lib B (227, 233)			
Possible Changes:	$LIV_2FMA_2S_2T_2$	$LIV_2FMA_2S_2T_2$	
Residue:	**L227**	**L233**	Other
Nonselective Variants			
*NS2	S	wt	Q223Stop
NS3	wt	S	
Selective Variants			
S1	I	I	
S4	wt	wt	C410Y
S10	wt	wt	C410Y

Table 3.13: Rational Mutagenic Approach: hVDR Subset Library C Sequencing Results
*= variant contains frame-shift

hVDR Lib C (237, 238)		
Possible Changes:	S_2TCFI	$LIV_2FMA_2S_2T_2$
Residue:	**S237**	**I238**
Nonselective Variants		
*NS3	wt	wt
NS4	wt	F
Selective Variants		
*S6	S	M

Table 3.14: Rational Mutagenic Approach: hVDR Subset Library E Sequencing Results

*= variant contains frame-shift

hVDR Library E (295)	
Possible Changes:	YFSCHNDIVGLR
Residue:	**Y295**
Nonselective Variants	
NS2	H
*NS4	I
Selective Variants	
S3	R
S4	R

Table 3.15: Rational Mutagenic Approach: hVDR Subset Library F Sequencing Results

hVDR Library F (397, 401)			
Possible Changes:	HYNKQstop	saturated	
Residue:	**H397**	**Y401**	other
Nonselective Variants			
NS2	Q	W	
NS3	N	wt	V421M
-			
Selective Variants			
S1	wt	wt	
S6	wt	wt	C410Y
S9	wt	wt	C410Y

3.7 Materials and Methods

Ligands

Amoxicillin, cloxacillin, penicillin G, ampicillin, oxacillin, γ-1-oxo-pyrenebutyric acid, cholecalciferol and resveratrol were purchased from Sigma-Aldrich (St. Louis, MO). 17-β-estradiol, hexestrol, 9-*cis* retinoic acid and lithocholic acid were purchased from MP Biomedicals, LLC (Solon, OH). 10 mM stocks of all ligands were made with 80 % ethanol: 20 % dimethyl sulfoxide (DMSO) and stored at 4 °C.

Hybridization and PCR to Create Full Insert Cassettes for hVDR Libraries 1 & 2

For each hVDR library, 100 ng of each oligonucleotide (Operon, Huntsville, AL) was combined in a PCR tube with 10X *Pfu* buffer, dNTPs, *Pfu* polymerase and 125 ng of the corresponding forward and reverse primers (Operon, Huntsville, AL). Cassettes were created via PCR using the following thermocycler program: 95 ºC 3 minutes, 95 ºC 1 minute, 60 ºC 1 minute, 72 ºC 2 minutes, repeat 15 cycles, 95 ºC 1 minute, 45 ºC 1 minute, 72 ºC 4 minutes, repeat 15 cycles, 72 ºC 5 minutes. The full insert cassette (1096 bp) for each library was created via PCR using the same thermocycler program and the following primers: 5'-atg atc ctg aag cgg aag gag gag-3' and 5'- tga cag gct gtg ccc caa agt c-3' (Operon, Huntsville, AL). The full insert cassettes were purified using the QIAprep® Spin Miniprep Kit (Qiagen, Valencia, CA).

Construction of a hVDR Background Plasmid

A hVDR background plasmid was constructed to decrease the expression of the wild-type hVDR in the designed libraries. *SacII* and *KpnI* restriction sites were introduced into the pGBDhVDR yeast expression plasmid (discussed in Chapter 2) towards the beginning and end of the hVDR gene, respectively, using site-directed mutagenesis (Stratagene, Santa Clara, CA) to create the pGBDhVDRSacIIKpnI plasmid. This plasmid

was digested with *SacII* and *KpnI*, removing a portion of the wild-type hVDR gene. A 145 bp segment of random DNA ('junk') from a pMSCVeGFP plasmid was amplified via PCR (55 ºC as the annealing temperature) using 125 ng of the following primers: 5'-atc ccc cgc ggg ggt ctt tca tgg gta aca gtt tct-3' and 5'-gcc ggg tac ccg ctg tcc ata atg aac tat ttc agg-3' (Operon, Huntsville, AL), digested and ligated between the *SacII* and *KpnI* sites in the pGBDhVDRSacIIKpnI plasmid. The underlined sequences denote *SacII* and *KpnI* restriction sites, respectively. The ligation was transformed into Z-competent™ XL-1 Blue *Escherichia coli* (*E.coli)* cells (Zymo, Orange, CA). When expression of the resulting plasmid, pGBDhVDRBackground, takes place three STOP codons are translated, resulting in a non-functional protein. Therefore background with the wild-type hVDR is reduced in the libraries. All DNA was purified using the QIAprep® Spin Miniprep Kit (Qiagen, Valencia, CA). The pGBDhVDRBackground plasmid was sequenced for confirmation (Operon, Huntsville, AL).

Yeast Transformation Using the PJ69-4A Strain

For each hVDR library, using the TRAFCO yeast transformation protocol, 1 µg of the full insert cassette and 0.3 µg of the yeast expression plasmids, pGBDhVDRBackground (containing a tryptophan marker, digested) and pGAD10BAACTR (containing the Gal4 AD fused to ACTR and a leucine marker), were transformed into the yeast strain PJ69-4A [21]. Transformants were plated onto non-selective agar plates (SC-LW), as well as adenine and histidine selective agar plates (SC-ALW or SC-HLW+0.1 mM 3-AT) with 10 µM of ligand set 1 (amoxicillin, cloxacillin, penicillin G, 17-β-estradiol and γ-OPBA), 10 µM of ligand set 2 (ampicillin, oxacillin, hexestrol, 9-*cis* retinoic acid, and resveratrol) and LCA (10 µM) and chole (10 µM) individually. Plates were incubated at 30 ºC for 3-4 days.

Liquid Quantitation Assays of Chemical Complementation in Yeast

Variants obtained from the yeast transformation were grown overnight in non-selective SC-LW media, at 30 ºC with shaking at 300 rpm. A 4:1 ratio of selective media (SC-ALW or SC-HLW+0.1 mM 3-AT with and without ligand at varying concentrations): cells (yeast resuspended in water) were aliquoted into 96-well plates. Plates were then incubated at 30 ºC with shaking at 170 rpm for 48 hours, with optical density readings at a wavelength of 630 nm (OD630) taken at 0, 24 and 48 hours. All data points represent the mean of at least duplicate experiments and the bars indicate standard deviation. The lowest ligand concentration data points for all plots contain no ligand. EC_{50} values were calculated using GraphPad Prism and a non-linear regression extrapolation.

Using Klenow to Create Full Insert Cassettes for hVDR Libraries 1 & 2

Followed a revised version of the protocol proposed by Holowachuk and Ruhoff [17]. 500 ng of each oligonucleotide (Operon, Huntsville, AL), NEBuffer 2 (New England Biolabs, Ipswich, MA) and distilled water were combined in a tube, heated to 95 ºC for 5 minutes, 50 ºC for 5 minutes and cooled to 25 ºC. After this hybridization step, *Klenow* polymerase (New England Biolabs, Ipswich, MA) and dNTPs were added, and the mixture was cooled at 25 ºC for 15 minutes and heated to 75 ºC for 20 minutes to extend the oligonucleotides. Cassettes were then combined and amplified via PCR, with 10X *Pfu* buffer, dNTPs, *Pfu* polymerase and 125 ng of the corresponding forward and reverse primers (Operon, Huntsville, AL).

Error-Prone PCR

A section of the hVDR ligand binding domain (LBD) (full-insert cassette) was amplified from the pGBDhVDR yeast expression plasmid via PCR (55 ºC as the annealing temperature) using 500 ng of the following primers: 5'-atg atc ctg aag cgg aag

gag gag-3' and 5'- tga cag gct gtg ccc caa agt c-3' (Operon, Huntsville, AL), in addition to 10x *Taq* buffer, dNTPs, $MgCl_2$, $MnCl_2$ and *Taq* polymerase (Omega Bio-Tek, Norcross, GA). The full insert cassettes were purified using the QIAprep® Spin Miniprep Kit (Qiagen, Valencia, CA).

Hybridization and PCR to Create Full Insert Cassettes for hVDR Libraries B, C, E & F

For each hVDR library, 100 ng of each oligonucleotide (Operon, Huntsville, AL) was combined in a PCR tube with 10X *Pfu* buffer, dNTPs, *Pfu* polymerase and 125 ng of the corresponding forward and reverse primers (Operon, Huntsville, AL). For hVDR libraries B & F the following primers were used: 5'- gat cct gaa gcg gaa gga gg-3' and 5'- gtc cag gca ggg tgg cca gaa cgg gtg ggc aca aag gat gga cta gtt cag gag atc tca ttg cca aac act tcg ag-3'. For hVDR libraries C & D the following primers were used: 5'- gat cct gaa gcg gaa gga gg-3' and 5'- gtc cag gca ggg tgg cc-3'. The full insert cassette for each library (1014 bp) was created using the following thermocycler program: 95 ºC 1 minute, 59 ºC 1 minute, 72 ºC 2 minutes, repeat 20 cycles, 95 ºC 1 minute, 56.6 ºC 1 minute, 72 ºC 2 minutes, repeat 20 cycles, 72 ºC 3 minutes. The full insert cassettes were purified using the QIAprep® Spin Miniprep Kit (Qiagen, Valencia, CA).

Construction of Mammalian Expression Plasmids

The Gal4 DBD fused to full-length hVDR (GBDhVDR) as well as the hVDRC410Y variant (GBDhVDRC410Y), was amplified from the respective pGBD yeast expression plasmid via PCR (55 ºC as the annealing temperature) using 125 ng of the following primers: 5'-tcc <u>ccg cgg</u> atg aag cta ctg tct tct atc gaa caa g-3' and 5'- aag gaa aaa a<u>gc ggc cgc</u> tca gga gat ctc att gcc aaa ca-3' (Operon, Huntsville, AL). The underlined sequences denote *SacII* and *NotI* restriction sites, respectively. The fusion constructs and mammalian expression plasmid, pCMX, which contains a

cytomegalovirus (CMV) promoter, were digested with *SacII* and *NotI*, ligated, and transformed into Z-competent™ XL-1 Blue *Escherichia coli* (*E.coli)* cells (Zymo, Orange, CA). The resulting plasmids were pCMXGRhVDR and pCMXGRhVDRC410Y. All DNA was purified using the QIAprep® Spin Miniprep Kit (Qiagen, Valencia, CA). The pCMXGRhVDR and pCMXGRhVDRC410Y plasmids were sequenced for confirmation (Operon, Huntsville, AL).

Mammalian Cell Culture Assays

Human embryonic kidney 293T cells (HEK 293T, ATCC, USA) were transfected with the pCMX mammalian expression plasmids discussed above, along with the p17*4TATAluc and pCMXβ-gal reporter plasmids as described by Taylor et al., using Lipofectamine 2000 (Invitrogen, Carlsbad, CA) as the cationic lipid [2]. p17*4TATAluc contains the *Renilla* luciferase gene under the control of four Gal4 response elements, while pCMXβ-gal contains the β-galactosidase gene under the control of the mammalian CMV promoter. Cells were harvested ~36-48 hours after the addition of ligand at varying concentrations, and analyzed for luciferase and β-galactosidase activity. All data points represent the mean of triplicate experiments normalized against β-galactosidase activity and the bars indicate standard deviation. The lowest ligand concentration data points for all plots contain no ligand. EC_{50} values were calculated using GraphPad Prism and a non-linear regression extrapolation. Fold activations were calculated by dividing the highest level of activation by the lowest level of activation in triplicate experiments.

3.8 Literature Cited

1. Schwimmer, L.J., P. Rohatgi, B. Azizi, K.L. Seley, and D.F. Doyle, *Creation and discovery of ligand-receptor pairs for transcriptional control with small molecules.* Proc. Natl. Acad. Sci. U.S.A., 2004. **101**(41): p. 14707-14712.

2. Taylor, J.L., P. Rohatgi, H.T. Spencer, D.F. Doyle, and B. Azizi, *Characterization of a molecular switch system that regulates gene expression in mammalian cells through a small molecule.* BMC Biotechnol., 2010. **10**: p. 15.

3. Elander, R.P., *Industrial production of beta-lactam antibiotics.* Appl. Microbiol. Biotechnol., 2003. **61**(5-6): p. 385-392.

4. Rochel, N., J.M. Wurtz, A. Mitschler, B. Klaholz, and D. Moras, *The crystal structure of the nuclear receptor for vitamin D bound to its natural ligand.* Mol. Cell, 2000. **5**(1): p. 173-179.

5. Humphrey, W., A. Dalke, and K. Schulten, *VMD: Visual molecular dynamics.* J. Mol. Graphics, 1996. **14**(1): p. 33-38.

6. Reddy, M.D., L. Stoynova, A. Acevedo, and E.D. Collins, *Residues of the human nuclear vitamin D receptor that form hydrogen bonding interactions with the three hydroxyl groups of 1alpha,25-dihydroxyvitamin D3.* J. Steroid Biochem. Mol. Biol., 2007. **103**(3-5): p. 347-351.

7. Choi, M.W., K. Yamamoto, H. Masuno, K. Nakashima, T. Taga, and S. Yamada, *Ligand recognition by the vitamin D receptor.* Bioorg. Med. Chem., 2001. **9**(7): p. 1721-1730.

8. Yamamoto, K., M. Choi, D. Abe, M. Shimizu, and S. Yamada, *Alanine scanning mutational analysis of the ligand binding pocket of the human Vitamin D receptor.* J. Steroid Biochem. Mol. Biol., 2007. **103**(3-5): p. 282-285.

9. Choi, M., K. Yamamoto, T. Itoh, M. Makishima, D.J. Mangelsdorf, D. Moras, H.F. DeLuca, and S. Yamada, *Interaction between vitamin D receptor and vitamin D ligands: Two-dimensional alanine scanning mutational analysis.* Chem. Biol., 2003. **10**(3): p. 261-270.

10. Yamada, S. and K. Yamamoto, *Ligand recognition by vitamin D receptor: Total alanine scanning mutational analysis of the residues lining the ligand binding pocket of vitamin D receptor.* Curr. Top. Med. Chem., 2006. **6**(12): p. 1255-1265.

11. Yamamoto, K., D. Abe, N. Yoshimoto, M. Choi, K. Yamagishi, H. Tokiwa, M. Shimizu, M. Makishima, and S. Yamada, *Vitamin D receptor: Ligand recognition and allosteric network.* J. Med. Chem., 2006. **49**(4): p. 1313-1324.

12. Gietz, R.D. and R.H. Schiestl, *High-efficiency yeast transformation using the LiAc/SS carrier DNA/PEG method.* Nat. Protoc., 2007. **2**(1): p. 31-34.

13. Watkins, R.E., G.B. Wisely, L.B. Moore, J.L. Collins, M.H. Lambert, S.P. Williams, T.M. Willson, S.A. Kliewer, and M.R. Redinbo, *The human nuclear xenobiotic receptor PXR: Structural determinants of directed promiscuity.* Science, 2001. **292**(5525): p. 2329-2333.

14. Jurutka, P.W., P.D. Thompson, G.K. Whitfield, K.R. Eichhorst, N. Hall, C.E. Dominguez, J.C. Hsieh, C.A. Haussler, and M.R. Haussler, *Molecular and functional comparison of 1,25-dihydroxyvitamin D_3 and the novel vitamin D receptor ligand, lithocholic acid, in activating transcription of cytochrome P450 3A4.* J. Cell. Biochem., 2005. **94**(5): p. 917-943.

15. Higuchi, R., B. Krummel, and R.K. Saiki, *A general-method of invtro preparation and specific mutagenesis of DNA fragments - Study of protein and DNA interactions.* Nucleic Acids Res., 1988. **16**(15): p. 7351-7367.

16. Lundberg, K.S., D.D. Shoemaker, M.W.W. Adams, J.M. Short, J.A. Sorge, and E.J. Mathur, *High-fidelity amplification using a thermostable DNA polymerase isolated from pyrococcus furiosus.* Gene, 1991. **108**(1): p. 1-6.

17. Holowachuk, E.W. and M.S. Ruhoff, *Efficient gene synthesis by Klenow assembly extension - Pfu polymerase amplification (KAPPA) of overlapping oligonucleotides.* PCR Methods Appl., 1995. **4**(5): p. 299-302.

18. Islam, K.M.D., M. Dilcher, C. Thurow, C. Vock, I.K. Krimmelbein, L.F. Tietze, V. Gonzalez, H.M. Zhao, and C. Gatz, *Directed evolution of estrogen receptor proteins with altered ligand-binding specificities.* Protein Eng. Des. Sel., 2009. **22**(1): p. 45-52.

19. Tindall, K.R. and T.A. Kunkel, *Fidelity of DNA synthesis by the thermus aquaticus DNA polymerase.* Biochemistry, 1988. **27**(16): p. 6008-6013.

20. Pritchard, L., D. Corne, D. Kell, J. Rowland, and M. Winson, *A general model of error-prone PCR.* J. Theor. Biol., 2005. **234**(4): p. 497-509.

21. Gietz, R.D. and R.A. Woods, *Transformation of yeast by lithium acetate/single-stranded carrier DNA/polyethylene glycol method*, in *Guide to Yeast Genetics and Molecular and Cell Biology, Pt B*. 2002, Academic Press Inc: San Diego. p. 87-96.

CHAPTER 4

ENGINEERING THE HVDRC410Y VARIANT AND INVESTIGATING THE MUTATIONAL TOLERANCE OF RESIDUE C410 IN THE HUMAN VITAMIN D RECEPTOR

4.1 Engineering hVDRC410Y and Investigating hVDR Residue C410

To investigate the structure-function relationships between the human vitamin D receptor (hVDR) and its ligands, as well as gain insight into the role and tolerance of specific residues, a mutational analysis of residues in the hVDR's ligand binding domain (LBD) was performed. As discussed in Chapter 3, libraries of hVDR variants were engineered by methods of rational and random mutagenesis and tested using chemical complementation. One variant containing an undesigned mutation at the C410 position to a tyrosine, hVDRC410Y, displayed a 100-fold increase in sensitivity towards a known hVDR ligand, lithocholic acid (LCA), in comparison to the wild-type receptor. This variant was also activated by a novel small molecule ligand, cholecalciferol (chole), whereas the wild-type receptor is not (Figure 4.1).

In this work, several approaches were taken to investigate the hVDRC410Y variant and residue C410 further. In an attempt to discover a variant with even higher sensitivity for LCA and/or chole, the C410Y variant was subjected to random mutagenesis via error-prone PCR (epPCR). Residue C410 does not line the hVDR's ligand binding pocket (LBP) and as a result does not make direct contacts with the natural ligand, 1α, 25$(OH)_2D_3$, yet surprisingly contributes towards enhanced activation with LCA and chole. *In-silico* docking of these ligands with C410Y was performed, in quest of gaining structural insight into this variant. The mutational tolerance of residue C410 was also investigated, using site-directed mutagenesis to change the residue to

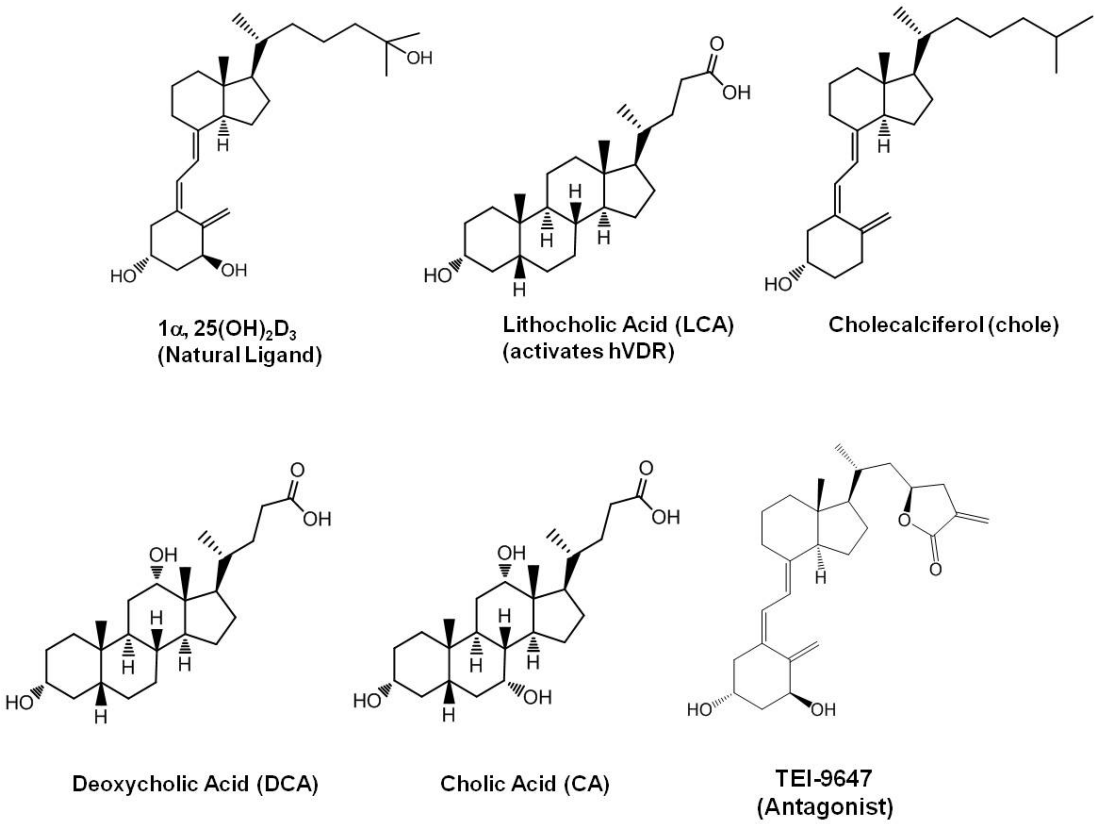

Figure 4.1: Structures of hVDR Ligands and Molecules of Interest

amino acids of varying chemical and physical properties. Lastly, the effects of combining the C410Y mutation with other hVDR mutations previously obtained in our lab were explored.

4.2 Engineering hVDRC410Y: Error-Prone PCR Libraries

The C410Y variant was obtained from one of the libraries created in Chapter 3 using the rational mutagenic approach. Interestingly, residue C410 was not one of the positions chosen for mutation in the designed libraries, yet through the power of selection in the chemical complementation method, this variant was obtained in the designed libraries numerous times. To determine whether selective pressure would allow for the directed evolution of a variant with further enhanced sensitivity for LCA and/or chole, while overcoming the five angstroms bias introduced in the rational mutagenic approach, the C410Y variant was used as the template for random mutagenesis via epPCR using *Taq* polymerase. As previously discussed in Chapter 3, *Taq* polymerase lacks proof-reading capabilities and the addition of $MnCl_2$ can be used to control the fidelity of the enzyme, with higher concentrations of $MnCl_2$ resulting in higher numbers of mutations [1, 2]. Various concentrations of $MnCl_2$ (2-200 μM) were used to amplify the hVDRC410Y LBD (full insert cassette) via PCR.

For each epPCR library, the full insert cassette, the digested background plasmid (pGBDhVDRBackground, containing a tryptophan marker and the Gal4 DNA Binding Domain (GBD) fused to a portion of the hVDR followed by a 'junk' sequence), and the coactivator plasmid (pGAD10BAACTR, containing a leucine marker and the Gal4 activation domain (GAD) fused to the activator for thyroid and retinoid receptors (ACTR)) were transformed into the PJ69-4A yeast strain. Transformants were plated onto non-selective synthetic complete agar plates lacking leucine and tryptophan (SC-LW) to select for both plasmids, and to determine whether homologous recombination between

the insert cassette and background plasmid occurred. The PJ69-4A yeast strain contains the *HIS3* and *ADE2* genes, essential genes in the corresponding histidine or adenine biosynthetic pathway, under the control of Gal4 response elements. As a result, transformants were also plated onto adenine and histidine selective agar plates (SC-ALW and SC-HLW+0.1 mM 3-AT) containing individual ligands.

Since the C410Y variant displayed ligand activated growth with LCA at 100 nM and with chole at 10 μM in histidine selective media when tested in chemical complementation, and the goal was to obtain a variant with further enhanced sensitivity, individual selective plates containing 10 nM LCA and 1 μM chole were used (Chapter 3, Figures 3.12 and 3.13). In addition to the ligand sets discussed in Chapter 3 (section 3.2.2), individual selective plates containing 10 μM deoxycholic acid (DCA) and cholic acid (CA) were used. Like LCA, DCA and CA are bile acids; their structures being extremely similar to each other. Compared to LCA, DCA has one additional hydroxyl group while CA has two additional hydroxyl groups (Figure 4.1). Besides increasing the sensitivity of C410Y for LCA and chole, part of the goal was to determine if a variant could be engineered to activate in response to another novel small molecule ligand. Due to the structural similarities between LCA, DCA and CA, activation with these molecules can provide significant insight into specific receptor-ligand interactions, perhaps on the importance of hydrogen bonding for the stability and function of the receptor.

Engineering hVDRC410Y: Results for Error-Prone PCR Libraries

The non-selective (SC-LW) plates were used to determine the experimental library size and transformation efficiency of each C410Y library. The transformations produced a library size of ~10^3 variants for each library, with transformation efficiencies of ~10^5 cfu/μg plasmid DNA per library. Unfortunately, no ligand activated variants were obtained on the selective plates with ligand.

Homologous recombination between the insert cassette and background plasmid occurred successfully for each C410Y epPCR library, as variants were obtained on non-selective plates. To confirm that the lack of selective ligand activated variants was not due to an unreasonable number of mutations being introduced into the C410Y template, ten non-selective variants (several from each library) were submitted for sequencing. Mutational frequencies similar to those obtained for the hVDR epPCR libraries created in Chapter 3 were observed, and as expected, an overall increase in mutations was observed with increasing concentration of $MnCl_2$. These results suggest that for these libraries ligand activated variants were not obtained due to the lack of a variant with enhanced sensitivity for LCA/chole or activation with any of the other ligands tested, and not due to nonsense mutations or truncated proteins.

4.3 hVDR Residue C410 and *In-Silico* Docking of wthVDR and hVDRC410Y

Structurally, cysteines have been shown to play an important role in the maintenance of protein conformation, primarily due to the formation of strong disulfide bonds that contribute to protein stability. Disulfide bonds are covalent bonds formed by the coupling of two thiol groups. Early biochemical experiments on the hVDR suggested that amino acids with sulfhydryl-containing side chains may play a crucial role in ligand binding, potentially by contributing to the proper conformation of the LBP [3, 4]. However in the case of the C410Y variant a cysteine residue was mutated to a tyrosine, resulting in enhanced activity with a known ligand and activation with a novel small molecule.

Residue C410 is located in the loop between helices 11 and 12 of the hVDR's LBD and is part of a compact hydrophobic core involving residues from helix 3n (L221 and L224), helix 3 (L227) and helix 11 (L404) (Figure 4.2a) [5, 6]. In the crystal structure of the hVDR with its natural ligand, 1α, $25(OH)_2D_3$, this residue is 8.48 Å from the 25-

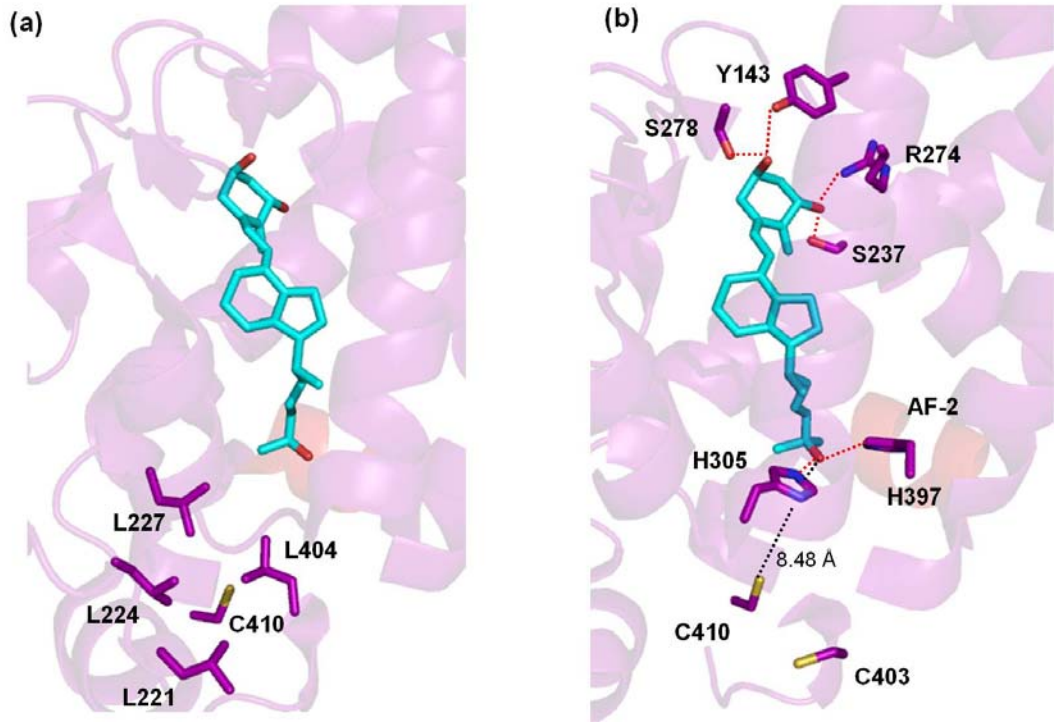

Figure 4.2: hVDR Residue C410. Cysteine 410 is part of a hydrophobic core and is 8.48 Å from 1α,25$(OH)_2D_3$'s 25-hydroxyl group. Ligand (Cyan), hVDR residues (Purple), AF-2 Domain (Red Helix), hydrogen bonds (Red Lines), distance measured (Black Line), PDB:1DB1

hydroxyl group of the ligand and is not involved in direct contacts with the small molecule (Figure 4.2b) [5]. Interestingly, cysteine 410 also happens to be one of three residues (L378, C403, and C410) that differ in the C-terminal regions of the rat VDR (rVDR) and hVDR LBDs [7-10]. Along with C403, this residue has been implicated to be involved in mediating opposing effects in the two species despite the fact that neither of these residues is close enough to make direct contacts with the ligand [7-12]. Specifically, the small molecule TEI-9647 (a 1α,25$(OH)_2D_3$ derivative) has been shown to have an antagonistic effect on the hVDR, while an agonistic effect has been observed on the rVDR (Figure 4.1).

Molecular models with 1α, 25$(OH)_2D_3$ have shown that the R-groups of the corresponding rVDR loci (S399 and N406) form additional hydrogen bonds not formed by the hVDR C403 and C410 thiol groups, providing helix 12 with additional stability and enhanced rVDR-coactivator interactions thus gene activation [8, 10, 12, 13]. Recent work on the VDR has elucidated the mechanisms underlying the opposing effects of TEI-9647 between the hVDR and rVDR [7, 10, 14]. Work by Kakuda *et al.* indicates that for the hVDR, TEI-9647 hydrogen bonds to residue H305 resulting in a conformational change of the receptor, such that residue C403 or C410 are shifted towards the ligand. A covalent bond between the thiol group of C403 or C410 and the TEI-9647 25-methylene group is then formed, along with the disruption of hydrophobic contacts with helix 12 thus gene repression [14].

To visualize the structural impact of the C410Y mutation on the hVDR, *in-silico* docking of 1α, 25$(OH)_2D_3$, LCA and chole with the wild-type hVDR and hVDRC410Y was performed using AutoDock Vina [15]. *In-silico* docking programs such as AutoDock Vina predict how well a given molecule will fit into the binding site of a target structure. In general docking consists of two steps; sampling of the ligand's possible conformations in

the binding site, and scoring of the poses [16, 17]. During docking simulations with AutoDock Vina, the ligand is flexible while the protein is held rigid. When the wild-type hVDR and variant C410Y docked structures were superimposed, as expected only slight structural changes were observed. For 1α, 25$(OH)_2D_3$ a small upward shift of the ligand (docked into the variant) in the pocket resulted in closer proximity of the aliphatic chain 25-hydroxyl group to residue H305, an important hydrogen bonding residue in the hVDR (Figure 4.3a). For LCA the ring system of both docked structures overlap with each other, however the side chain of the ligand docked into the variant is curved towards the center and away from the end of the pocket consisting of residue C410. In this case the carboxyl group on the side chain is positioned further from two important hydrogen bonding residues (H305 and H397) (Figure 4.3b). This is surprising due to the enhanced activation observed for C410Y with LCA. The docked structure for chole with the variant shows a very similar conformation, compared to the natural ligand docked into the wild-type hVDR (Figure 4.3c). These theoretical models may not accurately represent the positioning of the ligands in the pocket, nevertheless we can conclude that the increased bulkiness at the C410 position, with a tyrosine substituting a cysteine, may be contributing to a shift (upwards in the pocket) and/or repositioning (curvature into the center of the pocket) of the ligand. The subtle and contradicting structural effects of residue C410 on the hVDR limit our conclusions to these generalizations, yet the effect on ligand specificity and activation continue to be surprising, considering how distant this residue is located within the hVDR LBD.

4.4 Mutational Tolerance of Residue C410

Naturally, the fact that residue C410 was not targeted in the designed libraries and that the mutation C410Y resulted in a unique activation profile with both LCA and chole led to further investigation of this position; particularly on the role and tolerance of

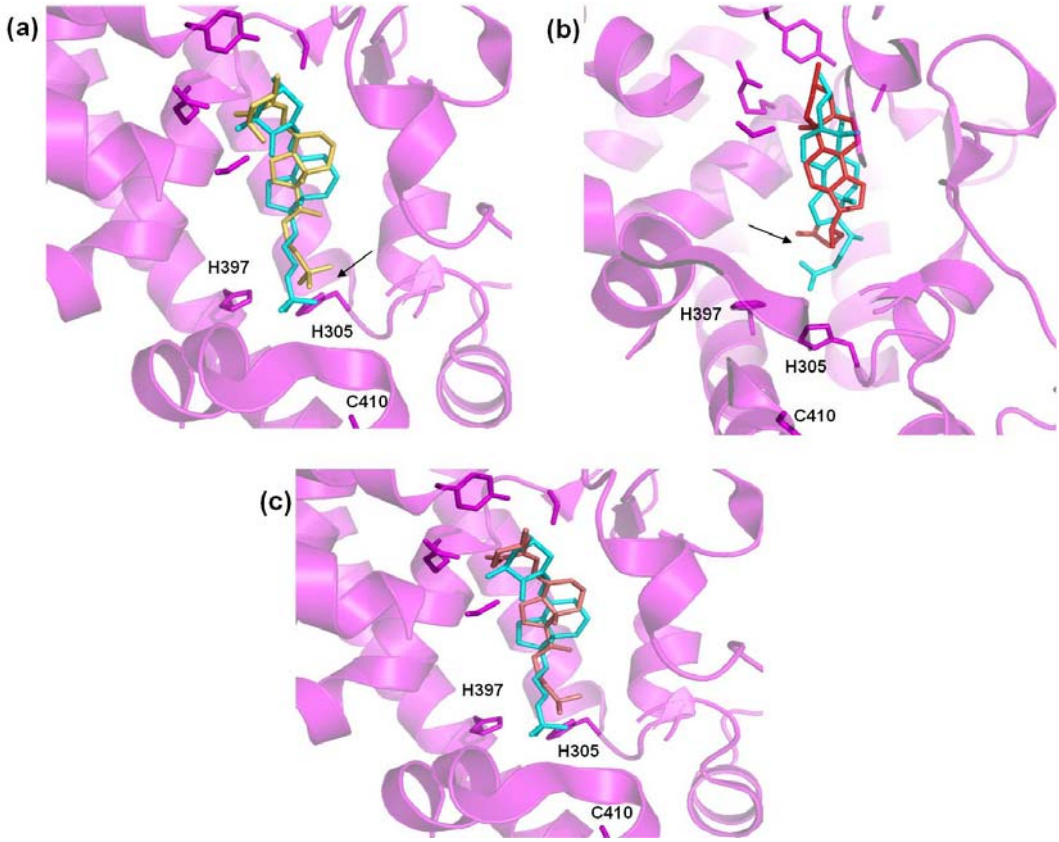

Figure 4.3: *In-silico* Docking of wthVDR and hVDRC410Y with Various Ligands hVDR residues (Purple), PDB:1DB1

(a) Wild-type docked structure: 1α, 25$(OH)_2D_3$ (Cyan),
Variant docked structure: 1α, 25$(OH)_2D_3$ (Yellow)

(b) Wild-type docked structure: LCA (Cyan),
Variant docked structure: LCA (Red)

(c) Wild-type docked structure: 1α, 25$(OH)_2D_3$ (Cyan),
Variant docked structure: chole (Pink)

this residue on activation of the receptor by various ligands. Gaining an understanding on the tolerance of specific residues in the hVDR's LBD provides insight into the structural and functional parameters of this domain. Insight from an evolutionary perspective can also be gained. For example, in this specific case evolution selected a cysteine at position 410 of the hVDR and an asparagine for the rat ortholog (rVDR). This may be due to the presence of different metabolites in these organisms, such that an asparagine may accommodate the metabolites found in rat versus those found in mammalian cells. By investigating the tolerance of this position, information on what types of amino acids are preferred, as well as which ones contribute towards the activation of the receptor can be gained. This knowledge can be applied towards the development of small molecules for therapeutic use, especially non-natural ligands which may not contribute to the 'traditional or common' interactions but may compensate for them in other ways.

In order to determine whether (1) the enhanced C410Y activity was specifically due to the presence of a tyrosine, (2) a physical or chemical property of the residue was responsible for the observed activation profiles (e.g. increased bulkiness and hydrogen bonding capability) and (3) another amino acid would display a similar activation profile as the C410Y variant, this residue was mutated to amino acids of varying polarity, shape and volume (e.g. phenylalanine, alanine, serine, asparagine, tryptophan, histidine, leucine, methionine, threonine and lysine) using site-directed mutagenesis and the yeast expression plasmid, pGBDhVDR, as the template. Each variant was transformed into the PJ69-4A yeast strain along with the coactivator plasmid (pGAD10BAACTR) and tested using chemical complementation, where yeast growth would be an indication of a small molecule binding and activating the variant (ligand activated growth). Overall, no drastic changes would have been expected in the behavior of these variants due to the location of the residue in the LBD. However, in looking at the crystal structure, the presence of a

cavity at the end of the pocket containing residue C410 suggests that the increase in bulk at the C410 position may attribute to the filling of this cavity and possibly leading to the molecular interactions necessary for the enhanced and novel activation observed with LCA and chole, respectively.

Mutational Tolerance of Residue C410: Results for hVDRC410 Variants in Chemical Complementation

When tested in liquid quantitation assays of chemical complementation with 1α, 25$(OH)_2D_3$, LCA and chole in histidine selective media (SC-HLW + 0.1 mM 3-AT), most of the C410 variants behaved similar to the wild-type hVDR (Figures 4.4a-c). More specifically, with 1α, 25$(OH)_2D_3$ ligand activated growth was observed for C410F, C410A, C410S, C410N, C410H, C410L, C410M, C410T, and C410K at 10 nM with an ~EC_{50}>10 nM, indicating a wide range of tolerance at this position for different types of residues (Figure 4.4a). Ligand activated growth was not observed for variant C410W, which could imply that excessive bulk is not tolerated at this position (Figure 4.4a). Overall, position C410 is fairly tolerant of mutations with the variants studied displaying profiles similar to that of the wild-type receptor and C410Y (~EC_{50}>10 nM vs. EC_{50}≈ 2 nM) but with a 10-fold decrease in sensitivity when tested with 1α,25$(OH)_2D_3$ (Figure 4.4a). Despite residue C410's distance from 1α, 25$(OH)_2D_3$, the fact that this position tolerated a wide range of amino acids including alanine was surprising, indicating that perhaps this residue does not contribute to the activation of the hVDR by its natural ligand; as seen with the rat VDR (rVDR) where the presence of an asparagine at this position results in comparable activation with 1α, 25$(OH)_2D_3$. However, there seems to be some limitation to this tolerance as observed with C410W. Tryptophan has the largest volume among all amino acids (227.8 $Å^3$) [18]. The lack of ligand activation for this

variant and 1α, 25$(OH)_2D_3$ may be due to the significantly increased bulkiness at the C410 position, which may disrupt residue packing within the ligand binding domain.

Despite the fact that with 1α, 25$(OH)_2D_3$ a range of tolerance was observed at the C410 position, the same trend does not seem to be observed with other ligands. When tested with LCA, similar to the C410Y variant, C410F exhibited ligand activated growth at 100 nM with an EC_{50}= 54 nM (EC_{50}= 29 nM for C410Y) (Figure 4.4b). Similar to the wild-type hVDR, ligand activated growth at 10 μM with an ~EC_{50}> 10 μM was observed for the rest of the C410 variants (Figure 4.4b). C410W which did not show growth with the natural ligand, also displayed ligand activated growth with LCA at 10 μM (~EC_{50}> 10 μM), indicating that the increase of bulk and packing of the cavity at this end of the pocket contributes to activation with LCA (Figure 4.4b). When tested with chole, C410F once again exhibited a ligand activated growth profile similar to that of C410Y with growth at 10 μM and an ~EC_{50}> 10 μM (Figure 4.4c). Like the wild-type hVDR, the rest of the C410 variants (including C410W) did not display ligand activated growth with chole (Figure 4.4c).

Interestingly, as shown in this work, the presence of a tyrosine at the C410 position results in a novel activation profile with both LCA and chole in comparison to the wild-type hVDR. In addition to the tyrosine, the same activation profile is observed with C410F, emphasizing the importance of bulkiness for activation with both ligands, as well as suggesting that the presence of a hydrogen bonding residue versus a hydrophobic one at C410 does not seem to affect the overall activity obtained with these ligands. Both LCA and chole have reduced molecular volumes compared to the natural ligand,

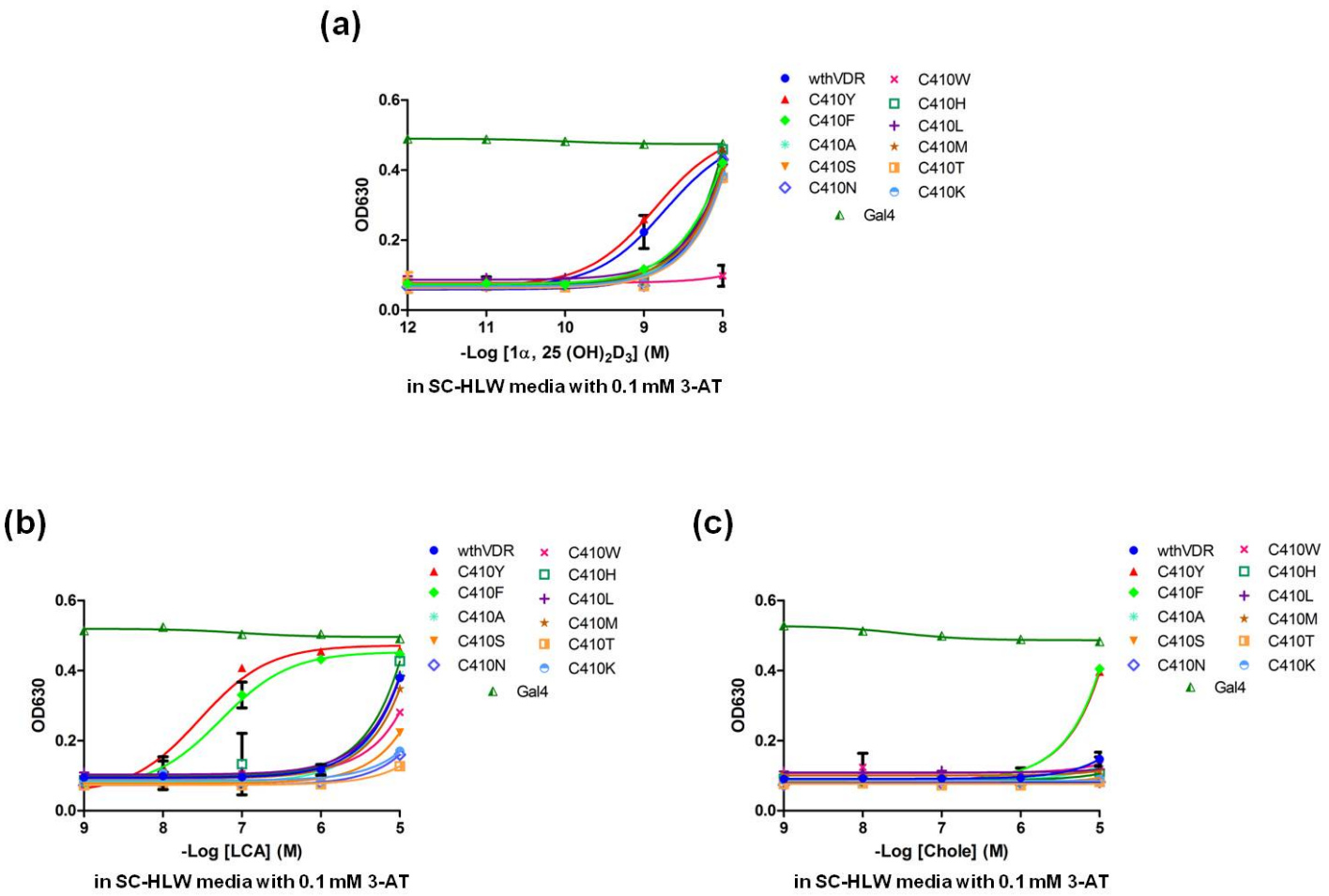

Figure 4.4: Mutational Tolerance of Residue C410 in the hVDR: hVDRC410 Variants in Chemical Complementation. Histidine selective media with (a) 1α, 25$(OH)_2D_3$, (b) LCA and (c) chole

1α, 25$(OH)_2D_3$. As a result, the increased bulkiness at the C410 position (volumes: cysteine 108.5 $Å^3$, phenylalanine 189.9 $Å^3$, and tyrosine 193.6 $Å^3$) may contribute additional contacts by decreasing the overall volume of the hVDR's LBP, and filling the cavity present at that end of the pocket [18].

4.5 Enhancing the Sensitivity of hVDRC410Y

Previously in our lab via random mutagenesis, a hVDR variant, H305F;H397Y, was engineered to activate in response to cholecalciferol (Ousley *et al*., manuscript submitted). Interestingly, both of the residues mutated in this variant and residue C410 are positioned on the same end of the hVDR's LBP (Figure 4.2b). Additionally, the aliphatic chain of 1α, 25$(OH)_2D_3$ which is also positioned on this end of the pocket upon binding the hVDR has been the main target of chemical modifications during drug development, as the cycloalkane rings have not been successfully changed without loss of ligand activation (Figure 4.2b) [5]. Receptor activation has been maintained or enhanced with many of the developed analogs and the currently discussed hVDR variants, suggesting that receptor-ligand interactions in this region of the LBP have some flexibility in terms of tolerating structural variations.

To determine the effects of combining the H305F, H397Y and C410Y mutations on ligand activation, different combinations of these mutations were introduced into the hVDR. Mammalian expression plasmids (pCMX, with a cytomegalovirus promoter) containing the variants under investigation were transfected into human embryonic kidney 293T (HEK 293T) cells along with the p17*4TATALuc (containing a luciferase gene under the control of four Gal4 response elements) reporter plasmid (as described by Taylor *et al*.) [19]. Cell culture assays were performed with 1α, 25$(OH)_2D_3$, LCA and chole, where luciferase activity would be an indication of a small molecule binding and

activating the variant. Overall, an increase in sensitivity for LCA and chole was expected for these variants as the hypothesis that the combination of the H305F, H397Y and C410Y mutations would have an additive effect on the activation of the hVDR was developed.

Enhancing the Sensitivity of hVDRC410Y: Results for hVDR Variants in Mammalian Cell Culture Assays

The variants H305F and C410Y showed EC_{50} values of 4 nM and 1 nM with $1\alpha,25(OH)_2D_3$, and ~10 μM and 3 μM with LCA, respectively. The variant H305F;C410Y displayed slightly higher sensitivity for $1\alpha,25(OH)_2D_3$ and enhanced sensitivity for LCA (~10-fold compared to C410Y), compared to the other variants tested with an EC_{50}< 1 nM and a 54-fold activation and an EC_{50}= 0.3 μM and a 28-fold activation, respectively (Figures 4.5a and 4.5b, and Table 4.1). With chole, the variants H305F and C410Y showed EC_{50} values of 2 μM and 4 μM, respectively. H305F;H397Y and H305F;C410Y shared the same enhanced sensitivity for chole (~10-fold compared to C410Y), with an EC_{50}= 0.3 μM and a 42-fold activation and an EC_{50}= 0.2 μM and a 14-fold activation, respectively (Figure 4.5c and Table 4.1). Interestingly, the variant H305F;H397Y;C410Y displayed constitutive activity, indicating that the receptor is in an active conformation, with activation observed in the absence of an exogenous small molecule ligand (Figures 4.5a-c).

Based on these results, some of the explored mutations did have a slight additive effect when combined. As previously mentioned with the C410Y mutation individually, the enhanced activity observed for the variant H305F;C410Y may be due to the increased bulkiness at the H305 and C410 positions (volumes: histidine 153.2 $Å^3$ and phenylalanine 189.9 $Å^3$) contributing additional or making up for a loss of receptor

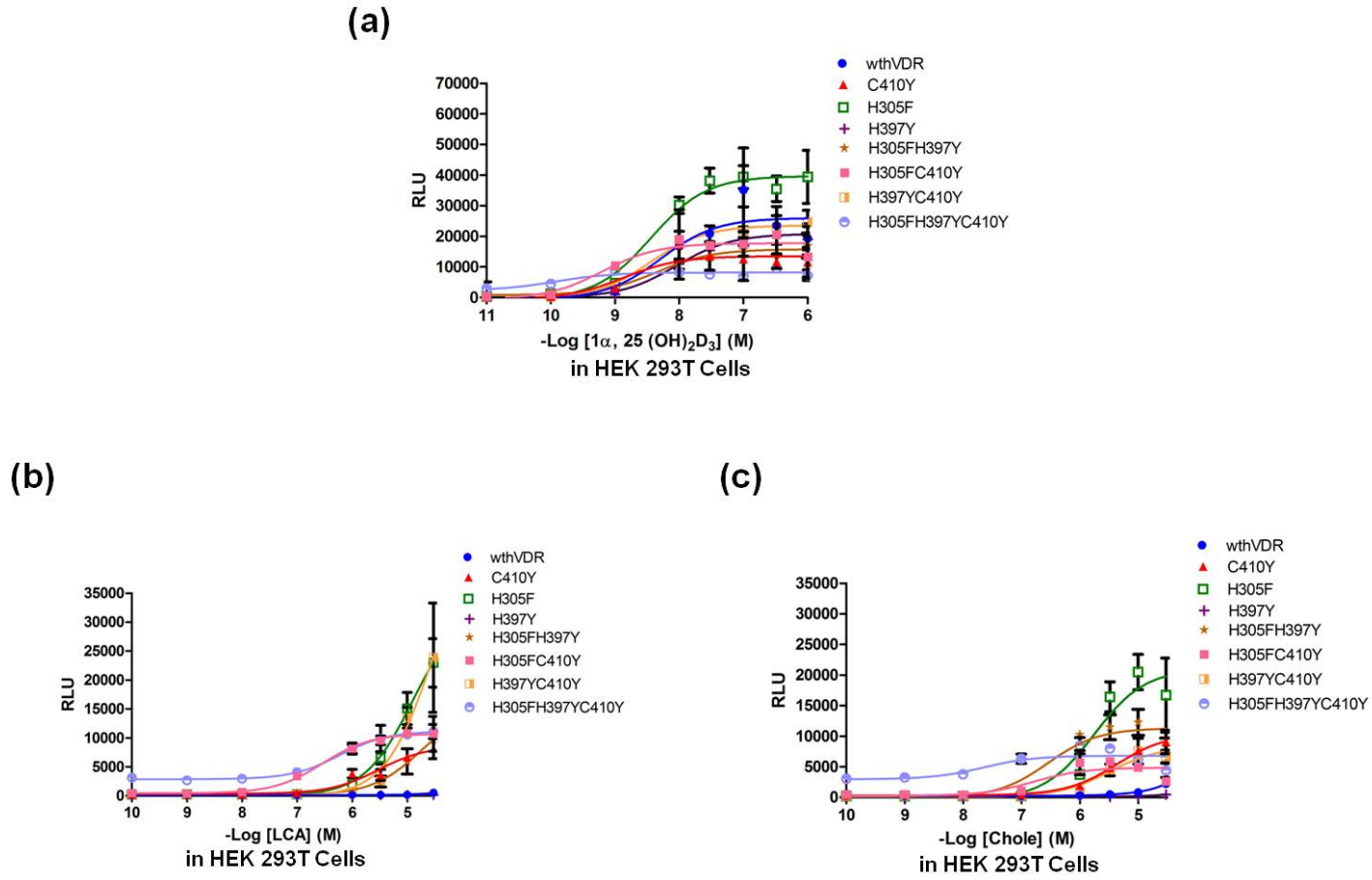

Figure 4.5: Enhancing the Sensitivity of hVDRC410Y. hVDR Variants in Mammalian Cell Culture Assays with (a) 1α, 25$(OH)_2D_3$, (b) LCA and (c) chole

Table 4.1: EC_{50} and Fold- Activation Values for hVDR Constructs Tested in Mammalian Cell Culture Assays Using HEK 293T Cells with 1α, 25(OH)$_2$D$_3$, LCA and chole. C.A. indicates constitutive activity.

	1α,25(OH)$_2$D$_3$		LCA		Chole	
hVDR Construct	EC_{50}	Fold Activation	EC_{50}	Fold Activation	EC_{50}	Fold Activation
wthVDR	5 nM	198±83	>32 μM	<10	>32 μM	<10
C410Y	1 nM	76±57	3 μM	34±7	4 μM	25±5
H305F	4 nM	135±30	~10 μM	103±22	2 μM	98±31
H397Y	9 nM	201±88	>32 μM	<10	>32 μM	<10
H305F;H397Y	4 nM	75±31	~10 μM	38±3	0.3 μM	42±9
H305F;C410Y	<1 nM	54±25	0.3 μM	28±13	0.2 μM	14±12
H397Y;C410Y	4 nM	119±22	~10 μM	99±41	3 μM	32±13
H305F;H397Y;C410Y	C.A.	<5	C.A.	<5	C.A.	<5

contacts with the smaller molecular volume ligands [18]. For the H305F;H397Y;C410Y variant however, the dramatic decrease in the overall volume of the hVDR's LBP when changing one residue to a phenylalanine and two to tyrosines resulted in a constitutively active receptor. This may potentially be due to an 'over-stabilized' active conformation and/or significantly enhanced hVDR-coactivator interactions. The results obtained with the hVDR variants studied thus far suggest that the end of the hVDR ligand binding pocket consisting of residues H305, H397 and C410 not only tolerates mutations, but is also capable of compensating for these changes such that enhanced activation is obtained.

4.6 Summary

We have explored the effects of mutating a residue (C410) that does not line the human vitamin D receptor's (hVDR) ligand binding pocket (LBP) and that as a result does not make direct contacts with the natural ligand. *In-silico* docking results of LCA and chole with hVDRC410Y do not show drastic changes in the ligand-receptor poses compared to the wild-type hVDR, yet the mutation C410Y contributes towards enhanced activation with both ligands. When the C410Y mutation was combined with an additional mutation on the same end of the LBP, H305F, the receptor's sensitivity for these ligands was enhanced further, emphasizing the importance of bulkiness at this end of the pocket for activation with both ligands.

Previous work on the hVDR has focused on residues lining the receptor's ligand binding pocket; however the unforeseen effects of mutating residue C410 on specificity and activation with the ligands studied not only serve as an example of the significant impact distant residues can have on receptor activation with different ligands but also emphasize the important role physical properties of residues, such as volume, can play for specific ends of the LBP compared to chemical properties. Future work investigating

the effects of C410Y on ligand binding and receptor-coactivator interactions would provide insight into the indirect effects of this mutation on the activation of the hVDR.

4.7 Materials and Methods

Ligands

Amoxicillin, cloxacillin, penicillin G, ampicillin, oxacillin, γ-1-oxo-pyrenebutyric acid, cholecalciferol, resveratrol and cholic acid were purchased from Sigma-Aldrich (St. Louis, MO). 17-β-estradiol, hexestrol, 9-*cis* retinoic acid, lithocholic acid and deoxycholic acid were purchased from MP Biomedicals, LLC (Solon, OH). 1α,25-dihydroxyvitamin D_3 was purchased from BIOMOL (Plymouth Meeting, PA). 10 mM stocks of all ligands, except 1α,25-dihydroxyvitamin D_3, for which a 13.3 μM stock was made, were made with 80 % ethanol: 20 % dimethyl sulfoxide (DMSO) and stored at 4 °C.

Error-Prone PCR

A section of the hVDRC410Y LBD (full-insert cassette) was amplified from the pGBDhVDRC410Y yeast expression plasmid via PCR (55 ºC as the annealing temperature) using 500 ng of the following primers: 5'- gat cct gaa gcg gaa gga gg-3' and 5'- gtc cag gca ggg tgg cca gaa cgg gtg ggc aca aag gat gga cta gtt cag gag atc tca ttg cca aac act tcg ag-3' (Operon, Huntsville, AL), in addition to 10x *Taq* buffer, dNTPs, $MgCl_2$, $MnCl_2$ and *Taq* polymerase (Omega Bio-Tek, Norcross, GA). The full insert cassettes were purified using the QIAprep® Spin Miniprep Kit (Qiagen, Valencia, CA).

Yeast Transformation Using the PJ69-4A Strain

For each hVDR library, using the TRAFCO yeast transformation protocol, 1 μg of the full insert cassette and 0.3 μg of the yeast expression plasmids, pGBDhVDRBackground (containing the Gal4 DBD fused to a portion of the hVDR

followed by the 'junk' sequence and a tryptophan marker, digested (discussed in Chapter 3)) and pGAD10BAACTR (containing the Gal4 AD fused to ACTR and a leucine marker), were transformed into the yeast strain PJ69-4A [20]. Transformants were plated onto non-selective agar plates (SC-LW), as well as adenine and histidine selective agar plates (SC-ALW or SC-HLW+0.1 mM 3-AT) with 10 μM of ligand set 1 (amoxicillin, cloxacillin, penicillin G, 17-β-estradiol and γ-OPBA), and 10 μM of ligand set 2 (ampicillin, oxacillin, hexestrol, 9-*cis* retinoic acid, and resveratrol). Selective plates containing 10 nM LCA, 1 μM chole, 10 μM DCA and 10 μM CA individually were also used. Plates were incubated at 30 ºC for 3-4 days.

Liquid Quantitation Assays of Chemical Complementation in Yeast

Transformants obtained from the yeast transformation were grown overnight in non-selective SC-LW media, at 30 ºC with shaking at 300 rpm. A 4:1 ratio of selective media (SC-ALW or SC-HLW+0.1 mM 3-AT with and without ligand at varying concentrations): cells (yeast resuspended in water) were aliquoted into 96-well plates. Plates were then incubated at 30 ºC with shaking at 170 rpm for 48 hours, with optical density readings at a wavelength of 630 nm (OD630) taken at 0, 24 and 48 hours. All data points represent the mean of at least duplicate experiments and the bars indicate standard deviation. The lowest ligand concentration data points for all plots contain no ligand. EC_{50} values were calculated using GraphPad Prism and a non-linear regression extrapolation.

In-Silico Docking of Wild-type hVDR and hVDRC410Y

The structure of the hVDRC410Y variant was prepared *in-silico* using the program TRITON 4.0.0 (National Centre for Biomolecular Research, Czech Republic) and its external program MODELLER (National Centre for Biomolecular Research,

Czech Republic). A computational site-directed mutagenesis method, where the wild-type protein is used for homology modeling was employed [21, 22]. The atomic coordinates of the crystal structure of the hVDR ligand binding domain (Δ165-215) were retrieved from the Research Collaboratory for Structural Bioinformatics (RCSB) Protein Data Bank (PDB) (PDB ID: 1DB1) [5, 23].

The wild-type hVDR and hVDRC410Y structures were prepared for docking using the UCSF CHIMERA-interactive molecular graphics program by: (1) removing the ligand and water molecules, (2) adding polar hydrogens, and (3) assigning Gasteiger charges [24]. The three-dimensional structure of each ligand was constructed and minimized using ChemBioDraw Ultra 11.0 and ChemBio3D Ultra 11.0 (Cambridge Soft, USA) [25]. AutoDockTools was used to add Gasteiger charges to each ligand structure, setting the partial charge property of each atom. Docking simulations were performed using AutoDock Vina with default parameters, such that the protein was held rigid and the ligand was allowed free rotation [15]. The receptor-ligand poses of lowest free energy of binding were analyzed further.

Site-Directed Mutagenesis

Mutations were introduced into the yeast expression plasmid, pGBDhVDR, using PCR (Stratagene, Santa Clara, CA) and the corresponding mutagenic primers (Operon, Huntsville, AL). All plasmids were purified using the QIAprep® Spin Miniprep Kit (Qiagen, Valencia, CA) and sequenced for confirmation (Operon, Huntsville, AL).

Construction of Mammalian Expression Plasmids

The Gal4 DBD fused to the hVDR variants H305F, H397Y, H305F;H397Y, H305F;C410Y, H397Y;C410Y, and H305F;H397Y;C410Y, was amplified from the respective pGBD yeast expression plasmid via PCR (55 ºC as the annealing

temperature) using 125 ng of the following primers: 5'-tcc ccg cgg atg aag cta ctg tct tct atc gaa caa g-3' and 5'- aag gaa aaa agc ggc cgc tca gga gat ctc att gcc aaa ca-3' (Operon, Huntsville, AL). The underlined sequences denote *SacII* and *NotI* restriction sites, respectively. The fusion constructs and mammalian expression plasmid, pCMX (discussed in Chapter 3), were digested with *SacII* and *NotI*, ligated, and transformed into Z-competent™ XL-1 Blue *Escherichia coli* (*E.coli)* cells (Zymo, Orange, CA). The resulting plasmids pCMXGRhVDRH305F, pCMXGRhVDRH397Y, pCMXGRhVDRH305F;H397Y, pCMXGRhVDRH305F;C410Y, pCMXGRhVDRH397Y;C410Y, and pCMXGRhVDR H305F;H397Y;C410Y were purified using the QIAprep® Spin Miniprep Kit (Qiagen, Valencia, CA) and sequenced for confirmation (Operon, Huntsville, AL).

Mammalian Cell Culture Assays

Human embryonic kidney 293T cells (HEK 293T, ATCC, USA) were transfected with the pCMX mammalian expression plasmids discussed above, along with the p17*4TATAluc and pCMXβ-gal reporter plasmids (discussed in Chapter 3) as described by Taylor et al., using Lipofectamine 2000 (Invitrogen, Carlsbad, CA) as the cationic lipid [19]. Cells were harvested ~36-48 hours after the addition of ligand at varying concentrations, and analyzed for luciferase and β-galactosidase activity. All data points represent the mean of triplicate experiments normalized against β-galactosidase activity and the bars indicate standard deviation. The lowest ligand concentration data points for all plots contain no ligand. EC_{50} values were calculated using GraphPad Prism and a non-linear regression extrapolation. Fold activations were calculated by dividing the highest level of activation by the lowest level of activation in triplicate experiments.

4.8 Literature Cited

1. Tindall, K.R. and T.A. Kunkel, *Fidelity of DNA synthesis by the thermus aquaticus DNA polymerase.* Biochemistry, 1988. **27**(16): p. 6008-6013.

2. Pritchard, L., D. Corne, D. Kell, J. Rowland, and M. Winson, *A general model of error-prone PCR.* J. Theor. Biol., 2005. **234**(4): p. 497-509.

3. Nakajima, S., J.C. Hsieh, P.W. Jurutka, M.A. Galligan, C.A. Haussler, G.K. Whitfield, and M.R. Haussler, *Examination of the potential functional role of conserved cysteine residues in the hormone binding domain of the human 1,25-dihydroxyvitamin D-3 receptor.* J. Biol. Chem., 1996. **271**(9): p. 5143-5149.

4. Coty, W.A., C.L. McConkey, and T.A. Brown, *A specific binding-protein for 1-alpha,25-dihydroxyvitamin-D in the chick-embryo chorioallantoic membrane.* J. Biol. Chem., 1981. **256**(11): p. 5545-5549.

5. Rochel, N., J.M. Wurtz, A. Mitschler, B. Klaholz, and D. Moras, *The crystal structure of the nuclear receptor for vitamin D bound to its natural ligand.* Mol. Cell, 2000. **5**(1): p. 173-179.

6. Ciesielski, F., N. Rochel, and D. Moras, *Adaptability of the Vitamin D nuclear receptor to the synthetic ligand Gemini: Remodelling the LBP with one side chain rotation.* J. Steroid Biochem. Mol. Biol., 2007. **103**(3-5): p. 235-242.

7. Ochiai, E., D. Miura, H. Eguchi, S. Ohara, K. Takenouchi, Y. Azuma, T. Kamimura, A.W. Norman, and S. Ishizuka, *Molecular mechanism of the vitamin D antagonistic actions of (23S)-25-dehydro-1 alpha-hydroxyvitamin D-3-26,23-lactone depends on the primary structure of the carboxyl-terminal region of the vitamin D receptor.* Mol. Endocrinol., 2005. **19**(5): p. 1147-1157.

8. Perakyla, M., F. Molnar, and C. Carlberg, *A structural basis for the species-specific antagonism of 26,23-lactones on vitamin D signaling.* Chem. Biol., 2004. **11**(8): p. 1147-1156.

9. Ishizuka, S., N. Kurihara, Y. Hiruma, D. Miura, J.I. Namekawa, A. Tamura, Y. Kato-Nakamura, Y. Nakano, K. Takenouchi, Y. Hashimoto, K. Nagasawa, and G.D. Roodman, *1 alpha,25-dihydroxyvitamin D-3-26,23-lactam analogues function as vitamin D receptor antagonists in human and rodent cells.* J. Steroid Biochem. Mol. Biol., 2008. **110**(3-5): p. 269-277.

10. Mizwicki, M.T., C.M. Bula, P. Mahinthichaichan, H.L. Henry, S. Ishizuka, and A.W. Norman, *On the mechanism underlying (23S)-25-dehydro-1alpha(OH)-vitamin D3-26,23-lactone antagonism of hVDRwt gene activation and its switch to a superagonist.* J. Biol. Chem., 2009. **284**(52): p. 36292-36301.

11. Kittaka, A., N. Saito, S. Honzawa, K. Takenouchi, S. Ishizuka, T.C. Chen, S. Peleg, S. Kato, and M.A. Arai, *Creative synthesis of novel vitamin D analogs for health and disease.* J. Steroid Biochem. Mol. Biol., 2007. **103**(3-5): p. 269-276.

12. Carlberg, C. and F. Molnar, *Detailed molecular understanding of agonistic and antagonistic vitamin D receptor ligands.* Curr. Top. Med. Chem., 2006. **6**(12): p. 1243-1253.

13. Mizwicki, M.T., C.M. Bula, J.E. Bishop, and A.W. Norman, *New insights into Vitamin D sterol-VDR proteolysis, allostery, structure-function from the perspective of a conformational ensemble model.* J. Steroid Biochem. Mol. Biol., 2007. **103**(3-5): p. 243-262.

14. Kakuda, S., S. Ishizuka, H. Eguchi, M.T. Mizwicki, A.W. Norman, and M. Takimoto-Kamimura, *Structural basis of the histidine-mediated vitamin D receptor agonistic and antagonistic mechanisms of (23S)-25-dehydro-1 alpha-hydroxyvitamin D-3-26,23-lactone.* Acta Crystallogr., Sect. D: Biol. Crystallogr., 2010. **66**: p. 918-926.

15. Trott, O. and A.J. Olson, *AutoDock Vina: Improving the speed and accuracy of docking with a new scoring function, efficient optimization, and multithreading.* J. Comput. Chem., 2009.

16. Chen, H.M., P.D. Lyne, F. Giordanetto, T. Lovell, and J. Li, *Evaluating molecular-docking methods for pose prediction and enrichment factors.* J. Chem. Inf. Model., 2006. **46**(1): p. 401-415.

17. Feher, M., *Consensus scoring for protein-ligand interactions.* Drug Discov. Today, 2006. **11**(9-10): p. 421-428.

18. Reichert, J. and J. Suhnel, *The IMB Jena Image Library of Biological Macromolecules: 2002 update.* Nucleic Acids Res., 2002. **30**(1): p. 253-254.

19. Taylor, J.L., P. Rohatgi, H.T. Spencer, D.F. Doyle, and B. Azizi, *Characterization of a molecular switch system that regulates gene expression in mammalian cells through a small molecule.* BMC Biotechnol., 2010. **10**: p. 15.

20. Gietz, R.D. and R.A. Woods, *Transformation of yeast by lithium acetate/single-stranded carrier DNA/polyethylene glycol method*, in *Guide to Yeast Genetics and Molecular and Cell Biology, Pt B*. 2002, Academic Press Inc: San Diego. p. 87-96.

21. Sali, A. and T.L. Blundell, *Comparative protein modeling by satisfaction of spatial restraints.* J. Mol. Biol., 1993. **234**(3): p. 779-815.

22. Damborsky, J., M. Prokop, and J. Koca, *TRITON: graphic software for rational engineering of enzymes.* Trends Biochem. Sci., 2001. **26**(1): p. 71-73.

23. Berman, H.M., J. Westbrook, Z. Feng, G. Gilliland, T.N. Bhat, H. Weissig, I.N. Shindyalov, and P.E. Bourne, *The Protein Data Bank.* Nucleic Acids Res., 2000. **28**(1): p. 235-242.

24. Pettersen, E.F., T.D. Goddard, C.C. Huang, G.S. Couch, D.M. Greenblatt, E.C. Meng, and T.E. Ferrin, *UCSF chimera - A visualization system for exploratory research and analysis.* J. Comput. Chem., 2004. **25**(13): p. 1605-1612.

25. Sanner, M.F., *Python: A programming language for software integration and development.* J. Mol. Graphics Modell, 1999. **17**(1): p. 57-61.

CHAPTER 5

INVESTIGATING THE ROLE AND MUTATIONAL TOLERANCE OF TYROSINES 143 AND 147 IN THE HUMAN VITAMIN D RECEPTOR'S LIGAND BINDING POCKET

5.1 Tyrosines and the Two Anchoring Ends of the hVDR's Ligand Binding Pocket

Most nuclear receptors and their ligands are involved in forming key molecular interactions that are crucial for the activation and function of the receptor. These interactions include hydrophobic and electrostatic interactions (e.g. Van der Waals and hydrogen bonding). For example, 17-β estradiol forms two hydrogen bonds with residues located on opposite ends of the estrogen receptor's ligand binding pocket [1]. Glutamate 353, arginine 394 and a water molecule form a network of hydrogen bonds with the 3-hydroxyl group of estradiol, while histidine 524 on the other end of the pocket forms a hydrogen bond with the 17-hydroxyl group of the ligand [1, 2]. Hydrogen bonding residues are important, as they often anchor ligands in the pockets of nuclear receptors [3, 4]. Additionally, they contribute significantly to the three-dimensional structures adopted by these receptors.

While engineering the human vitamin D receptor (hVDR) to bind and activate in response to a novel small molecule ligand, a key characteristic observed was the importance of forming and maintaining hydrogen bonding potentials for interactions between the receptor and its ligands. The role of H305, H397 and C410 were investigated and discussed in Chapter 4. Residues Y143, S237, R274, S278, H305 and H397 form important hydrogen bonds with the hVDR's natural ligand, 1α, 25$(OH)_2D_3$, serving as anchors on each end of the ligand binding pocket (LBP) (Figure 5.1) [5]. The activation profiles obtained with the hVDR variants studied in Chapter 4 suggest that the end of the LBP consisting of two of these anchoring residues, H305 and H397, and

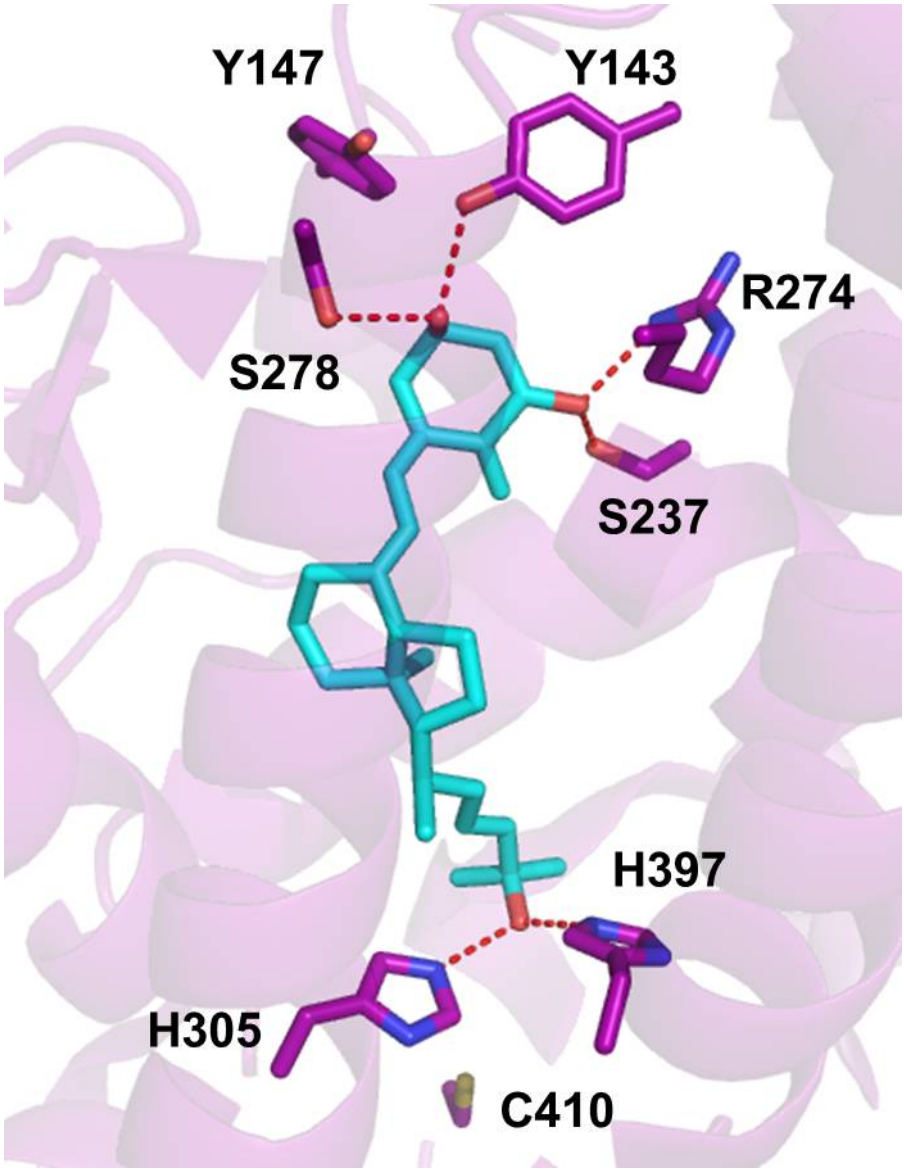

Figure 5.1: The hVDR and 1α, 25(OH)$_2$D$_3$,
hVDR residues (Purple), 1α, 25(OH)$_2$D$_3$ (Cyan), hydrogen bonds (Red Lines), PDB:1DB1

residue C410, tolerates structural variations, as numerous variants with mutations at these positions displayed enhanced activity in chemical complementation and mammalian cell culture assays. The hVDR's structure contains two tyrosines located at the exact opposite end of the pocket, involved in either direct or indirect contacts with the ligand. Thus, the role of these residues at the other end of the pocket was investigated.

Tyrosines 143 and 147 were two of the residues targeted for mutagenesis in hVDR library 2 (a rationally designed library discussed in Chapter 3), and interestingly these residues are positioned on the opposite end of the LBP compared to the H305, H397 and C410 residues (Figure 5.1). Both residues are within four angstroms of 1α, 25$(OH)_2D_3$; Y143 (helix 1) forms a hydrogen bond with the 3β-hydroxyl group of the ligand, while Y147 (loop 1-3) shares hydrophobic interactions with the ligand [5]. These aromatic residues have also been hypothesized to aid in stabilizing the many loop structures in the neighboring region and contributing to the ligand-mediated folding of the receptor [6-8]. In an effort to gain further insight into the role of residues at the other anchoring end of the ligand binding pocket, mutagenesis was performed to assess the tolerance of tyrosines 143 and 147.

5.2 Reversal of the hVDR Ligand Anchors

Previous protein engineering of the hVDR showed that residues H305 and H397 changed to tyrosines lead to enhanced activation with lithocholic acid (LCA) and cholecalciferol (chole) [9]. Based on these results and those obtained with the C410Y variant, where tyrosines on one end of the LBP seem to enhance activity, we chose to investigate the role of tyrosines on the other end of the hVDR's LBP. In previous work by Choi et al. and based on performed *in-silico* docking, different conformational poses have been obtained for ligands in the hVDR's LBP [8, 10]. For example, the positioning of the side chain carboxyl group of LCA towards helix 12, and that of 3-keto LCA

towards the opposite end of the LBP (~180º rotation) has been observed by Choi et al. Similar results have been observed for other receptor-ligand pairs when *in-silico* docking was performed using the program AutoDock Vina, such as the A-ring and side chain of cholecalciferol (chole) positioned on opposite ends of the LBP, compared to the structure of 1α, 25$(OH)_2D_3$ (Figure 5.2) [11]. Although the crystal structures of the hVDR with LCA, chole and 3-keto LCA are currently unavailable, receptor activation profiles obtained via alanine scanning mutational analyses with LCA and 3-keto LCA support these docking models [10].

To comprehensively assess the role of Y143 and Y147, several hypotheses were developed and tested. Since mutating H305 and H397 to tyrosines led to enhanced activation with LCA and chole, the first question asked was whether modifying Y143 and Y147 to histidines would allow wild-type activity with these ligands. Using site-directed mutagenesis, residues Y143 and Y147 in the hVDR were mutated to histidines in combination with H305Y;H397Y ("reversal of the hVDR ligand anchors") to determine whether the reversal of the residues on opposite ends of the pocket would allow for binding and activation (potentially due to binding of a ligand in the LBP in a ~180 º rotated conformation). This "reversal" would also provide insight into the tolerance of Y143 and Y147, as well as, the impact of secondary shell residues neighboring and surrounding these positions. Hence, part of the goal was to determine whether maintaining the hydrogen bonding potentials of the anchors on each end of the pocket was sufficient for activation, or whether a greater network of molecular interactions exists that is involved in ligand binding and activation.

To further assess the tolerance of residues Y143 and Y147 on their own (double variant), these amino acids were changed to histidines via site-directed mutagenesis. Each variant was transformed into the PJ69-4A yeast strain along with the coactivator plasmid (pGAD10BAACTR) and tested using chemical complementation, where yeast

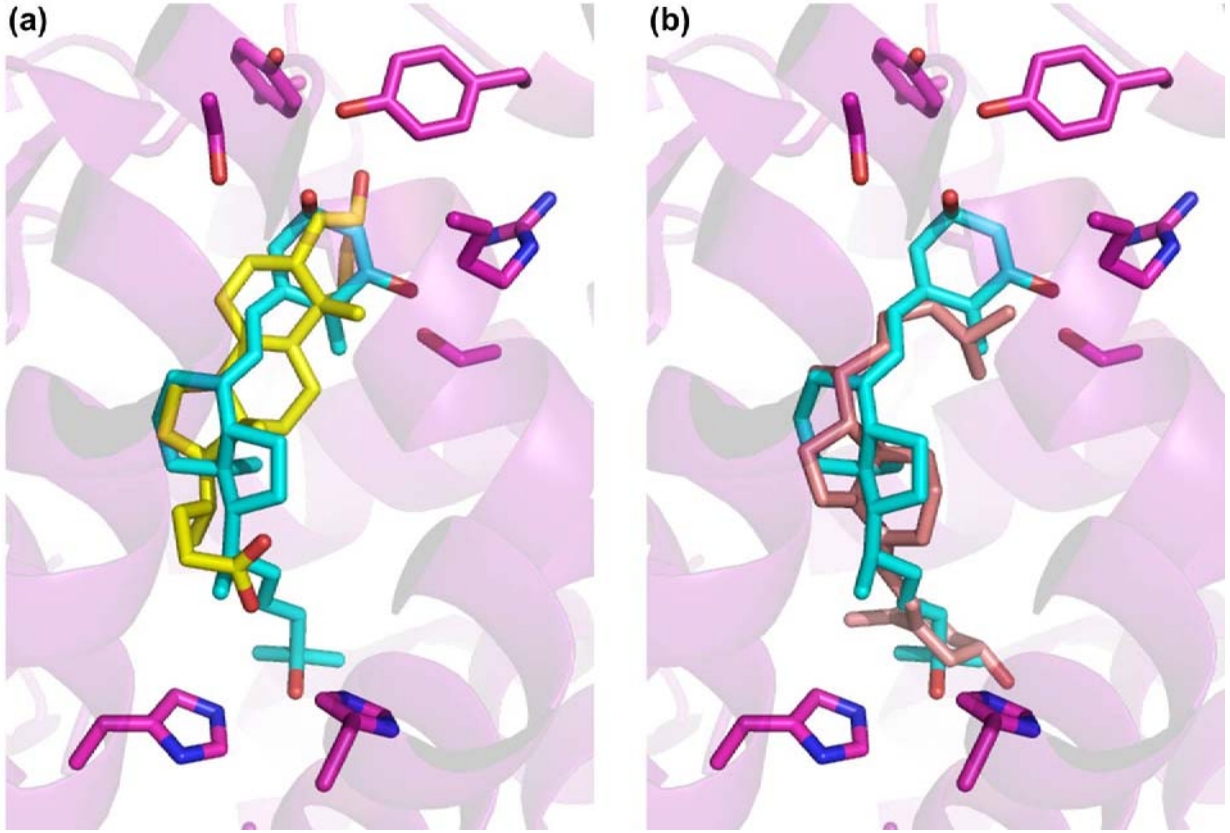

Figure 5.2: *In-silico* Docking of the wt hVDR with (a) LCA and (b) Chole.
hVDR residues (Purple), 1α, 25$(OH)_2D_3$ (Cyan), Lithocholic Acid (Yellow), Cholecalciferol (Pink), PDB:1DB1

growth would be an indication of a small molecule binding and activating the variant (ligand activated growth).

Reversal of the hVDR Ligand Anchors: Results from Chemical Complementation

When tested in liquid quantitation assays of chemical complementation with 1α, 25$(OH)_2D_3$ in adenine selective media (-ALW) and with LCA and chole in histidine selective media (SC-HLW + 0.1 mM 3-AT), ligand activated growth was only observed for the wild-type hVDR and the H305Y;H397Y variant (Figures 5.3a-c). More specifically, the wild-type hVDR and variant H305Y;H397Y shared the same ligand activated growth profile with 1α,25$(OH)_2D_3$ displaying an EC_{50}≈ 5 nM (Figure 5.3a). Ligand activated growth was not observed for variants Y143H;Y147H and Y143H;Y147H;H305Y;H397Y with this ligand (Figure 5.3a). As expected due to previous results in our lab, H305Y;H397Y displayed enhanced ligand activated growth compared to the wild-type hVDR when tested with LCA (EC_{50}= 0.4 μM vs. ~EC_{50}> 10 μM) and chole (EC_{50}> 10 μM vs. no growth for the wild-type hVDR) (Figures 5.3b and 5.3c). Once again, no ligand activated growth was observed for variants Y143H;Y147H and Y143H;Y147H;H305Y;H397Y with LCA or chole (Figures 5.3b and 5.3c). Mutating tyrosines 143 and 147 to histidines had a detrimental effect on the function of the receptor.

No ligand activated growth was obtained when Y143 and Y147 were changed to histidines on their own or in combination with H305Y;H397Y, yet enhanced growth is observed for the H305Y;H397Y variant with both LCA and chole. These results are not surprising and agree with previously discussed data, once again suggesting that the end of the hVDR's ligand binding pocket consisting of residues H305, H397 and C410

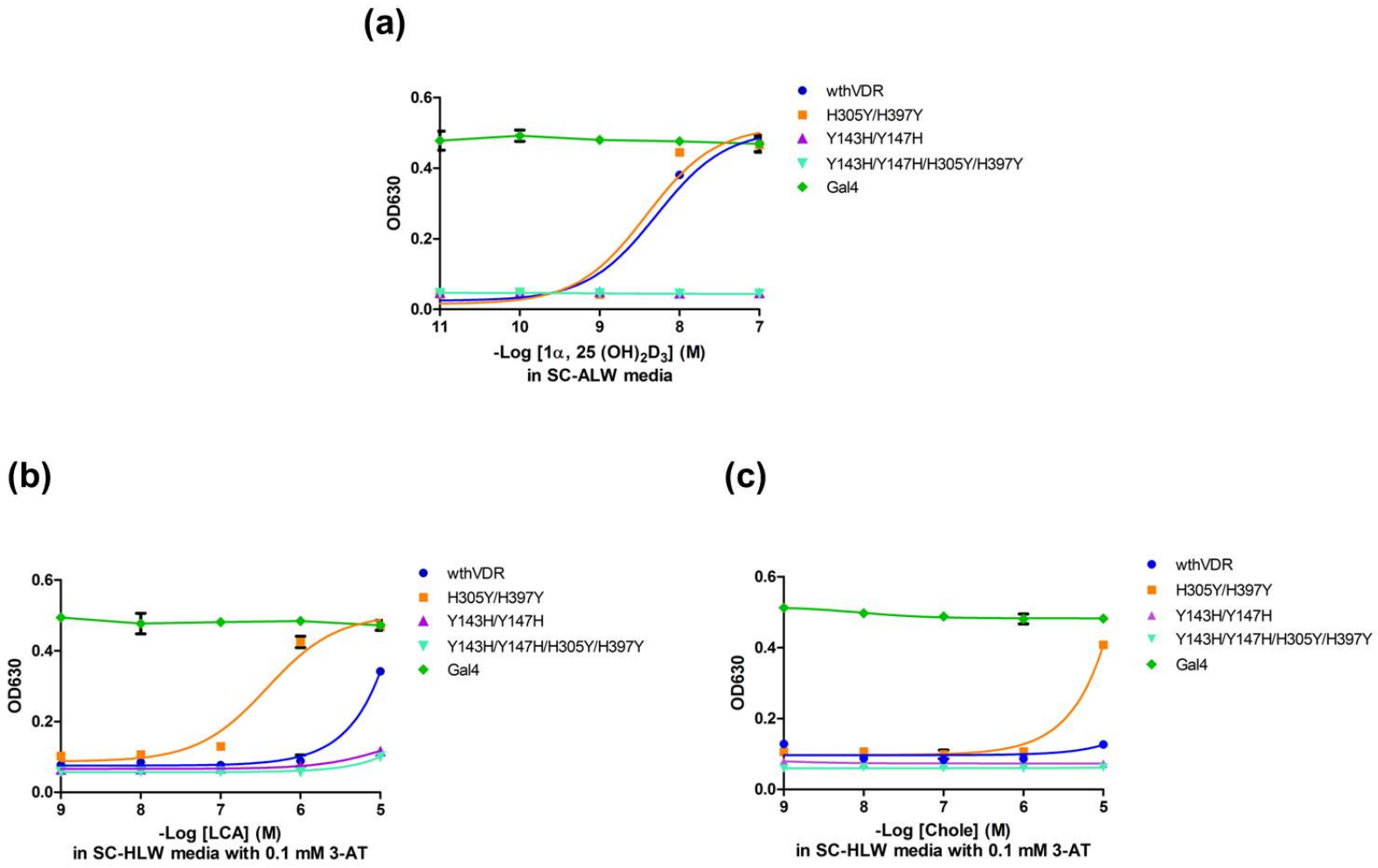

Figure 5.3: Reversal of the hVDR Ligand Anchors: hVDR Variants in Chemical Complementation. Adenine selective media with (a) 1α, 25$(OH)_2D_3$, Histidine selective media with (b) LCA and (c) chole

tolerates structural changes, in some instances with mutations leading to enhanced function of the receptor. These results also suggest that the end of the ligand binding pocket consisting of residues Y143 and Y147 is not as tolerant, in terms of allowing structural changes without resulting in loss of function.

5.3 Eliminating the Constitutive Activity of A hVDR Variant

Previous protein engineering of the hVDR showed that residues H305 and H397 changed to phenylalanines lead to constitutive activation of transcription or constitutive activity [9]. Constitutive activity refers to a nuclear receptor (NR) showing growth or activation without the presence of an exogenous small molecule ligand. As discussed in Chapter 1, helix 12 of most NRs forms the ligand dependent activation function domain (AF-2) which serves as a mobile lid over the LBP and is involved in interactions with transcriptional coregulators. In some cases, such as that of the constitutive androstane receptor (CAR) constitutive activity can result from a fixed active conformation of this domain or the binding of an endogenous ligand [12-15].

The “reversal of the hVDR ligand anchors” resulted in no ligand activated growth due to the detrimental effect of mutating tyrosines 143 and 147 to histidines. To determine whether the same effect would be observed for a constitutively active variant, residues Y143 and Y147 in the hVDR were mutated to histidines in combination with H305F;H397F via site-directed mutagenesis. Each variant was transformed into the PJ69-4A yeast strain along with the coactivator plasmid (pGAD10BAACTR) and tested using chemical complementation.

Eliminating the Constitutive Activity of A hVDR Variant: Results from Chemical Complementation

When tested in liquid quantitation assays of chemical complementation with LCA and chole in histidine selective media (SC-HLW + 0.1 mM 3-AT), constitutive activity was observed for variants H305F;H397F and Y143H;H305F;H397F (Figures 5.4a and 5.4b). Interestingly, the wild-type hVDR and variant Y147H;H305F;H397F shared similar ligand activated growth profiles with LCA with an EC_{50}> 10 μM (Figure 5.4a). Y147H;H305F;H397F also displayed ligand activated growth with chole with an EC_{50}> 10 μM. Due to the expense of the hVDR's natural ligand, 1α, 25$(OH)_2D_3$, only LCA and chole were used to collect this set of data.

As expected, mutating both tyrosines, 143 and 147, to histidines in combination with H305F;H397F (resulting in variant Y143H;Y147H;H305F;H397F) had a detrimental effect on the function of the receptor. As with the variants for the "reversal of the hVDR ligand anchors", no ligand activated growth was observed for Y143H;Y147H;H305F;H397F. However, when Y143H and Y147H were introduced into H305F;H397F individually, the results obtained were quite surprising. Y147H seems to reverse the constitutive activity observed with H305F;H397F, such that the variant displays ligand activated growth with LCA and chole. Introducing Y143H however does not have the same effect, as constitutive activity is still observed. This set of data suggests that although mutations at the end of the ligand binding pocket consisting of residues Y143 and Y147 seem to be detrimental to the function of the receptor, thus far position Y147 is possibly less tolerant than Y143 as the presence of Y147H in combination with H305F;H397F eliminates the constitutive activity of the double variant.

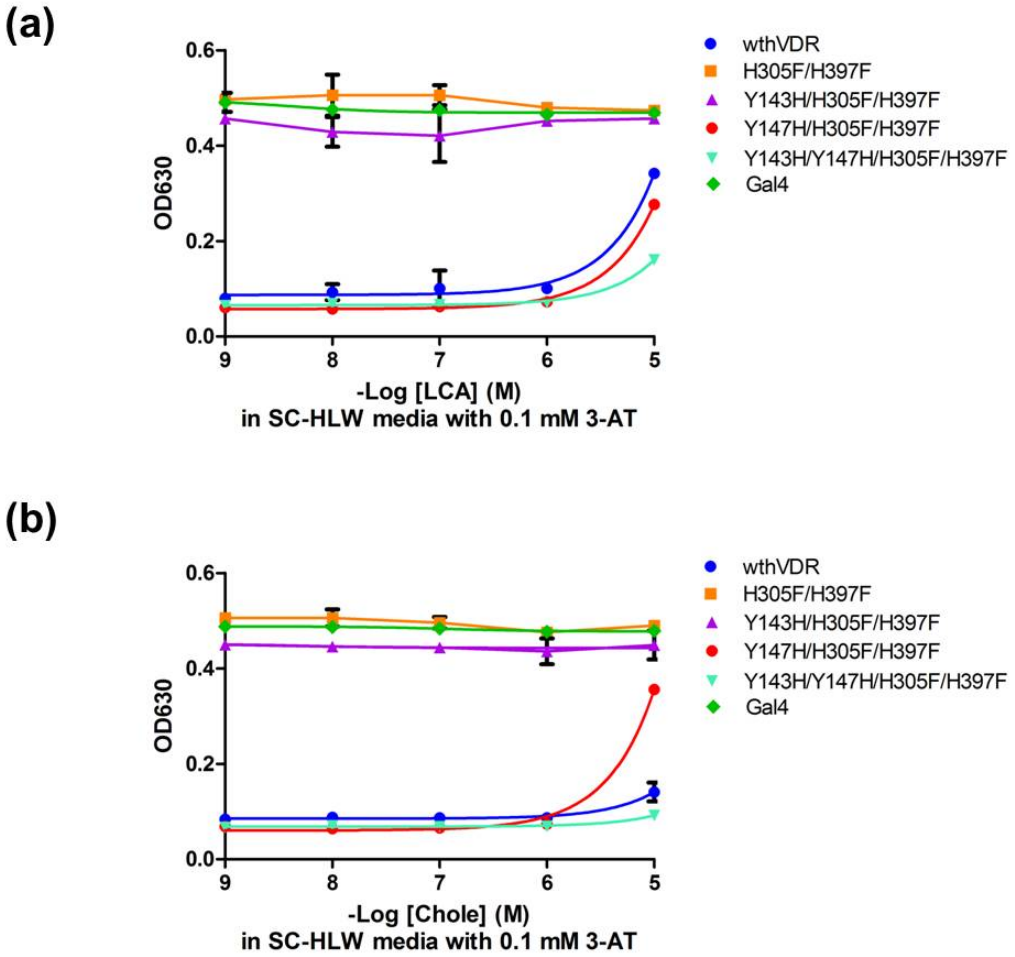

Figure 5.4: Eliminating the Constitutive Activity of A hVDR Variant: hVDR Variants in Chemical Complementation.
Histidine selective media with (a) LCA and (b) chole

5.4 Mutational Tolerance of hVDR Residues Y143 and Y147

Residues Y143 and Y147 are within four angstroms of 1α, 25$(OH)_2D_3$. Y143 forms a hydrogen bond with the ligand, while Y147 is involved in hydrophobic interactions. In previous work, mutating Y143 to alanine has been shown to drastically reduce activity, while mutating Y147 to alanine nearly eliminates activity [7, 8]. Additionally, Y143A has resulted in large effects on ligand binding, while Y147A has had a larger influence on receptor activity [7]. Tyrosines 143 and 147 are also known to be part of an important cluster of aromatic residues in the hVDR's ligand binding pocket (LBP) consisting of residues F150, W286 and Y295 (Figure 5.5) [7, 8]. These aromatic residues have been hypothesized to aid in stabilizing the many loop structures in the region and contributing to the ligand-mediated folding of the receptor [6-8].

To explore these residues beyond alanine mutagenesis and gain a better understanding of the mutational tolerance at these positions, residues Y143 and Y147 were changed to amino acids of varying properties via site-directed mutagenesis. The amino acids histidine, phenylalanine, lysine, tryptophan, leucine, and serine were chosen, as they exhibit diverse characteristics in terms of residue shape, size and polarity. Each single and double (Y143 and Y147 positions simultaneously mutated to the same amino acid) variant was transformed into the PJ69-4A yeast strain along with the coactivator plasmid (pGAD10BAACTR) and tested using chemical complementation. A subset of variants was also tested in mammalian cell culture assays. Overall, we expected variants with amino acids of similar shape and size to tyrosine at the Y143 and Y147 positions to exhibit activation profiles similar to that of the wild-type hVDR. For example, variants Y143F and Y147F were hypothesized to display better activity than Y143S and Y147S despite the fact that both tyrosine and serine have a hydroxyl group. Previous work in our lab showed that at positions 305 and 397, the volume of the residue was critical in maintaining the function of the receptor with the natural ligand [9].

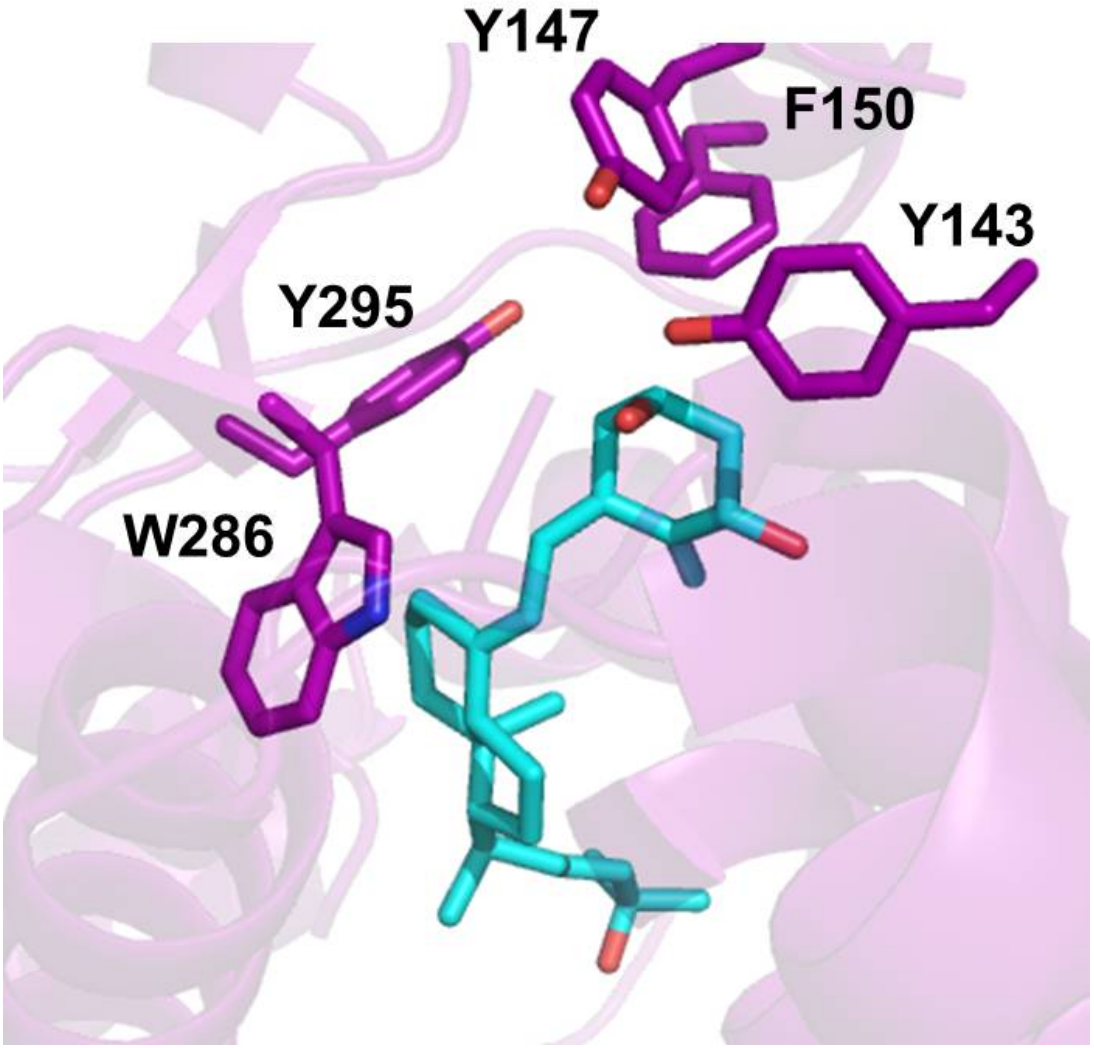

Figure 5.5: hVDR Residues Y143 and Y147.
Tyrosines 143 and 147 are part of an important cluster of aromatic residues in the hVDR's ligand binding pocket. hVDR residues (Purple), 1α, 25$(OH)_2D_3$ (Cyan), PDB:1DB1

The same concept may apply to the residues at the other end of the pocket.

Mutational Tolerance of hVDR Residues Y143 and Y147: Results for Single and Double Variants in Chemical Complementation

When tested in liquid quantitation assays of chemical complementation with $1\alpha,25(OH)_2D_3$ in adenine selective media (-ALW) and with LCA and chole in histidine selective media (SC-HLW + 0.1 mM 3-AT), ligand activated growth was observed for only a few of the single and double Y143 and Y147 variants (Figures 5.6a-c, 5.7a-c and 5.8). When tested with $1\alpha,25(OH)_2D_3$, variants Y143H, F and W showed a slight (~10-fold) decrease in sensitivity compared to the wild-type hVDR with an ~EC_{50}> 100 nM (vs. EC_{50}= 18 nM) (Figure 5.6a)**.** Variants Y147H, F and W showed a similar behavior with $1\alpha,25(OH)_2D_3$, displaying an ~EC_{50}> 100 nM (Figure 5.7a). Only one of the double variants, Y143F;Y147F, exhibited ligand activated growth with $1\alpha,25(OH)_2D_3$ with an ~EC_{50}> 100 nM (Figure 5.8).

As expected, ligand activated growth was observed for the wild-type hVDR with LCA at 10 μM (Figures 5.6b and 5.7b). For several of the single Y143 and Y147 variants, very little ligand activated growth was obtained with LCA at 10 μM (Figures 5.6b and 5.7b). No growth was obtained for any of the variants with chole (Figures 5.6c and 5.7c).

Thus far only bulky (residue volumes: tyrosine 193.6 $Å^3$, histidine 153.2 $Å^3$, phenylalanine 189.9 $Å^3$, and tryptophan 227.8 $Å^3$) amino acids also consisting of an aromatic ring have contributed to ligand activated growth with hVDR's natural ligand in chemical complementation [16]. Considering that tryptophan has the largest volume among all amino acids, we did not expect the ligand activated growth displayed by the Y143W and Y147W variants. However, mutating Y143 and Y147 simultaneously may potentially lead to a disruption of residue packing within the ligand binding pocket, as

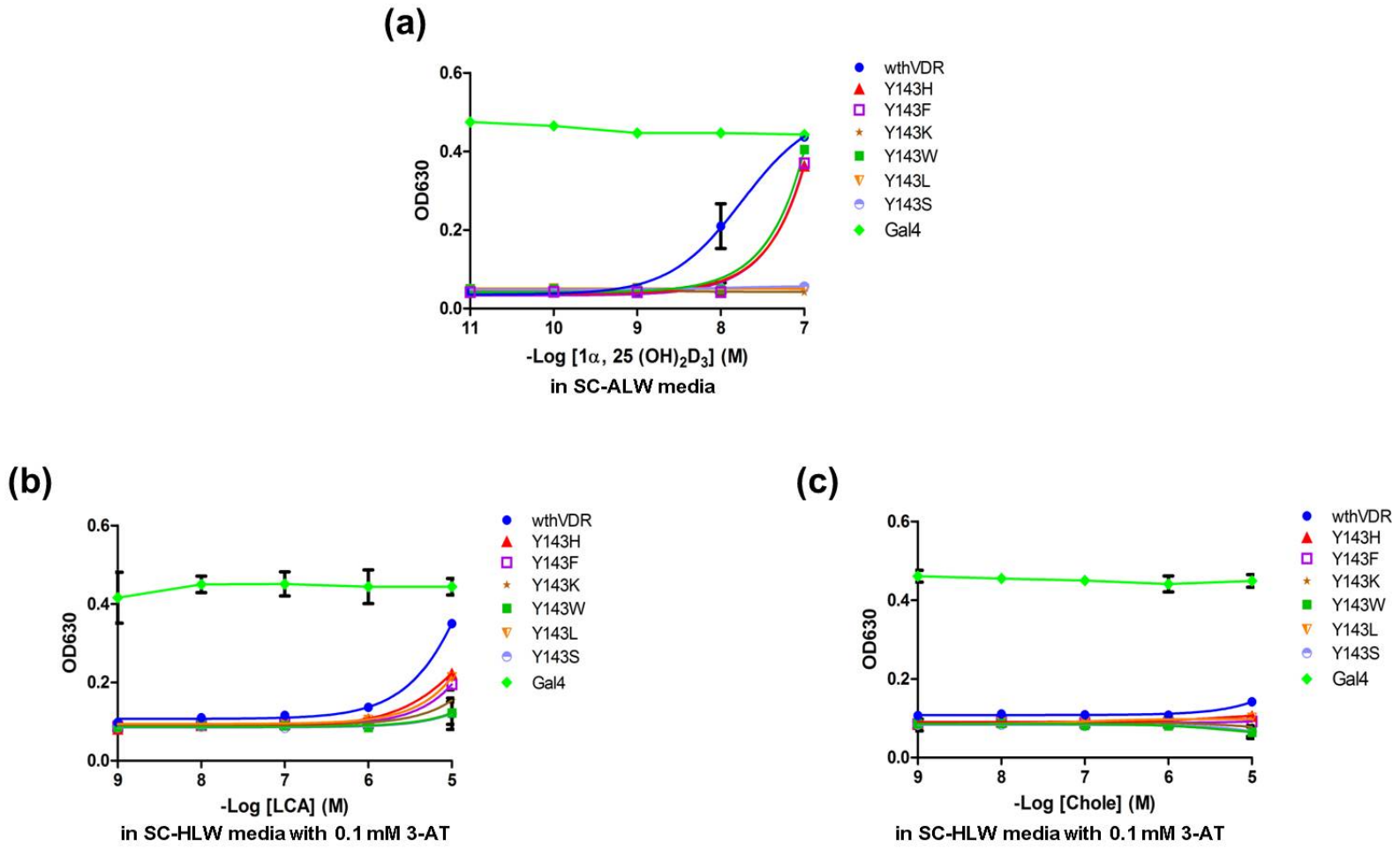

Figure 5.6: Mutational Tolerance of hVDR Residue Y143: Single Variants in Chemical Complementation. Adenine selective media with (a) 1α, 25$(OH)_2D_3$, Histidine selective media with (b) LCA and (c) chole

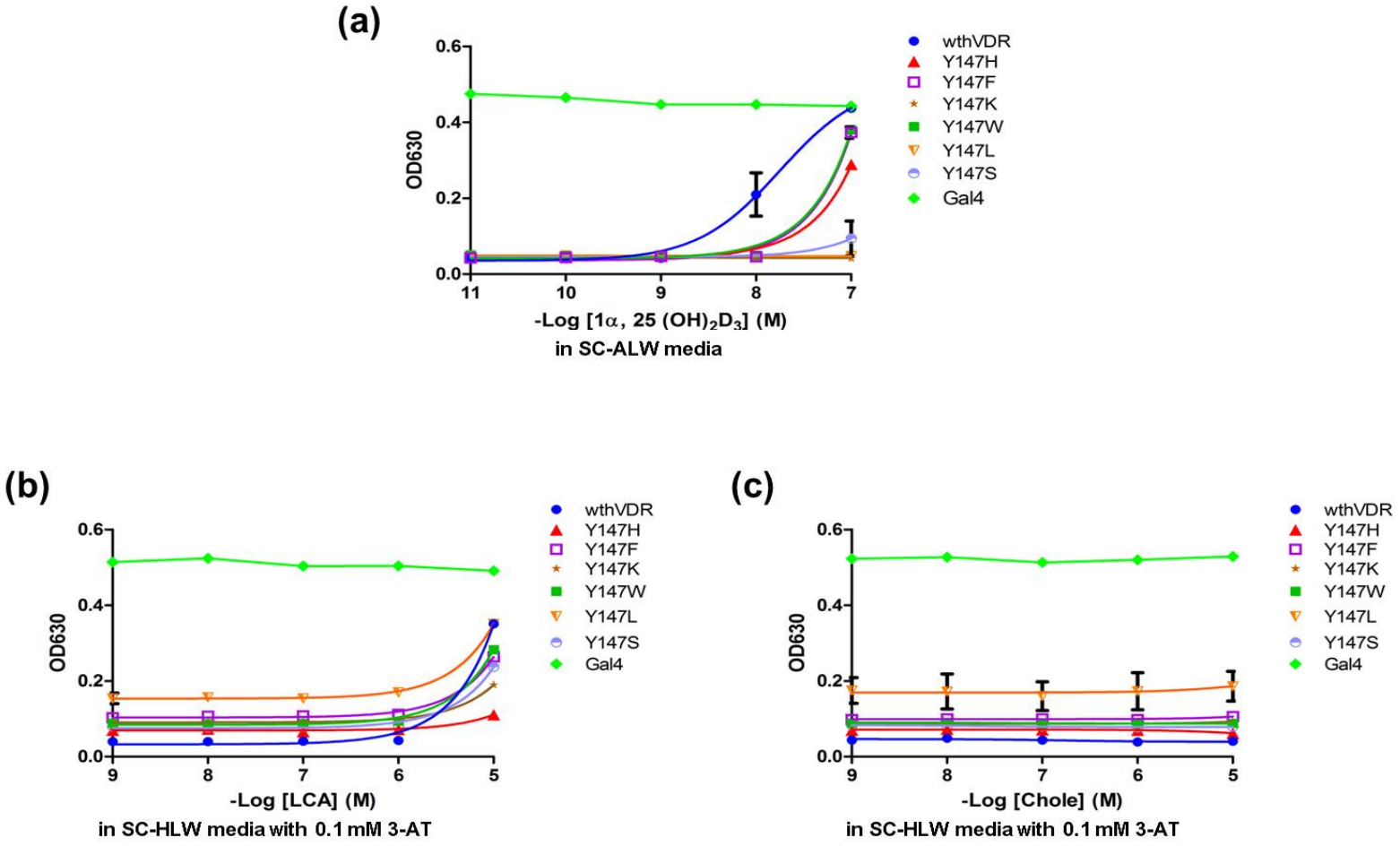

Figure 5.7: Mutational Tolerance of hVDR Residue Y147: Single Variants in Chemical Complementation. Adenine selective media with (a) 1α, 25$(OH)_2D_3$, Histidine selective media with (b) LCA and (c) chole

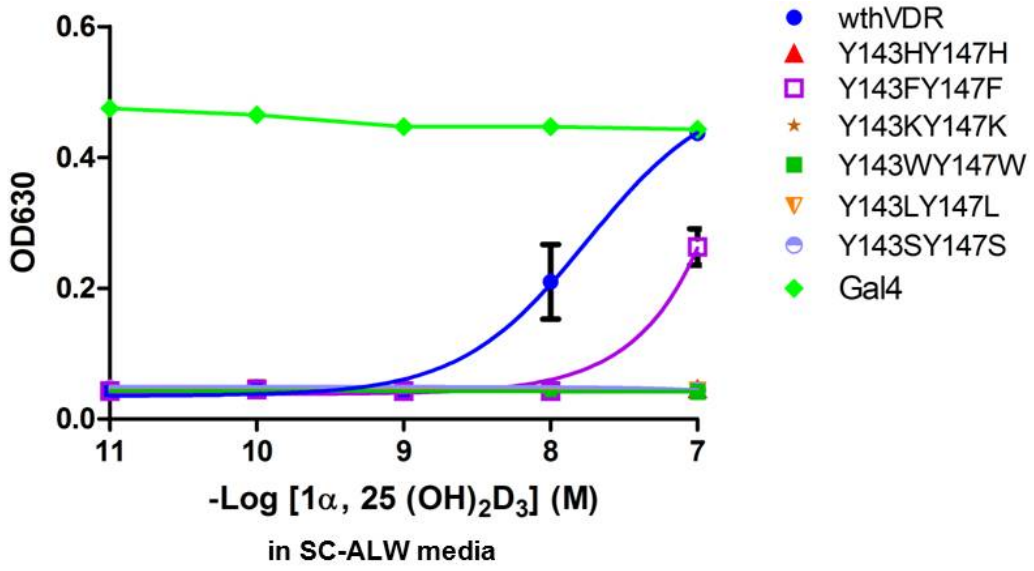

Figure 5.8: Mutational Tolerance of hVDR Residues Y143 and Y147: Double Variants in Chemical Complementation.
Adenine selective media with 1α, 25$(OH)_2D_3$

ligand activated growth was only observed for one of the double variants (Y143F;Y147F). This was not surprising, as phenylalanine is the amino acid most similar in properties, shape and size, to tyrosine.

Mutational Tolerance of hVDR Residues Y143 and Y147: Results for Single and Double Variants in Mammalian Cell Culture Assays

To determine whether the results obtained in yeast with the hVDR Y143 and Y147 variants were consistent in mammalian cell culture assays, mammalian expression plasmids (pCMX, with a cytomegalovirus promoter) containing a subset of the variants with interesting ligand activated growth profiles were transfected into human embryonic kidney 293T (HEK 293T) cells along with the p17*4TATALuc (containing a luciferase gene under the control of four Gal4 response elements) reporter plasmid (as described by Taylor *et al*.) [17]. Cell culture assays were performed with 1α, 25$(OH)_2D_3$, where luciferase activity would be an indication of a small molecule binding and activating the variant.

When tested with 1α,25$(OH)_2D_3$, the overall trend observed for the Y143 and Y147 single variants was consistent with the results obtained in chemical complementation. An EC_{50}= 5 nM and a 97-fold activation was observed for the wild-type hVDR, which displayed the best activity compared to all the variants tested. Residue Y143 exhibited preference for phenylalanine (EC_{50}= 6 nM and 79-fold activation), followed by tryptophan (EC_{50}= 50 nM and 161-fold activation) and histidine (EC_{50}= 76 nM and 130-fold activation) (Figure 5.9 and Table 5.1). Residue Y147 exhibited preference for phenylalanine (EC_{50}= 16 nM and 131-fold activation), followed by histidine (EC_{50}= 47 nM and 69-fold activation) and tryptophan (EC_{50}= 118 nM and 101-fold activation) (Figure 5.10 and Table 5.1). Most of the other Y143 and Y147 single variants tested

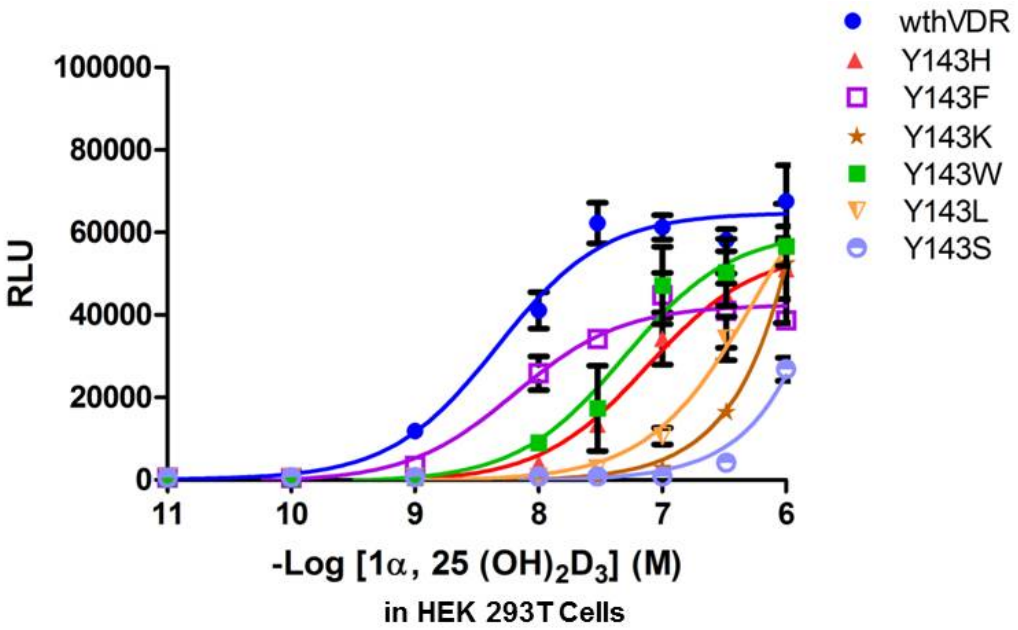

Figure 5.9: Mutational Tolerance of hVDR Residue Y143:
Single Variants in Mammalian Cell Culture Assay with 1α, 25$(OH)_2D_3$

Table 5.1 EC_{50} and Fold-Activation Values for hVDR Constructs Tested in Mammalian Cell Culture Assays Using HEK293T Cells with 1α, 25(OH)$_2$D$_3$. (-----) indicates less than 2-fold activation observed.

1α, 25(OH)$_2$D$_3$									
hVDR Construct	**EC_{50}**	**Fold-Activation**	**hVDR Construct**	**EC_{50}**	**Fold-Activation**	**hVDR Construct**	**EC_{50}**	**Fold-Activation**	
wthVDR	5 nM	97±24							
Y143H	76 nM	130±28	**Y147H**	47 nM	69±20	**Y143HY147H**	~178 nM	137±17	
Y143F	6 nM	79±11	**Y147F**	16 nM	131±23	**Y143FY147F**	37 nM	12±3	
Y143K	~316 nM	126±35	**Y147K**	~ 316 nM	75±18				
Y143W	50 nM	161±23	**Y147W**	118 nM	101±26	**Y143WY147W**	----------	---------	
Y143L	~316 nM	79±8	**Y147L**	~178 nM	93±20				
Y143S	>1000 nM	41±8	**Y147S**	206 nM	75±15	**Y143SY147S**	>316 nM	59±5	

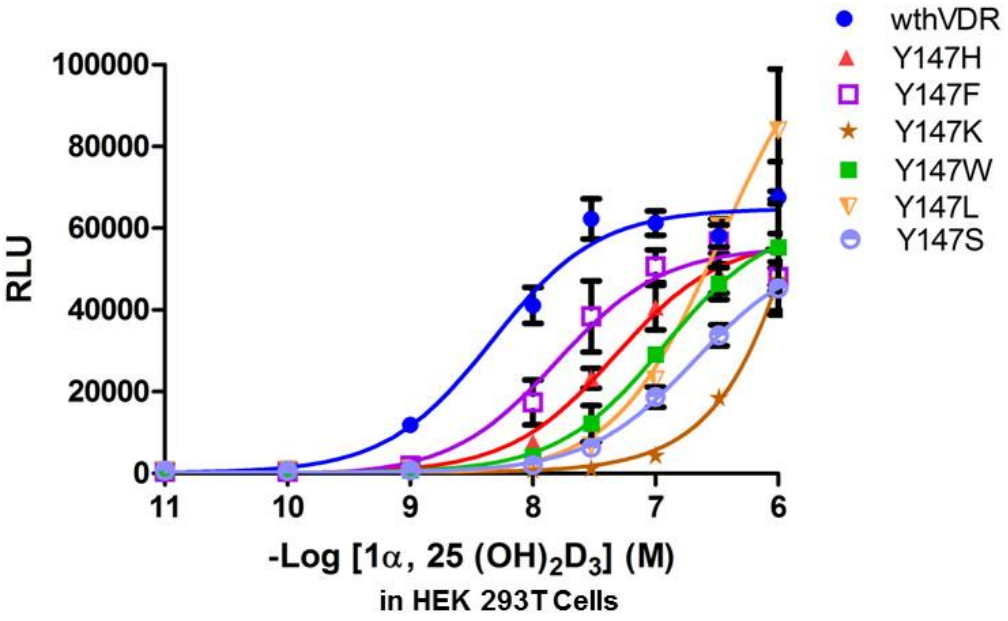

Figure 5.10: Mutational Tolerance of hVDR Residue Y147:
Single Variants in Mammalian Cell Culture Assay with 1α, 25$(OH)_2D_3$

displayed activity with 1α,25$(OH)_2D_3$, but at much higher concentrations (Figures 5.9 and 5.10, and Table 1). In agreement with the results obtained in yeast, mutating Y143 and Y147 simultaneously to the same amino acid proved to be detrimental in all cases suggesting that a disruption of residue packing and/or important interactions within the ligand binding pocket was caused (Figure 5.11 and Table 5.1).

Overall, the results obtained in yeast and mammalian cell culture assays for the hVDR Y143 and Y147 single and double variants demonstrate that most changes at these positions are detrimental to the function of the receptor. Once again, this data supports the hypothesis that this end of the hVDR's ligand binding pocket is less tolerant of structural variations, compared to the opposite end consisting of residues H305, H397 and C410. None of the mutations studied resulted in enhanced receptor function, however the conservative change to phenylalanine and semi-conservative changes to histidine and tryptophan resulted in activation similar to that of the wild-type hVDR. This is probably due to the presence of an aromatic group which might continue to interact favorably with the important cluster of aromatic residues Y143 and Y147 are a part of (Figure 5.5). The other amino acids tested may disrupt or not satisfy these interactions, resulting in little to no hVDR activation. These results suggest that maintaining proper residue packing within the ligand binding pocket may be more important than maintaining the hydrogen bonding interactions, as suggested by previous research [18].

5.5 Summary

Previously discussed variants (Chapter 4) with enhanced activity compared to the wild-type human vitamin D receptor have indicated that the end of the receptor's ligand binding pocket (LBP) consisting of residues H305, H397 and C410, tolerates mutations and can compensate for structural variations. Tyrosines 143 and 147 were two of the residues targeted for mutagenesis in one of the rationally designed

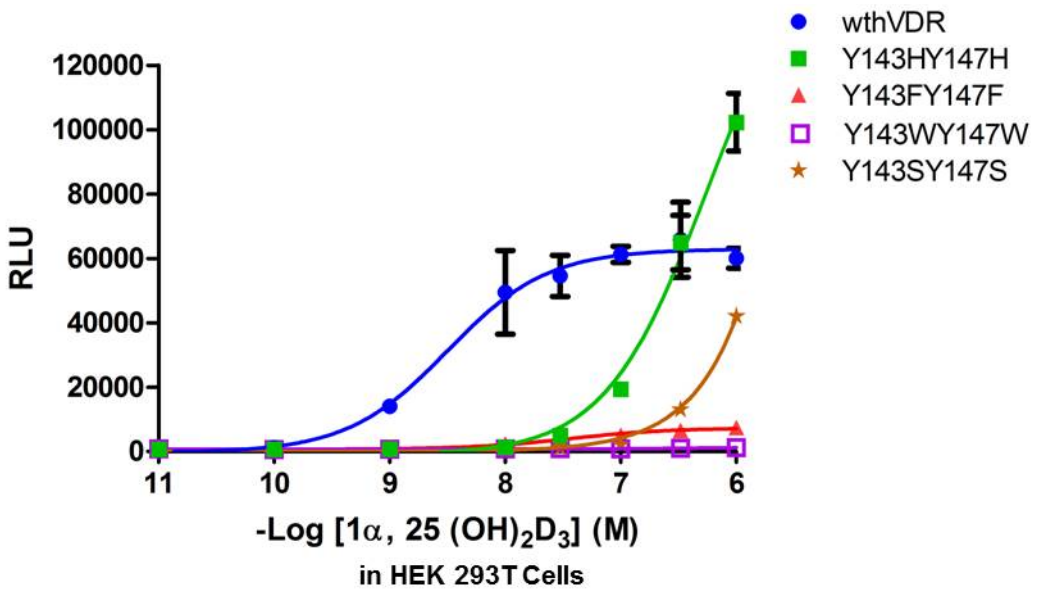

Figure 5.11: Mutational Tolerance of hVDR Residues Y143 and Y147: Double Variants in Mammalian Cell Culture Assay with 1α, 25$(OH)_2D_3$

libraries discussed in Chapter 3, and interestingly these residues are positioned on the opposite end of the hVDR's LBP (Figure 5.1). In this work we explored the end of the ligand binding pocket consisting of residues Y143 and Y147, using mutagenesis to gain insight on the role and mutational tolerance of these residues. Overall, most changes at these positions proved to be detrimental to the function of the receptor supporting the hypothesis that this end of the LBP is less tolerant of structural changes.

This work consisted of testing double variants where residues Y143 and Y147 were simultaneously changed to the same amino acid, while future work can focus on mutating these residues to different amino acids. This will help determine whether other combinations of amino acid properties work well together at these positions. Additional structural studies on the important aromatic cluster formed by residues Y143, Y147, F150, W286 and Y295 would also be useful for protein engineering, providing insight into how this cluster provides stability for the rest of the protein structure and how important each position is in contributing towards this role.

5.6 Materials and Methods

Ligands

1α, 25-dihydroxyvitamin D_3, lithocholic acid and cholecalciferol were purchased from BIOMOL (Plymouth Meeting, PA), MP Biomedicals, LLC (Solon, OH) and Sigma-Aldrich (St. Louis, MO), respectively. 10 mM stocks of LCA and chole, and a 13.3 μM stock of 1α,25-dihydroxyvitamin D_3 were made with 80 % ethanol: 20 % dimethyl sulfoxide (DMSO) and stored at 4 °C.

In-silico Docking of Wild-type hVDR

The atomic coordinates of the crystal structure of the hVDR ligand binding domain (Δ165-215) were retrieved from the Research Collaboratory for Structural

Bioinformatics (RCSB) Protein Data Bank (PDB) (PDB ID: 1DB1) [5, 19]. The structure was prepared for docking using the UCSF CHIMERA-interactive molecular graphics program by: (1) removing the ligand and water molecules, (2) adding polar hydrogens, and (3) assigning Gasteiger charges [20]. The three-dimensional structure of each ligand was constructed and minimized using ChemBioDraw Ultra 11.0 and ChemBio3D Ultra 11.0 (Cambridge Soft, USA) [21]. AutoDockTools was used to add Gasteiger charges to each ligand structure, setting the partial charge property of each atom. Docking simulations were performed using AutoDock Vina with default parameters, such that the protein was held rigid and the ligand was allowed free rotation [11]. The receptor-ligand poses of lowest free energy of binding were analyzed further.

Site-Directed Mutagenesis

Mutations were introduced into the yeast expression plasmid, pGBDhVDR, using PCR (Stratagene, Santa Clara, CA) and the corresponding mutagenic primers (Operon, Huntsville, AL). All plasmids were purified using the QIAprep® Spin Miniprep Kit (Qiagen, Valencia, CA) and sequenced for confirmation (Operon, Huntsville, AL).

Yeast Transformation Using the PJ69-4A Strain

Using the 1x TRAFCO yeast transformation protocol, ~500 ng of the yeast expression plasmids, pGBDhVDR (containing the Gal4 DBD fused to the full-length hVDR with the corresponding mutation(s) and a tryptophan marker) and pGAD10BAACTR (containing the Gal4 AD fused to ACTR and a leucine marker), were co-transformed into the yeast strain PJ69-4A [22]. Transformants were plated onto non-selective synthetic complete agar plates lacking leucine and tryptophan (SC-LW) to select for both fusion plasmids. Plates were incubated at 30 ºC for 3-4 days.

Liquid Quantitation Assays of Chemical Complementation in Yeast

Transformants obtained from the yeast transformation were grown overnight in non-selective SC-LW media, at 30 ºC with shaking at 300 rpm. A 4:1 ratio of selective media (SC-ALW or SC-HLW) with and without ligand at varying concentrations: cells (yeast resuspended in water) were aliquoted into 96-well plates. Plates were then incubated at 30 ºC with shaking at 170 rpm for 48 hours, with optical density readings at a wavelength of 630 nm (OD630) taken at 0, 24 and 48 hours. All data points represent the mean of at least duplicate experiments and the bars indicate standard deviation. The lowest ligand concentration data points for all plots contain no ligand. EC_{50} values were calculated using GraphPad Prism and a non-linear regression extrapolation.

Construction of Mammalian Expression Plasmids

The Gal4 DBD fused to the hVDR for each of the Y143 and Y147 single and double variants was amplified from the respective pGBD yeast expression plasmid via PCR (55 ºC as the annealing temperature) using 125 ng of the following primers: 5'-tcc <u>ccg cgg</u> atg aag cta ctg tct tct atc gaa caa g-3' and 5'- aag gaa aaa a<u>gc ggc cgc</u> tca gga gat ctc att gcc aaa ca-3' (Operon, Huntsville, AL). The underlined sequences denote *SacII* and *NotI* restriction sites, respectively. The fusion constructs and mammalian expression plasmid, pCMX (discussed in Chapter 3), were digested with *SacII* and *NotI*, ligated, and transformed into Z-competent™ XL-1 Blue *Escherichia coli* (*E.coli)* cells (Zymo, Orange, CA). The resulting plasmids were purified using the QIAprep® Spin Miniprep Kit (Qiagen, Valencia, CA) and sequenced for confirmation (Operon, Huntsville, AL).

Mammalian Cell Culture Assays

Human embryonic kidney 293T cells (HEK 293T, ATCC, USA) were transfected with the pCMX mammalian expression plasmids discussed above, along with the p17*4TATAluc and pCMXβ-gal reporter plasmids (discussed in Chapter 3) as described by Taylor et al., using Lipofectamine 2000 (Invitrogen, Carlsbad, CA) as the cationic lipid [17]. Cells were harvested ~36-48 hours after the addition of ligand at varying concentrations, and analyzed for luciferase and β-galactosidase activity. All data points represent the mean of triplicate experiments normalized against β-galactosidase activity and the bars indicate standard deviation. The lowest ligand concentration data points for all plots contain no ligand. EC_{50} values were calculated using GraphPad Prism and a non-linear regression extrapolation. Fold activations were calculated by dividing the highest level of activation by the lowest level of activation in triplicate experiments.

5.7 Literature Cited

1. Brzozowski, A.M., A.C.W. Pike, Z. Dauter, R.E. Hubbard, T. Bonn, O. Engstrom, L. Ohman, G.L. Greene, J.A. Gustafsson, and M. Carlquist, *Molecular basis of agonism and antagonism in the oestrogen receptor.* Nature, 1997. **389**(6652): p. 753-758.

2. Huang, P.X., V. Chandra, and F. Rastinejad, *Structural overview of the nuclear receptor superfamily: Insights into physiology and therapeutics.* Annu. Rev. Physiol., 2010. **72**: p. 247-272.

3. Greschik, I. and D. Moras, *Structure-activity relationship of nuclear receptor-ligand interactions.* Curr. Top. Med. Chem., 2003. **3**(14): p. 1573-1599.

4. Moore, J.T., J.L. Collins, and K.H. Pearce, *The nuclear receptor superfamily and drug discovery.* ChemMedChem, 2006. **1**(5): p. 504-523.

5. Rochel, N., J.M. Wurtz, A. Mitschler, B. Klaholz, and D. Moras, *The crystal structure of the nuclear receptor for vitamin D bound to its natural ligand.* Mol. Cell, 2000. **5**(1): p. 173-179.

6. Yamamoto, K., M. Choi, D. Abe, M. Shimizu, and S. Yamada, *Alanine scanning mutational analysis of the ligand binding pocket of the human Vitamin D receptor.* J. Steroid Biochem. Mol. Biol., 2007. **103**(3-5): p. 282-285.

7. Yamamoto, K., D. Abe, N. Yoshimoto, M. Choi, K. Yamagishi, H. Tokiwa, M. Shimizu, M. Makishima, and S. Yamada, *Vitamin D receptor: Ligand recognition and allosteric network.* J. Med. Chem., 2006. **49**(4): p. 1313-1324.

8. Yamada, S. and K. Yamamoto, *Ligand recognition by vitamin D receptor: Total alanine scanning mutational analysis of the residues lining the ligand binding pocket of vitamin D receptor.* Curr. Top. Med. Chem., 2006. **6**(12): p. 1255-1265.

9. Ousley, A.M., *Engineering the Human Vitamin D Receptor to Bind A Novel Small Molecule: Investigating the Structure-Function Relationship Between Human Vitamin D Receptor and Various Ligands* in *unpublished thesis (PhD). Georgia Institute of Technology, Atlanta.* 2010.

10. Choi, M., K. Yamamoto, T. Itoh, M. Makishima, D.J. Mangelsdorf, D. Moras, H.F. DeLuca, and S. Yamada, *Interaction between vitamin D receptor and vitamin D*

ligands: Two-dimensional alanine scanning mutational analysis. Chem. Biol., 2003. **10**(3): p. 261-270.

11. Trott, O. and A.J. Olson, *AutoDock Vina: Improving the speed and accuracy of docking with a new scoring function, efficient optimization, and multithreading.* J. Comput. Chem., 2009.

12. Sonoda, J., L.M. Pei, and R.M. Evans, *Nuclear receptors: Decoding metabolic disease.* FEBS Lett., 2008. **582**(1): p. 2-9.

13. Noy, N., *Ligand specificity of nuclear hormone receptors: Sifting through promiscuity.* Biochemistry, 2007. **46**(47): p. 13461-13467.

14. Suino, K., L. Peng, R. Reynolds, Y. Li, J.Y. Cha, J.J. Repa, S.A. Kliewer, and H.E. Xu, *The nuclear xenobiotic receptor CAR: Structural determinants of constitutive activation and heterodimerization.* Molecular Cell, 2004. **16**(6): p. 893-905.

15. Xu, R.X., M.H. Lambert, B.B. Wisely, E.N. Warren, E.E. Weinert, G.M. Waitt, J.D. Williams, J.L. Collins, L.B. Moore, T.M. Willson, and J.T. Moore, *A structural basis for constitutive activity in the human CAR/RXR alpha heterodimer.* Mol. Cell, 2004. **16**(6): p. 919-928.

16. Reichert, J. and J. Suhnel, *The IMB Jena Image Library of Biological Macromolecules: 2002 update.* Nucleic Acids Res., 2002. **30**(1): p. 253-254.

17. Taylor, J.L., P. Rohatgi, H.T. Spencer, D.F. Doyle, and B. Azizi, *Characterization of a molecular switch system that regulates gene expression in mammalian cells through a small molecule.* BMC Biotechnol., 2010. **10**: p. 15.

18. Reddy, M.D., L. Stoynova, A. Acevedo, and E.D. Collins, *Residues of the human nuclear vitamin D receptor that form hydrogen bonding interactions with the three hydroxyl groups of 1alpha,25-dihydroxyvitamin D3.* J. Steroid Biochem. Mol. Biol., 2007. **103**(3-5): p. 347-351.

19. Berman, H.M., J. Westbrook, Z. Feng, G. Gilliland, T.N. Bhat, H. Weissig, I.N. Shindyalov, and P.E. Bourne, *The Protein Data Bank.* Nucleic Acids Res., 2000. **28**(1): p. 235-242.

20. Pettersen, E.F., T.D. Goddard, C.C. Huang, G.S. Couch, D.M. Greenblatt, E.C. Meng, and T.E. Ferrin, *UCSF chimera - A visualization system for exploratory research and analysis.* J. Comput. Chem., 2004. **25**(13): p. 1605-1612.

21. Sanner, M.F., *Python: A programming language for software integration and development.* J. Mol. Graphics Modell, 1999. **17**(1): p. 57-61.

22. Gietz, R.D. and R.A. Woods, *Transformation of yeast by lithium acetate/single-stranded carrier DNA/polyethylene glycol method*, in *Guide to Yeast Genetics and Molecular and Cell Biology, Pt B*. 2002, Academic Press Inc: San Diego. p. 87-96.